INTERMITTENCY-A PRIOR INDICATOR OF COMBUSTION INSTABILITY AND FLAME BLOWOUT IN A TURBULENT COMBUSTOR

A THESIS

submitted by

GIREESHKUMARAN THAMPI B. S.

for the award of the degree

of

DOCTOR OF PHILOSOPHY

DEPARTMENT OF AEROSPACE ENGINEERING
INDIAN INSTITUTE OF TECHNOLOGY MADRAS.

October 2015

THESIS CERTIFICATE

This is to certify that the thesis titled **INTERMITTENCY- A PRIOR INDICATOR OF COMBUSTION INSTABILITY AND FLAME BLOWOUT IN A TURBULENT COMBUSTOR**, submitted by **Gireeshkumaran Thampi. B.S.**, to the Indian Institute of Technology, Madras, for the award of the degree of **Doctor of Philosophy**, is a bona fide record of the research work done by him under our supervision. The contents of this thesis, in full or in parts, have not been submitted to any other Institute or University for the award of any degree or diploma.

Prof. (Dr) R.I. Sujith
Research Guide
Professor
Dept. of Aerospace Engineering
IIT-Madras, 600 036

Place: Chennai
Date: 7th October 2015

Dedicated to my parents

Late

N. Bhaskaran Thampi and Savithri Amma

ACKNOWLEDGEMENTS

I would like to thank and acknowledge the support rendered by all the people during my past six years of research in combustion and flow diagnostic lab. It was a very good experience for me to perform my Ph.D., in this pleasing aura. During these years a good number of people have influenced my academic career at several occasions.

First and foremost I would like to thank my advisor, Prof. R.I. Sujith for his extraordinary support and guidance. His enthusiasm and exceptional efforts that he puts in understanding new things and implementing those things in research is amazing. He has given a particular shape to my career and taught me lot of things, both academic and nonacademic. He has been there for me during the situations where results were not coming.

I would like to express my sincere gratitude to the members of my doctoral committee, Prof. S.R. Chakravarthy, Dr. Sunetra Sarkar, Prof. Srinivasan. K, Dr. Shamit Bakshi for their valuable remarks and suggestions during the doctoral committee meetings. I would like to thank our HODs Prof. P. Sriram and Prof. K. Bhaskar for their support and encouragement during my tenure in Aerospace Department. My sincere thanks to all teachers for their exceptional lectures. I would like acknowledge the great help provided by the administrative staff and staff members in the central and aero workshop during my fabrication work. Especially Mr. Shankarakumarasamy and Biju at the time of purchase and settling the bill. Special thanks to Mr. John George (Central work shop) for his help during purchase of the material and for giving awareness of keeping safety aspects in the lab during the experiments with lasers. I am also thankful to Rama Dinakaran (PS to Prof.Sujith) for sending the scan copies of papers given by Prof. Sujith. I am also remembering in this occassion the late Mr. Ranganathan (machinist) for his help given to me during the fabrication work. I am also thankful to Dr. Sulochana Karuppusamy and Saravanan for their help for making a triggering circuit for my experimental purpose and an electronic control device for our patent.

Next, I would like to thank Dr. Vineeth Nair for the valuable suggestions and support

given by him during the time of experiments and paper writing. This acknowledgment would never be fulfilled, if I do not mention my other friends in our experimental and computational labs and also nearby labs, especially Shanmughadas, Vishnu R (Agni) and Ramgopal for their uncountable help during my experiment and computational work. Their night outs along with me during the hectic experimental schedule with sophisticated equipments is commendable. I am highly indebted to the senior research scholars especially Priya, Lipika, and Sathesh Mariappan for paving the way for doing research. I am also thankful to Mr. Vivekanandan (fearless man in the lab), for his help for doing the experiments with flame. I am also indebted to give special thanks to my colleagues in my parent institution for the help rendered to me during my period in IIT Madras. I am also very much thankful to my PG students Antonio Joseph, Viswajith and amaljith for their help during when I stuck with some computer problem.

Finally, I thank my parents (expired during the tenure of my period in IIT Madras) and all other family members for their support to achieve my goals. I would like to give a very special thanks to my wife Dr. Sreelatha and my wards Aiswarya (Achukutty) and Avinash (sambukuttan) and my niece Sruthi (Ammukutty) for their support and encouragement for my research activities and also their commendable help at the time of proof reading. I am also thankful to wife's family members for their support and careful attention given to my family in my absence. I am very much thankful to God Almighty for blessing me with very good health and happiness.

ABSTRACT

KEYWORDS: Lean premixed combustion; Swirl flows; Combustion dynamics; Nonlinear time series analysis; Limit cycle; 0-1 test; Stability margin; Intermittency; Blowout; Chemiluminescence imaging; Swirl stabilized combustor.

Combustors operating in the lean premixed mode often undergo unpredictable self-sustained high amplitude periodic oscillations, that results from the establishment of a positive feedback between unsteady heat release rate and chamber acoustic field. These periodic oscillations are referred to as combustion instability or thermoacoustic instability. The occurrence of these instabilities in the practical combustor is a challenging problem which results in the performance loss, structural degradation, reduced operational range and stability margin of the combustor. A small fraction of the heat released during combustion is sufficient enough to drive combustion instability. Thus, swirl combustor is more prone to combustion instability during fuel lean condition, where small perturbations in equivalence ratio produce large fluctuations in heat release rate. Even though several different mechanisms underlying the occurrence of instabilities are established, a basic understanding of the complex nonlinear interaction between unsteady combustion, acoustic and flow field involved is still lacking.

The present research work aims to characterize experimentally the nonlinear combustion dynamics such as limit cycle and intermittency in a partially premixed combustor using a swirl stabilized turbulent laboratory scale combustor. Experiments were performed by varying the global equivalence ratio between 0.92 and 0.33. The bifurcation diagram was plotted with the peak pressure amplitude for each operating condition as the measure and the flow Reynolds number, which varied up to blowout condition. Three different regime such as stable combustion (combustion noise), limit cycle oscillations, and irregular burst oscillations prior to blowout were identified using the bifurcation diagram. At higher equivalence ratios, the thermoacoustic system undergoes broadband low amplitude oscillations during stable operation, which is referred

to as combustion noise in literature. On reducing the equivalence ratio further, the broadband spectrum steepens and attains a single peak, indicating limit cycle oscillations. Secondary bifurcations such as irregular burst oscillations were observed at lower equivalence ratios nearing to blowout. At this state, the thermoacoustic system switch back and forth between periodic (noisy) and aperiodic (quiet) zone, termed as intermittency in dynamical system theory.

These nonlinear behaviors were characterized using nonlinear time series analysis of the acquired time series data of pressure fluctuations, which helps to detect hidden dynamical patterns and inherent nonlinearities in the system. The transition from stable combustion (combustion noise) to unstable combustion is shown qualitatively by drawing phase portraits, return maps, and recurrence plots. We observe that during the onset of instability, the thermoacoustic system undergoes intermittent bursts of high amplitude periodic oscillations among the regions of aperiodic low-amplitude oscillations. These excursions to instability oscillations last longer in time as the working condition approaches instability and finally the system attains instability. The dynamics during intermittent burst oscillations were quantified by measuring the recurrence rate of the dynamics using recurrence plots and also examining the scattering of the aperiodic phases. From the distribution of these aperiodic phases, robust advance notice of signals of an imminent combustion instability can be determined. We also implement a mathematical test for chaos, known as the 0-1 test for chaos in literature, as a measure of the closeness of the combustor to an imminent instability. The measure is powerful and shows a smooth transition for variation in flow conditions towards instability enabling a threshold to be set for operational boundaries.

At equivalence ratio nearing to blowout, the combustor undergoes secondary bifurcations. A uniformly black kite-like shape with white perforated structures are obtained in the recurrence plots indicating the intermittent behavior of the system. That is, prior to the blowout, the system undergoes a transition from instability oscillations to chaotic oscillations. The duration of the aperiodic phase lasts longer in time and finally the system attains complete chaotic oscillations prior to blowout. Thus, we can use intermittency as a signature prior to blowout.

From high-speed flame images, it is observed that the flame is sustained near to the chamber wall during stable combustion, indicated by low amplitude chaotic os-

cillations. The flame stabilizes near the dump plane and fills in the inner and outer recirculation zone during the occurrence of combustion instability. During intermittent behavior prior to blowout the flame consist of the dark zone, which is speculated to be corresponding to quiet phase and local pre-ignition zone of the flame corresponding to loud phase.

This research work strengthens the concept that the intermittent behavior can be used as an indicator prior to combustion instability and blowout in turbulent combustors. This helps the field operators to detect the occurrence of both thermoacoustic instability and blowout in advance. Thus, they can take necessary measures to avoid the instability oscillations and blowout, which increases both stability margin and operational range of practical turbulent combustors.

TABLE OF CONTENTS

LIST OF FIGURES

ABBREVIATIONS

CTRZ	Central Toroidal Recirculation Zone
ORZ	Outer Recirculation Zone
CRZ	Corner Recirculation Zone
WRZ	Wake Recirculation Zone
PVC	Precessing Vortex Core
LPG	Liquid Petroleum Gas
SLPM	Standard Litres per Minute
FTT	Fast Fourier Transform
FNN	False Nearest Neighbor
RR	Recurrence Rate
MLE	Maximal Lyapunov exponent
AMI	Average mutual information

NOTATION

Re	Reynolds number
ϕ	Equivalence ratio
λ	Maximal Lyapunov exponent
μ	Viscosity of the mixture
d	Burner diameter
ρ	Density of the mixture
ν	Bulk mean velocity
$\dot{m}_a$	Mass flow rate of air
$\dot{m}_f$	Mass flow rate of fuel
τ	Time lag
d_0	Optimum embedding dimension
$E_1(d)$	Measure used to compute optimum embedding dimension
$E_2(d)$	Measure used to check for determinism in CaoâĂŹs method
$p\prime(t)$	Unsteady pressure
$\bar{p}$	Mean pressure
ϵ	Attractor dimension
H	Heavy side step function
$R(i,j)$	Recurrence matrix
$P(v)$	Frequency distribution of vertical/horizontal black lines
v_{min}	Suitable lower limit for v
P_{rms}	Root mean square pressure
s	Shannon entropy
$P(l)$	Frequency distribution of the black diagonal line
$p(l)$	probability that a black diagonal line has length l
l_{min}	Minimum length of the diagonal line
k_c	Correlation of ξ and δ
K	Median of k_c

CHAPTER 1

INTRODUCTION

1.1 Background

Industrial gas turbines play a major role in the present world's power generation. The application of gas turbines extends from stationary power plants used for electrical power generation to aircraft engines, which is used for producing propulsive power (Mcmanus *et al.*, 1993). Lean premixed pre-vaporised (LPP) combustion technology is adopted in many gas turbine plants to meet stringent emission control measures. In this mode of combustion, a small quantity of fuel is sprayed into a large quantity of air stream at a distance upstream of the combustion chamber, such that fuel and air mixture introduced into the combustion chamber is in lean and well-mixed condition.

The lean premixed mode of combustion is believed to be the most promising solution to provide acceptable performance in terms of fuel economy, combustion efficiency and low pollutant emission (Annaswamy *et al.*, 1997). The relatively low flame temperature achieved at lean operating condition results in reduced NOx production. However at the lean condition, the premixed combustion introduces problems such as flame flashback and blowout. In addition, this combustor is prone to combustion instabilities, which are characterized by oscillations in pressure, the rate of heat release and the flow rate. The instabilities are sustained by the addition of a small portion of energy to the acoustic field from the unsteady combustion process. This dynamic phenomenon is a major threat to present combustion systems. They have troubled numerous propulsion and power generation systems such as solid and liquid rockets, ramjets and afterburners. These instabilities may cause large amplitude mechanical vibrations, which result in structural damage to the system (Samaniego *et al.*, 1993). These types of instabilities arises primarily from an interaction between the acoustic field and the unsteady combustion process. Amplified oscillations occur when the pressure oscillations and heat release rate oscillations are positively correlated in time as shown schematically in Fig. 1.1 (Samaniego *et al.*, 1993).

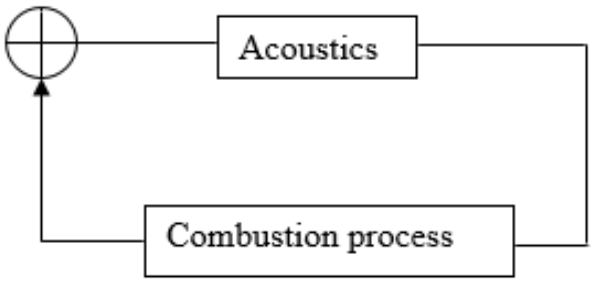

Figure 1.1: Schematic representation of the positive feedback loop between the acoustic field and combustion process.

1.2 Combustion instabilities

Combustion instabilities are self-excited and self-sustained large amplitude pressure and velocity oscillations in a combustor. These oscillations occur primarily due to the interaction between the acoustic waves and unsteady heat release rate. The heat release rate fluctuations are due to the fluctuations in the velocity field (Schuller *et al.*, 2003; Subramanian and Sujith, 2011) and the fuel-air ratio in the upstream side of the combustion chamber. When the heat release rate fluctuations interact with the acoustic field, it produces sound. That is a positive coupling between the acoustic field and unsteady heat release rate play an initial role in developing combustion instabilities (Mcmanus *et al.*, 1993). The other factors which influence the combustion instabilities are the formation of large-scale structures and fluctuations in the fuel-air ratio (Polifke, 2004).

In a confined environment, the pressure oscillations reflect back from the walls of the combustion chamber and it fluctuates the heat release rate. That is, a feedback loop is established between the chamber acoustics and the heat release rate oscillations as shown in Fig. 1.1. Self-excited oscillations occur when the acoustic oscillations and the fluctuations in heat release rate are in phase with each other. According to Rayleigh criteria (1878), the phase between the pressure and heat release rate fluctuations are within 90^0 is a necessary not sufficient condition for self-excited oscillations.

The term instability refers to the amplified pressure oscillations in the system. The pressure oscillations are amplified by the heat release rate fluctuations when they are

in phase (Rayleigh, 1878). Thus, the occurrence of combustion instability depends on the phase of the heat release rate fluctuations and the pressure oscillations at the flame. These amplified pressure oscillations then cause changes in heat release rate fluctuations through perturbations in the mean flow or the local equivalence ratio. A positive feedback results in the growth of the oscillations; this is referred to as thermoacoustic instability (Dowling, 2003; Rayleigh, 1878).

The velocity fluctuations associated with the acoustic waves perturb the flame and change the instantaneous rate of heat release. Since these fluctuations in heat release rate generate sound, the acoustic waves can gain energy from their interaction with the unsteady combustion process (Rayleigh, 1878). If this energy gain exceeds the losses at the ends of the duct and in the volume, the acoustic waves grow in amplitude into a finite amplitude self-excited oscillation.

1.2.1 Criteria for instability

Lord Rayleigh (1878) predicted a criterion for instability to occur. In this, Rayleigh assumed that the oscillations in an acoustic field accelerate the fluctuations in the unsteady heat release rate. Thus, the criterion developed by Rayleigh for the occurrence of a self-excited oscillations is that a direct coupling with regards to frequency and phase between unsteady heat release rate oscillations and acoustics fluctuations are necessary.

According to him: **"If heat is communicated to, and abstracted from, a mass of air vibrating in a cylinder bounded by a piston, the effect produced will depend upon the phase of the vibration at which the transfer of heat take place. If heat is given to the air at the moment of greatest condensation or to be taken from it at the moment of greatest rarefaction, the vibration is encouraged. On the other hand, if heat is given at the moment of greatest rarefaction or abstracted at the moment of greatest condensation, the vibration is discouraged."**

Thermoacoustic oscillations can occur whenever combustion takes place within a confined space. The unsteady heat release rate induces sound, which is propagated along the mean flow and reflected at the end of the combustion chamber, perturbs the flame, generating more unsteady heat release rate. Rayleigh identified that the relative phase of the pressure and the rate of heat release fluctuations as the parameter deter-

mining the stability of the system (Rayleigh, 1878). According to this criterion "for instability to occur, heat must be released at the moment of greatest compression".

1.2.2 Mechanism of combustion instabilities

The phase between the heat release rate fluctuations and the acoustic oscillations is the deciding factor for the occurrence of combustion instability. The pressure oscillations are amplified when they are in phase with heat release rate oscillations (Rayleigh, 1878). These amplified pressure oscillations oscillate the mean flow or the local equivalence ratios, which, in turn, fluctuate the heat release rate. A positive feedback results in the growth of these oscillations; this is referred to as thermoacoustic instability (Lieuwen *et al.*, 2011, Ducruix *et al.*, 2005). A driving process generates perturbations of the flow and these flow perturbations are coupled to the driving mechanism through a feedback process. This mechanism produces a resonant interaction that may lead to unpredictable oscillations. A schematic diagram of the process is as shown in Fig. 1.2. The amount of energy fed back into the initial perturbation is modulated by the acoustic boundaries of the plenum and the combustion chamber. This promotes the growth of modes of the natural frequency, which is close to the Eigen modes of the system (Fritsche *et al.*, 2007).

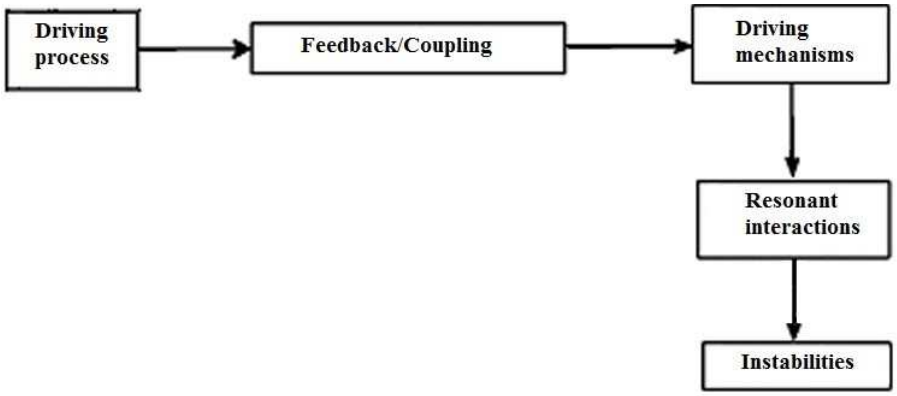

Figure 1.2: Schematic representation of the occurrence of combustion instability.

Figure 1.3 shows the influence of the acoustic perturbations on both upstream and downstream of the combustion chamber. The acoustic perturbations that generate during unstable combustion travel both upstream and downstream of the combustion cham-

ber. Acoustic oscillations that travel on the upstream side fluctuates the air and fuel flow rates, which in turn fluctuates mixing, atomization and vapourisation of the fuel and air mixture. However, the oscillations that travel on the downstream side of the combustor fluctuates the flame area, rate of reaction of the mixture and heat release rate. Acoustic oscillations also influence the interaction of vortex and flame.

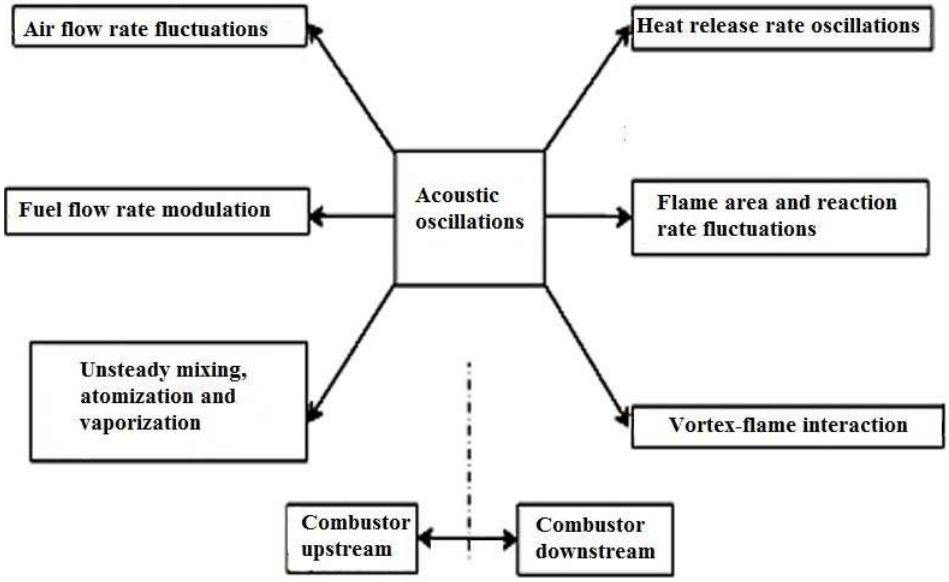

Figure 1.3: Schematic representation of the influence of acoustic oscillations on upstream and downstream of the combustion chamber.

The major driving mechanisms of combustion instabilities in lean premixed gas turbine engines are the equivalence ratio fluctuations, hydrodynamic instabilities, flame area variations, oscillatory fuel atomization and vaporization.

1.2.3 Causes of combustion instabilities

The understanding of the factors that affect the rate of heat release fluctuation and the effects of pressure oscillation to heat release rate oscillations is very much important in the study of combustion instabilities. The mechanisms that support heat release rate oscillations are shown in Fig. 1.4.

The major sources of heat release rate fluctuations are:

1. Flame - acoustic wave interaction

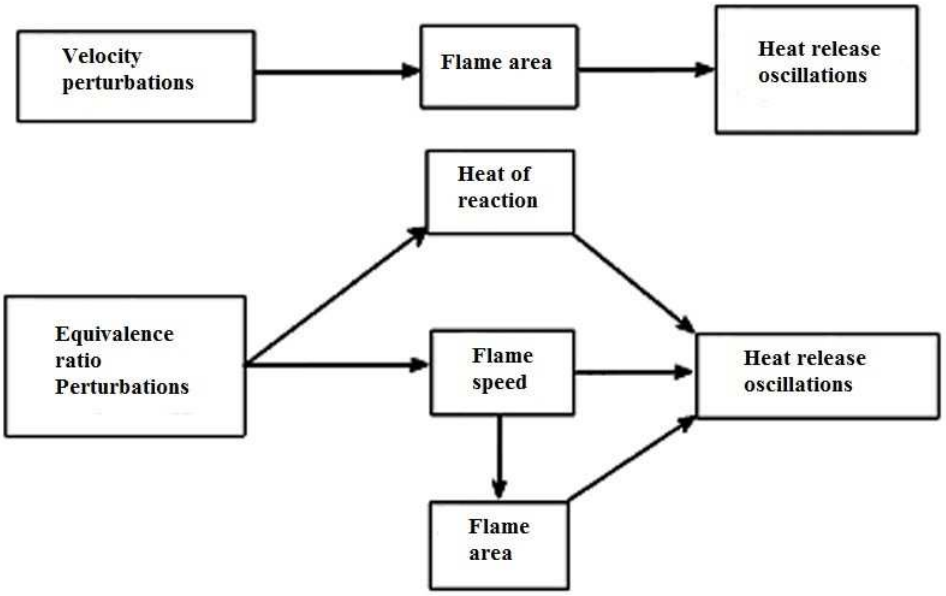

Figure 1.4: Schematic representation of mechanisms that support thermoacoustic instability.

2. Equivalence ratio oscillations
3. Flame - wall interactions
4. Flame - vortex interaction

Flame- acoustic wave interaction

In combustion systems, the flame act as an amplifier of acoustic waves. A small portion of available energy from the combustion process is added to the acoustic medium during certain phase between unsteady heat release rate oscillations and acoustic oscillations. This coupling between acoustic wave and the flame (Fig. 1.5) induces unsteadiness in the combustion process, which is responsible for self-excited oscillations (Lieuwen, 2001). Wu *et al.*, (2001) reported that in low-frequency regime the shape of the flame in a confined chamber is influenced by the acoustic source.

These high amplitude organized oscillations can cause structural damage. Such situations generally occur in combustors at natural acoustic modes. The direct effects of these interactions are the disturbance of flame structure such as flame surface area, flame positions, local burning area and wrinkling of flame etc.

Besides these effects, indirect oscillations are also exerted in the flow field by acoustic pressure and velocity oscillations. When the acoustic oscillations travel on the upstream side, they create disturbances in the premixing section, which in turn oscillate the fuel-air ratio of the reactive mixture. This oscillations travel through the mean flow and fluctuate the flame. The upstream velocity fluctuations or the density variation cause fluctuation in the mass flow rate of reactive mixtures into flame, oscillates the heat release rate, which in turn oscillate the chamber acoustic field and the process is repeated.

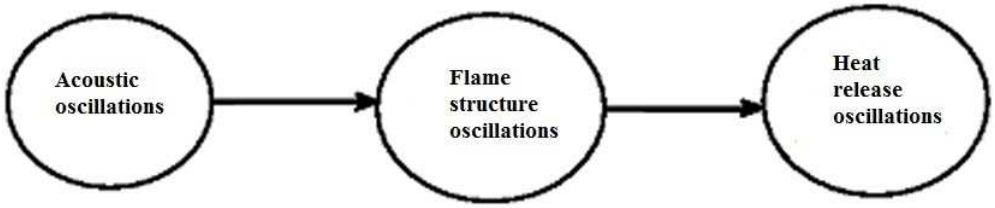

Figure 1.5: Schematic representation of flame-acoustic interactions.

Equivalence ratio fluctuations

Equivalence ratio (ϕ) is defined as the ratio of actual air and fuel ratio to the stoichiometric air and fuel ratio. i.e $\phi = (A/F)_a/(A/F)_s$. This indicates that the fluctuations in either flow rate of inlet air or fuel will fluctuate the equivalence ratio. Shreekrishna *et al.*, (2010) modelled the response of a premixed flame to fluctuating equivalence ratio of the reactant mixture. They established an underlying difference in response of a lean flame and a rich flame to fluctuating equivalence ratios. For a choked fuel injector, the equivalence ratio fluctuation is due to the fluctuation in inlet air velocity (Hong *et al.*, 2008, 2005). Relatively rich and lean equivalence ratios were obtained when the inlet air velocity is low and high respectively. This fluctuation in equivalence ratio fluctuate the heat release rate in the combustion chamber that could drive combustion instabilities (Atlay *et al.*, 2009). However in unchoked injectors, the time spent on the fuel in the feed line (or time lag τ) decides the equivalence ratio fluctuation. In this combustor, the fuel feed line pressure oscillates due to acoustic oscillations, which, in turn, fluctuates the pressure drop across the injector. The fluctuation in pressure across the fuel injector fluctuate the velocity of fuel flow and thus fluctuate the fuel flow rate (Hong *et*

al., 2005) at the upstream of the combustor. This causes the fluctuations in heat release rate during the combustion process. Equivalence ratio fluctuations which are driven by feedback from the combustion process and the resulting pressure and velocity oscillations can only cause combustion instability. That is, a feedback loop as shown Fig. 1.6 is needed to maintain instability.

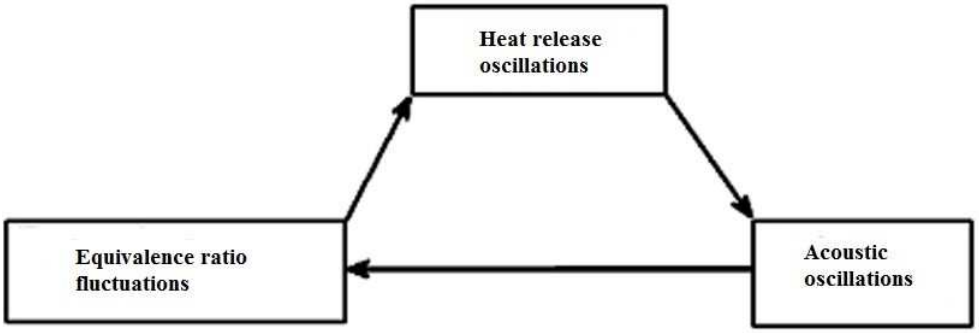

Figure 1.6: Schematic of the feedback mechanism needed to maintain instability.

Flame - wall interactions

Impingement of flame on a wall changes the flame area rapidly, which acts as a source of heat release rate oscillations. For a suitable phase and when the heat gain exceeds the losses, the rapid change in flame area during the interaction produces large amplitude heat release oscillations, which, in turn causes pressure oscillations (Durox *et al.*, 2002).

Under certain operating conditions, these interactions lead to self-sustained oscillations. Figure 1.7 shows schematically the effect of flame-solid wall interactions.

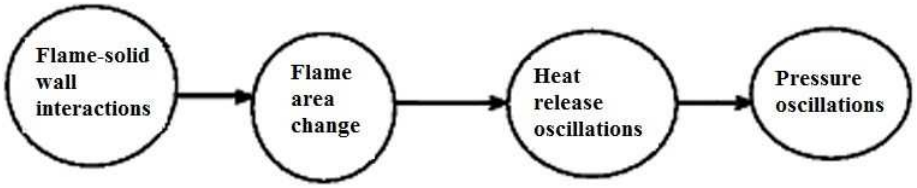

Figure 1.7: Schematic representation of the effect of flame-solid wall interactions.

Flame-Vortex interaction

Figure 1.8 shows the schematic representation of the interaction of flame with generated vortex in the combustion chamber. The flame is disturbed by vortical structures. The distortion of the flame front causes heat release oscillations due to flame area modulation. From studies involving flame-vortex interaction (Yu *et al.*, 1991, Hargrave and Jarvis 2006), it is clear that as the vortex traverses through the flame front, there is a marked change in the flame area which in turn affects the overall heat release rate. The instantaneous reaction rate and hence the instantaneous heat release rate can be measured using instantaneous flame surface area variation. The coupling between sound and flame occurs in a high-frequency region, where the acoustic time scales are comparable with the transit time of the flame. The generated sound modulates the flame and hence the flame surface area, which in turn modulates the heat release rate, thereby driving the chamber acoustics.

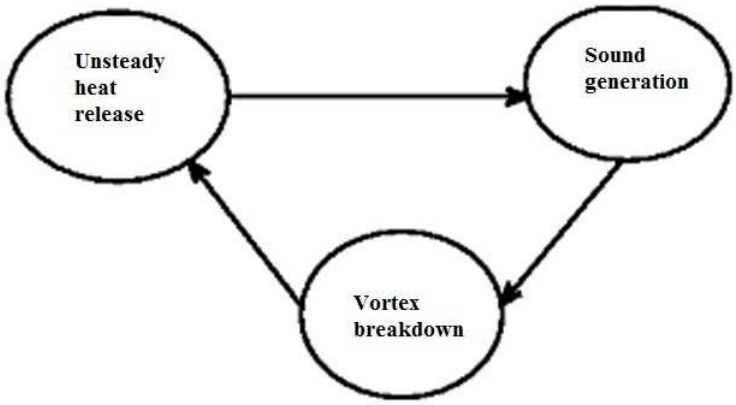

Figure 1.8: Schematic representation of flame-vortex interactions.

Further, the occurrence of coherent vortical structures causes heat release oscillations through large scale entrainment of reactive mixtures (Lieuwen, 2001).

Presence of large scale structures: Vortical structures that are developing depends on the stream injected into the combustion chamber. These structures are formed in the shear layer between a high-speed unburned mixture and the low-speed hot products. This high-velocity gradient exists between these two streams enhanced the mixing between the fresh fuel-air mixture and hot combustion products and the rate of burning in a premixed combustor (Paschereit *et al.*, 1999). Large scale structures in the shear layer

or highly shearing region are developed due to the flow instabilities and vortices. The shear layer develops instability in the initial region and then it is amplified by acquiring energy from the flow. After some threshold amount of energy gain, they start rolling up into vortices. The combustion process is significantly influenced by these vortex structures. The transport of fresh reactants into the burning region is also governed by these rolling structures. During vortex roll-up, the interface between the air, fuel mixture and hot products leading to fine scale turbulence, increases the heat release rate. The repetition of this process for each cycle of pressure oscillations causes periodic heat release rate. When there exists a proper phase (Rayleigh, 1878) between periodic heat release rate and pressure oscillations, high amplitude pressure oscillations are excited (Shadow, 2001). That is, undesired self-excited oscillations occur due to the interaction between large-scale structures related to flow instabilities, chamber acoustic modes and the rate of heat release processes. Coats (1996) reported that the coherent structure growth enhances heat release rate up to the generation of large amplitude combustion oscillations.

1.3 Swirling flows

A swirl flow occurs in modern gas turbine combustor and industrial burners (Gouldin *et al.*, 1984). These flows that are three-dimensional in nature have the characteristics of both turbulence and rotating motion (Reddy *et al.*, 2006). Periodic oscillations are also observed in swirling flows. The swirling magnitude depends on the coupling between flow driven swirling shear layer instabilities and flow instabilities due to sudden expansion and combustion geometry. Swirling motion promotes the flow reversal or vortex breakdown due to the occurrence of an adverse pressure gradient in the flow (Grinstein and Fureby 2005). The effect of swirl flow on longitudinal and azimuthal instability modes modifies the combustion process which leads to thermoacoustic instability.

High-frequency oscillations having comparable magnitude with the rotational frequency of the mean flow entering the test section are present in both cold and hot swirling flow. However in hot flow only low-frequency oscillations are prominent near the centre of the primary zone of the combustor. Hypothetically these fluctuations are periodic oscillations in the axial position of the recirculation zone and are driven by

coupling of combustion with the mechanism for the formation of the recirculation zone.

The swirl flows are characterized by swirl number, which is defined as the ratio of the axial flux of swirling momentum to the effective radius times the axial flux of axial momentum. In a confined chamber for no swirl condition, the wake recirculation zone (WRZ) and the outer recirculation zone (ORZ) are observed in the flow field due to sudden expansion of the flow (Najm and Ghonim, 1994). However, for flows with low swirl numbers, the flow structure consists of inner recirculation zone (IRZ), also called central toroidal recirculation zone (CTRZ), which is due to vortex breakdown along with the WRZ and ORZ. On increasing the swirl number further, the WRZ disappears by merging with CTRZ. At higher swirl numbers, the CTRZ move upstream and merges with ORZ. Thus the strength and axial position of CTRZ and ORZ is influenced by swirl number, which in turn depends on inlet flow velocity (Huang and Vigor 2005, Palies *et al.* 2010).

In swirl flows, the flame is stabilized at CTRZ and the combustion dynamics of swirl combustor are very much influenced by the flame stabilization at CTRZ. Najm and Ghonim (1994) reported that a rapid expansion of the flow causes a periodic detachment of the circulating flow in the ORZ, which in turn causes a flow roll up in the downstream direction. The oscillations in ORZ and CTRZ and the accompanying change in surface area of flame results in fluctuating heat release rate.

The swirling flows increase the residence time of the reactants in the swirl, which then increase the stability limits of the flame. The high rate of entrainment of ambient fluid and high rate of mixing between fuel and air accelerates the combustion process. The formation of CTRZ recirculates the hot combustion products and active chemical species to the upstream of the flame. Thus a lower velocity is required for the flame to stabilize in swirl flows (Syred and Beer 1974). Syred *et al.*, (1997) pointed out that the precessing vortex core (PVC) phenomena, due to high shear and turbulence in swirl flows, increases mixing. However, it damage the flame stabilization. Depending upon the operating conditions, a radially outward expanding flow is observed in swirling flows. The velocity at the central region is low compared to the velocity gradient in the shear layer (interface between CTRZ and CRZ). The magnitude of the velocity gradient reduces in the downstream direction. The turbulence intensity is higher near the swirl due to the flow from swirler and also from CTRZ and CRZ. A high momentum

transfer is also taking place through the shear layer between low-velocity CTRZ and high velocity swirling jet from the swirler.

The physical mechanisms responsible for the onset of thermoacoustic instability (Lieuwen *et al.* 2001, Ducruox *et al.* 2005) and the methods for its suppression (Shadow 2001) have been extensively investigated for various types of laboratory scale gas turbine combustor with swirling flows. A small fraction of the heat released during combustion is sufficient enough to drive combustion instability. Thus, swirl combustor is more prone to combustion instability during fuel lean condition, where a small perturbation in equivalence ratio can produce a large fluctuation in heat release rate. Kim *et al.* (2011) showed that the magnitude of the equivalence ratio fluctuations decide the linear and nonlinear regime of a flame. At higher equivalence ratio fluctuations, the flame shows a nonlinear behaviour. The nonlinear response becomes more pronounced at higher modulation frequencies and lower equivalence ratios. The inherent nonlinearity associated with the system dynamics can be extracted using the nonlinear dynamics to the acquired pressure data. The power spectral analysis of the acquired time evolution data provides only a limited understanding towards interpreting the complex system dynamics at various operating conditions.

1.4 Nonlinear Dynamics

1.4.1 Introduction to dynamical system theory

The dynamical systems approach aims to model the time evolving dynamics of a physical system. The time evolution of the system dynamics help us to get the information regarding the stability of the system and the related asymptotic state. However, this information is specific to the chosen system parameters and the applied initial condition. Thus, this individually obtaining evolutions in time to characterise the behaviour of the system for a range of parameter values and initial conditions are expensive. Both linear and nonlinear behaviour of the system can be investigated most efficiently and systematically by using the tools from dynamical system theory.

The complex nonlinear behaviour of the combustion dynamics of many combustion devices can be analysed using a set of tools for the nonlinear time series analysis. From

the time series data of a fluctuating variable (pressure), the characteristics and dynamical behaviour of systems at different operating conditions can be established (Hilborn, 2004, Kabiraj *et al.*, 2012a, Culick, 1994). Culick (1996) reported that the "measured pressure in a time histories of a combustion chamber will always show aspects of randomness as well as contributions from well-defined oscillations". The periodic, quasi-periodic or aperiodic behaviour of a thermoacoustic system can be characterized by embedding the experimentally acquired time series data of a fluctuating variable in an appropriate phase space using Takens' time delay embedding method (Takens, 1985). The qualitative change in the system dynamics during various operating condition can be observed through bifurcation diagrams.

1.5 Bifurcation

A sudden qualitative change in the behaviour of dynamical system on varying some of the controlling parameter by a small amount is called bifurcation in nonlinear dynamics. For example, a fixed point may change into a limit cycle indicating that the system now has acquired the capacity to oscillate. Such a change in the qualitative behaviour of a system is called bifurcation. During bifurcation, a qualitative change in the system behaviour is observed during a small and smooth variation of a system parameter above or below that of a particular value.

Basic types of local bifurcation are period-doubling, saddle node and Hopf bifurcation (Manneville and Pomeau, 1979). An infinite cascade of period doubling, leads to an aperiodic motion through an infinitely long period. A saddle node bifurcation occurs at points where the nonlinear oscillator curve turns over and the system undergoes instability. At Hopf bifurcation, self-excited limit cycle oscillations are generated.

A thermoacoustic system can undergo bifurcation leading to characteristically different nonlinear oscillations such as low amplitude stable oscillations to high amplitude limit cycle oscillations. However recent studies show that the limit cycle oscillations are just one of the possible end states of the system. The thermoacoustic system can undergo further bifurcation and attain states such as quasi-periodic, period doubling, frequency locked, intermittency and chaotic states.

Using bifurcation diagram, we can analyse the different regime such as stable com-

bustion (combustion noise) and its transition to instability oscillations and irregular burst oscillations a system can attain as and when a parameter is varied.

1.5.1 Combustion noise and its origin

Analysis of generation of noise induced by a flame is essential to understand the overall sound generation inside a combustion chamber at different operating conditions. In a confined chamber, the noise may be generated due to the impingement of flow with chamber wall, turbulence in flow (indirect noise), and coupling between acoustic oscillations and heat release rate fluctuations (Strahle, 1971). The noise due to the coupling between the sound field and combustion process is termed as direct noise (Bender *et al.*, 2008). In a combustion system, these generated noise having low amplitude is called combustion noise (Chiu and Summerfield, 1974). They also reported that the unsteady motion which produces both random fluctuations and coherent oscillations in ducts causes noise generation.

Combustion noise is also called flame induced noise. Any disturbance in flow field causes oscillations in the flame, resulting in sound generation. Candel *et al.*, (2004) reported that an acoustic emission is related to the rate of change of flame area due to the flow field interaction.

The physical processes that fluctuate flame surface area are flame-wall interaction, flame-flow interaction, flame-vortex interaction and impingement between vortices. These processes cause to change the flame area, which in turn oscillates the heat release rate, thus producing noise. Such types of noisy oscillations is always inherent in a turbulent combustor. A small portion of the energy available during the unsteady combustion process is supplied directly to the acoustic field; amplify the acoustic energy and produces oscillations with very high amplitude called combustion instability. In the premixed mode of combustion the coupling between unsteady combustion and pressure oscillations lead to large amplitude self-sustained oscillations known as thermoacoustic instabilities (Fritsche *et al.*, 2007, Fichera *et al.*, 2001). Unsteady combustion generates combustion noise and the resulting pressure oscillations induce more unsteadiness in the combustion process, generating high amplitude oscillations. In any thermodynamic system, the addition of heat at high pressure leads to a net energy input, which

is available to do work (Fichera *et al.*, 2001). If the energy gained from the unsteady combustion exceeds the rate of work done, then there occurs a growth in the amplitude of acoustic oscillations.

1.5.2 Transition from combustion noise to combustion instabilities

A low amplitude broadband noise is always present in a combustor having turbulent flows. When the operating conditions vary beyond the linear stability regime, the system undergoes a transition to high amplitude self-sustained instabilities from low amplitude noisy oscillations. Lieuwen (2002) observed that the inherent noise in a thermoacoustic system can strongly affect the limit cycle oscillations and under certain operating conditions they may even be responsible for causing the combustor to become stable under linearly unstable conditions. He also observed a phase drift characteristics of pressure oscillations due to the presence of noise. Chakravarthy *et al.*, (2007a and b) performed an experiment on a bluff body and backward facing step combustor and characterized that during combustion noise, the vortex shedding and chamber acoustics do not lock-on. However during instability oscillations the chamber acoustics and vortex shedding undergoes lock-on.

An understanding of the onset of these oscillations, the nature of oscillations and the nature of the transition from a stable state to an unstable state are very much essential to understand complex combustion dynamics. Linear analysis of the system provides an understanding of the existence of the thermoacoustic instabilities by revealing the unstable behaviour of the combustion process. However the linear analysis over simplified the view of the problem, which involves complex nonlinear interactions (Polifke, 2004). For a certain operating parameter the system undergoes secondary bifurcation such as intermittency.

1.5.3 Intermittency

Intermittency is referred to as the irregular switching of oscillations of the system between quiet and noisy regions under certain operating conditions (Pomeau and Manneville, 1980, Hammer*et al.*, 1994). For a system described by deterministic equations the switching appears to occur randomly. If the system behaviour seems to switch be-

tween periodic and chaotic behaviour, it is called intermittency. In this case for some control parameter value, the system behaviour is predominantly periodic with occasional burst of chaotic behaviour. For further change in the value of control parameter the time spent being chaotic increases with the decrease of time spent being periodic and eventually the system undergo chaotic all the time. As and when the control parameter value changes in the other direction the system behaviour is periodic all the time. The first type of intermittency is also called stable or tangent bifurcation intermittency. The second type of intermittency occurs when the system's behaviour seems to switch between periodic and quasi-periodic behaviour. In this type two frequencies are observed in the behaviour of the system in which one frequency corresponds to the original limit cycle, which disappears at the bifurcation point. At the bifurcation point, the limit cycle associated with the second frequency become unstable. The second type of intermittency is also called Hopf-bifurcation intermittency. In the third type of intermittency the amplitude of original periodic motion decreases, however the amplitude of sub harmonic behaviour which is created at the bifurcation point grows. The third type of intermittency is also called period-doubling intermittency. In fourth type of intermittency the behaviour of the system seems to alternate between very quiescent behaviour and chaotic bursts. The system is steady at some period of time. The fourth type of intermittency is called on-off intermittency (Kabiraj *et al.*. 2012 a and b, Klimaszewska and zebrowski, 2009).

For understanding the complex combustion dynamics and bifurcation characteristics of a themoacoustic system need an elaborate literature survey and is explained in Chapter 2.

CHAPTER 2

LITERATURE REVIEW

Combustion induced acoustic oscillations, called combustion instability is a resonance phenomenon associated with acoustic characteristics of the combustion chamber, the upstream duct and with the rate of unsteady heat release oscillations. The occurrence of such high amplitude oscillations is a challenging problem to the modern propulsion and power generation industry (Culick, 2006). Unpredictable large amplitude unsteady oscillations are easily established in these systems since only a small fraction of the available energy from the combustion process is sufficient to drive such oscillations. These oscillations result in performance loss, reduced operational range and structural degradation due to increased heat transfer (McManus *et al.*, 1993, Candel, 2002, Rogers and Marble, 1956).

Even in the absence of large amplitude oscillations, unsteady combustion process generates small amplitude noise, termed combustion noise (Strahle 1978, 1972, Nair *et al.*, 2013a).

2.1 Combustion noise

Combustion generated sound is an important aspect to consider in the development of modern energy and propulsion technology. The three main phenomenon encountered in this field are direct combustion noise, indirect combustion noise and combustion instabilities. Combustion systems such as aero engines produce direct and indirect combustion noise. Direct combustion noise is due to heat release rate oscillations (Strahle, 1978) and indirect combustion noise is due to temperature non-uniformities results from unsteady combustion (Schwarz and Janicka, 2009) that are convected through region with mean flow gradients such as nozzle. Experimental results showed that combustion noise is broadband with noise emissions above back ground noise levels for frequencies above 100Hz to over 20kHz. Combustion noise is generally peaked in a region of high back ground noise. Chakravarthy *et al.* (2007 a and b) performed experiments on

bluff body and backward facing step combustors and found that the regime of stable combustion is characterized by low amplitude broadband noise generation; i.e., stable combustion corresponds to the regime of combustion noise.

Combustion noise refers to one way coupling between acoustic field and flame, where turbulent fluctuations in the flow cause unsteadiness in the heat release rate, which, in turn, is a source of sound (Kotake, 1975). Traditionally the combustion noise has been thought of as a stochastic background such as flow turbulence and irregular low amplitude fluctuations present in the combustion dynamics in the midst of the flow, heat release rate and chamber acoustics. Thus the combustion dynamics are established with support of stochastic background such as flow turbulence and irregular low amplitude pressure oscillations, called combustion noise in literature. Through a series of determinism tests Nair *et al.* (2013a) showed that these aperiodic fluctuations are in fact chaotic of moderately high dimensions. They established that the combustion noise is deterministic chaos, which is in extreme contrast to the assumption as a stochastic back ground to the combustor dynamics. Thus the measurements acquired from a combustor is nothing but a signal modulated by combustion noise (Nair *et al.*, 2013a). This makes it difficult to predict a stability margin for turbulent combustors.

In a confined chamber, this low amplitude chaotic oscillations are transitioned to high amplitude instability oscillations at certain operating conditions. This is due to the fact that the acoustic waves caused by unsteady combustion are reflected from the boundaries and eventually return to the combustion chamber flow field and flame region, where they generate a further perturbation on the heat release rate. Under certain phase conditions, an unstable feedback may arise resulting in an amplification of the fluctuations until a distinct single frequency oscillation at well-defined amplitude is established called thermoacoustic instabilities.

2.2 Combustion noise leading to instability

The inherent system disturbances are self-excited through the interaction with the combustion process. A fluctuation in thermodynamic variable or flow, fluctuate the heat release rate from the combustion process. Any disturbance in the flow and acoustic field fluctuates the heat release rate that in turn fluctuates the disturbance in the flow

and acoustic field and thus heat release rate. This process repeats and thus the energy added to the chamber acoustic field during each cycle increases. Since the energy added to the field is greater than the energy loss (damping), the amplitude of the disturbance grows with time. Thus instability is initiated. An understanding of the physical mechanisms, which cause to change the behaviour of a system having fluctuations in flow, acoustics and unsteady combustion processes is critical.

The physical mechanisms underlying the onset of thermoacoustic instability and methods for its suppression have been extensively investigated for various types of laboratory scale gas turbine combustors with swirling flows. Huang and Yang (2009) summarizes that the major driving mechanisms of combustion instabilities in lean premixed gas turbine engines are equivalence ratio fluctuations, hydrodynamic instabilities, flame area variations, oscillatory fuel atomization and vaporization.

The response of the lean swirl stabilized flame to mixture ratio oscillations are quantitatively described by Kim *et al.* (2011) using flame transfer functions, defined as the ratio between the normalized heat release rate and the equivalence ratio fluctuations. They concluded that depending upon the magnitude of the equivalence ratio oscillations, the flame's response can be divided into linear and nonlinear regimes. At large equivalence ratio perturbations, heat release rate shows a nonlinear behaviour. The nonlinear response becomes more pronounced when the modulation frequencies increase and the mean equivalence ratio decreases. Komarek and Polifke (2010) measured the heat release rate response of a perfectly premixed swirl stabilized burner through flame transfer function (FTF), which relates the heat release rate oscillations to acoustic velocity fluctuations. For different positions of the swirler, they measured the velocity fluctuations using a constant temperature anemometer (CTA) and the heat release rate fluctuations using a photomultiplier with CH* filter.

Reddy *et al.* (2006) studied the flow field characteristics of a swirl flow through a sudden expansion geometry. They observed and characterized the swirling flow features such as corner recirculation zone (CRZ), precessing vortex core (PVC), and central toroidal recirculation zone (CTRZ). Thus, flow oscillations always exist in practical combustors even under stable operating conditions. Sutton and Biblas (2000) classified combustion with small amplitude pressure fluctuations as stable combustion and with large amplitude periodic pressure oscillations as unstable or oscillatory combustion.

According to Mongia *et al.*, (2005), instabilities occurring at frequencies lower than 30 Hz are often related to blowout phenomena. Instabilities occurring within the intermediate frequency range of 100-1000 Hz are associated with the coupling between fuel-air ratio and acoustic oscillations. They also observed high frequency oscillations above 1000 Hz, which are caused by the interaction between acoustic disturbance and flame evolution. Broda *et al.*, (1998) and Seo (2003) studied experimentally the combustion dynamics of a swirl stabilized combustor for a broad range of equivalence ratios. A significant difference in the overall flame structure was observed between stable and unstable combustion modes. The flame shape changes from a conical blue shape (steady state) to a deflected white flame with intense light emission (unstable state). Under unstable operating conditions, the inner recirculation zone is filled with flame, compared to stable combustion in which there is no flame within the inner recirculation zone.

Huang and Yang (2004) showed that in both stable and unstable flames, a central toroidal recirculation zone (CTRZ) is established at the centre of the combustion chamber under the effect of swirling flows. Vortex breakdown occurring within the CTRZ helps to stabilize the flame within this region, where the hot products are mixed with the incoming mixture of air and fuel. A corner recirculation zone (CRZ) is also formed downstream of the dump plane due to the sudden increase in area of cross section (Reddy *et al.*, 2006). Under stable operating conditions, the flame spreads from the corner of the centre body to the chamber wall. For unstable combustion, the flame is anchored by both the corner and the centre recirculation flows and forms a compact envelope. However in dump combustors, vortex shedding occurs instead of vortex breakdown, which causes instability.

Chakravarthy *et al.* (2007a and b) performed experiments in a confined backward-facing step and bluff body combustors by varying the operating conditions systematically. They observed that the vortex shedding and chamber acoustics do not lock when the pressure oscillations are characterized by low amplitude broadband oscillations. However, at the onset set of lock-on, these low amplitude oscillations are transformed to high amplitude tonal oscillations, which could be limit cycle oscillations. They concluded that after the onset of vortex-acoustic lock-on, the dominant frequency of the pressure fluctuations everywhere in the duct follow the pattern of the vortex shedding frequency. That is under the lock-on condition, the duct acoustic mode adjusts itself to match with the vortex-shedding behaviour with increasing Reynolds number. Further

Chakravarthy *et al.* (2007a) pointed out that in contrast to cold flow (for example, in the case of flow through an orifice in a duct) where the frequencies of oscillations are constant and the vortex shedding locks on to acoustics. However during combustion instability the acoustics locks on to vortex shedding and the frequency of oscillations are proportional to the mean flow velocity. The occurrences of instabilities in combustors arise from the interaction between pressure oscillations and heat release rate oscillations, which are nonlinear in general. Thus nonlinear analysis of the oscillations in the combustion chamber is essential to understand more about the combustion dynamics at different operating conditions.

2.3 Nonlinear flame dynamics

The nonlinear nature of the instabilities has been investigated through a series of experiments by different authors (Kim *et al.* 2011, Lieuwen 2002, Sterling 1993, Gotoda *et al.* 2011, Kabiraj *et al.* 2012c, Kabiraj and Sujith 2012a). Lieuwen (2002) presented time series data of chamber pressure oscillations in a gas turbine combustor using phase portraits. He observed that the transition from stable to an unstable operation occurs when the combustion processes nonlinearly interact with the chamber dynamics. He also showed that the instability frequency and pressure oscillations are proportional to the mean velocity of flow. Jahnke and Culick (1994) employed the numerical continuation method from dynamical system theory to study the nonlinear flow and flame dynamics in combustion systems, using numerical simulations. Sterling (1993) and Lieuwen (2002) characterized the measured pressure oscillations using methods such as time delay embedding method from dynamical system theory. Lieuwen (2002) concluded based on nonlinear time series analysis and statistical analysis that cycle to cycle variation of limit cycle oscillations in the combustor is due to the forcing of the system by background noise. He also observed that the inherent noise in a thermoacoustic system can strongly affect the limit cycles and under certain operating conditions may even be responsible for causing the combustor to become unstable under linearly stable conditions. Gotoda *et al.* (2011) experimentally investigated that the dynamic behaviour of the combustion instability undergoes a significant transition from stochastic fluctuation to periodic oscillation through low dimensional chaotic oscillations, as the equivalence ratio is varied. Nair *et al.* (2013b), Nair and Sujith (2014) and Nair (2014) shows that

a turbulent combustor undergoes a transition to high amplitude oscillations from low amplitude combustion noise during the reduction in equivalence ratio. They established this as a prior indicator of combustion instability. A thermoacoustic system can also undergo secondary bifurcations for a certain range of operating conditions.

2.4 Secondary bifurcations

Recent studies (Gotoda *et al.*, 2011, Kabiraj and Sujith 2012b, Kabiraj *et al.*, 2011) indicate that limit cycle is not the only possible final state. A thermoacoustic system can undergo further bifurcations and attain states such as quasi−periodic, period doubling, frequency locked, intermittent and chaotic states (Kabiraj*et al.*, 2011). Many combustors display intermittent oscillations under different operating conditions. The dynamical behaviour of pressure oscillations in a laboratory scale combustor was characterized using dynamical systems theory by Kabiraj *et al.* (2011). They investigated the features of nonlinear thermoacoustic oscillations using a simple setup, consisting of multiple flame configurations. They reported that as the bifurcation parameter (flame location) is varied, the system undergoes a series of bifurcations leading to characteristically different nonlinear oscillations such as periodic, aperiodic or chaotic oscillations. They pointed out that the thermoacoustic system undergoing limit cycle oscillations can undergo further bifurcations and attain states such as quasi-periodic, period doubling, frequency locking and chaotic states on further change of the flame location. They established route to chaos through quasi-periodic route, known as Ruelle-Takens scenario (Takens, 1985) and also a frequency locked oscillations (Kabiraj *et al.*, 2012c). Hong *et al.* (2005, 2008a, 2008b) investigated both numerically and experimentally the effect of fuel flow modulation due to pressure fluctuations in a swirl combustor. Flame characteristics with respect to equivalence ratio modulation up to blow out condition (1.0 to 0.42) were analysed experimentally using unchoked and choked fuel injection condition. The effect of unmixedness is investigated by changing the fuel injection location. They observed two representative instability modes in which mode 1 represents the "loud noise and vibration" for the choked flow condition and mode 2 shows the "alternate noisy and silent period" for an unchoked fuel flow condition. Arndt *et al.* (2010) observed similar behaviour in a premixed gas turbine model combustor during the transition between thermoacoustically stable and unstable states. They conducted OH* PLIF, OH*

chemiluminescence and stereoscopic PIV measurements simultaneously at a repetition rate of 5 kHz for a methane air mixture with a global equivalence ratio of 0.71. At this operating condition, the flame undergoes an unreliable transition from a state of self-excited thermoacoustic oscillations (noisy state) to a thermoacoustically stable burning state (quiet state).

This type of irregular switching of oscillations of the system between quiet and noisy regions under certain operating conditions is referred to as the intermittency in dynamical system theory (Kabiraj *et al.*, 2012a, Kabiraj and Sujith 2012a, Strogatz 2000, Klimaszewska and Zbrowski 2009, Kabiraj and Sujith 2012b). Such type of system behaviour was previously observed in thermoacoustic systems by different authors (Hong *et al.*, 2008a and b, Arndt *et al.*, 2010), although they did not explicitly refer to it as intermittency. Kabiraj *et al.* (2012c) recently established the occurrence of intermittency in a thermoacoustic system and observed a secondary bifurcation in a ducted premixed flame. They observed that the system undergoes limit cycle oscillations due to subcritical Hopf bifurcation for a particular flame location. For further variation of the flame location, the system exhibits quasi-periodic oscillations due to secondary Hopf bifurcation (Kabiraj *et al.* 2012c). When the flame location was further varied, irregular bursts referred to as intermittency in dynamical system theory was observed in the system. Using recurrence plots (Kabiraj *et al.*, 2012b, Kabiraj and Sujith 2012c) they established that these are an example of type-II intermittency that occurs in systems with secondary Hopf bifurcation. Recently by performing experiment in a turbulent combustor, Nair *et al.* (2014a) showed the presence of an intermittent periodic oscillations prior to the occurrence of combustion instability. Using this observation they developed a method for early detection of the onset of instabilities in a bluff body stabilized combustor. Different nonlinear characteristics due to successive bifurcation was observed by Kabiraj *et al.* (2015) in an imperfectly premixed model combustor. They pointed out that the system shows Ruelle-Takens scenario during its transition to low dimensional deterministic chaos from instability oscillations.

Combustion dynamics is dominated by complex dynamic processes involving a significant level of determinism when operating under the fuel lean condition. Presently, thermoacoustic systems are associated with limit cycle oscillations. Recently both experimental and computational studies indicated that a thermoacoustic system can undergo secondary bifurcation such as frequency locked, quasi-periodic, period doubling,

intermittent and chaotic states. However, these characteristics were investigated in laminar burners. Practical combustors are inherently noisy. They are often characterized by swirling turbulent flows and turbulent combustion. They display intermittent oscillations under a range of operating conditions. No studies have been performed to understand such intermittent oscillations. Therefore it is of great importance to apply the tools of dynamical systems theory to characterize the occurrence of intermittency in industrial combustors.

In the present study, the nonlinear behaviour of the combustion instability due to the nonlinear interaction between unsteady combustion and the chamber acoustic field in a lean premixed swirl stabilized combustor has been experimentally investigated by focusing on how the dynamic properties of the pressure fluctuations change with flow Reynolds number. The features of combustor pressure oscillations under stable and unstable operating conditions and the manner in which the combustor transitions from stable to unstable are determined using nonlinear time series analysis. Nair *et al.* (2013b) studied the flame behaviour prior to the transition from stable state to an unstable state. They developed a system, which helped the operators to detect the instabilities prior to its occurrence.

2.5 Detection and control of instability.

2.5.1 Conventional methods.

Controlling or avoiding and detecting the onset of these oscillatory instabilities are very much important and challenging. Various conventional techniques are proposed by researchers to control oscillatory instabilities in combustors and similar devices.

In one of the methods, instabilities are controlled by controlling the pressure in the fuel line using a delay feedback controller. This technique is partially successful in controlling instabilities in combustors as it requires external actuators, modification of combustor configuration and knowledge of frequency response of arbitrary input. This method fails to prevent instability, however it can control instability after its occurrence (Nair *et al.*, 2012).

In another conventional technique, the stability of the combustor is determined

based on the bandwidth of the vibrations of the combustor casing and the dynamic pressure measurements inside the combustor chamber. As and when the combustor approaches stability limit, the bandwidth decreases towards zero in the absence of noise. Presence of noise in the combustion chamber makes this technique inefficient (Nair *et al.*, 2012).

In yet another technique, the stability margin of the combustion chamber is determined by using exhaust flow and fuel injection rate modulation. However this technique is restricted by the need of acoustic drivers and pulsed fuel injectors. Furthermore, in another conventional technique, the instability of the combustor is tracked by a detector when the damping reduces to zero. The damping of the combustor is characterized by the autocorrelation of the acquired signal. However in this technique also the combustor should reach instability for the detector to work (Nair *et al.* 2012).

Further the combustor designers can incorporate sufficient stability margin in the design of the combustor to avoid combustion instabilities. However this leads to increased levels of NO_x emissions making it more difficult to meet the demanding emission norms.

These techniques require either incorporation of certain design features in the device or the incorporation of sensors or similar detectors that could detect and control the instability. However this process identifies the instabilities after its occurrence. Hence, there exists a need for a system and a method that could predetermine the instability and control various parameters of the device accordingly to control the instability and thus improve the stability margin.

2.5.2 Mathematical methods

Maximal Lyapunov exponent, λ

Usually the chaotic behaviour of a dynamical system whose equations are known is verified by calculating the maximal lyapunov exponent [MLE], λ (Gottwald and Melbourne 2004, Zachilas and Psarianos 2012). The value of $\lambda > 0$ indicates the trajectory deviate exponentially and $\lambda \leq 0$ indicates that the nearby trajectories remain in a close neighbourhood of each other. For experimental data, the value of λ can be obtained

by Takens phase space reconstruction method (Takens, 1985). However quite a lot of computing time is required for calculating the maximal lyapunov exponent.

Burst test for detecting instability

Method for determining the oscillatory instabilities in practical devices, before the occurrence of instabilities is essential to increase its life span and efficiencies. The burst test is one of the methods to detect the onset of oscillatory instabilities in devices where the transition from chaotic or noisy behaviour to oscillatory instability through intermittent bursts. By examining the intermittent bursting behaviour we can diagnose onset of instabilities very early (Nair *et al.*, 2013a).

Bursts which refer to a sudden spike in the amplitude of measured signal, leads to an intermittent switching behaviour of the signal between low and high amplitudes. The occurrence of such bursts is seen in high Reynolds number flow devices, where happens the transition from chaotic behaviour to oscillatory instabilities.

Peak method for detecting instability.

In this method the onset of combustion instability is identified by counting the number of peaks in the acquired signal above a defined threshold. The threshold value is fixed by the user and is corresponding to the stable operating regime. The combustor undergoes instability when the number of peaks in the acquired signal moving above the already fixed threshold value by the user. Then by taking required measures the user can avoid the occurrence of instability (Nair *et al.* 2014).

0-1 test

Usually the 0-1 test proposed by Gottwald and Melbourne (2004) is used for identifying chaos in a signal. Since the instabilities in turbulent combustor occurs from chaotic oscillations, combustion noise in literature, the prior information regarding the occurrence of combustion instability can also be determined using a 0-1 test. Using an algorithm based on 0-1 test, we can compute the time series data acquired from a system during different operating condition. An output value of 1 indicates chaotic oscillations and

0 indicates instability oscillations and the output value between 1 and 0 indicate the transition between chaotic oscillations to combustion instability. Thus, by looking at the output value of this mathematical method we can determined how close a system is towards impending instability.

Another major drawback in a premixed combustor is the blowout phenomenon.

2.6 Blowout phenomenon

At very lean condition (preferred to reduce pollution emissions) the combustor undergoes blowout. The early detection of an impending blowout is of utmost importance in practical combustors. Various researchers studied the dynamics near blowout. Stohr *et al.* (2011) observed local extinction and reignition prior to blowout in a swirl stabilized combustor. A fluid mechanic stretch, which cause a local flame extinction near blowout in a bluff body combustor is reported by Nair and Lieuewen (2007). They interpreted this local flame extinction as local hole in the flame. They observed that the occurrence of these holes and its reclosing happens prior to blow-off. This kind of extinction and reignition of flame prior to blowout is also observed by Muruganandam and Seitzman (2012). They performed an experiment with the flow seeded with olive oil droplets and identified the local extinction/local hole (disappearance) and reigniting/reclosing (appearance). The packets of unburned olive oil droplets indicate the local extinction zone. They keep away the system from the blowout by increasing the mixture ratio at the inlet of the combustor when the system approaches blowout. Muruganandam *et al.* (2005) also reported that aperiodic oscillations occur frequently in the combustor during its approach to lean blowout. They brought the system to safe margin of operational limit by developing an active control system near lean blowout. Low frequency combustion oscillations are also observed near lean blowout by Yi and Gutmark (2007) in multi swirl gas turbine combustor. They identified the lean blowout by mapping the indices, specifically, the normalized chemiluminescence RMS and the normalized cumulative duration of lean blowout precursor events. Bompelly *et al.* (2009) studied the lean blowout margin by using an event identification algorithm. They combine the event occurrence rate, the event duration and the strength of an event using a single parameter called Stability Index (SI). The dynamic range of stability index is higher at stable operating conditions

due to the high event occurring rate. Mukhopadhyay *et al.* (2013) predicted the lean blowout in gas turbine combustors using symbolic time series analysis. In this, a set of time series data is converted into a finite number of cells and assigned a symbol for each cell. They computed a state probability vector based on the number of occurrence of each symbol within a given time span, by keeping the condition sufficiently away from the lean blowout as the reference state. They detect the proximity of the lean blowout by using a parameter called anomaly measure, which is the measure of the deviation of the current state vector from the reference state. Significant change in the anomaly measure indicates the system approach to blowout. Gotoda *et al.* (2014) observed an intermittent burst oscillations during the transition to low dimensional chaos from an apparently periodic oscillations.

2.7 Motivation and goals

Industrial combustor uses swirl type burners and are almost entirely closed. The internal processes tending to attenuate combustion instability are weak. A small fraction of the heat released by combustion is sufficient enough to drive combustion instability. Thus, swirl combustor is more prone to combustion instability during fuel lean operating condition, where small perturbation in equivalence ratio (ϕ) produce large fluctuation in heat release. When these heat release fluctuation is in phase with chamber acoustic field, it results in large amplitude oscillations. In a swirl combustor due to enhanced mixing, the flame is short compared to acoustic wave length and is situated near the dump plane i.e. at the acoustic node of the combustor. Such an acoustically compact configuration is efficient in facilitating the interaction between oscillatory heat release, acoustic field and the unsteady flow making the combustor more prone to instability. Thus the stable combustion may become unstable during a small change in operating parameter. Also, once the system has become unstable, it is difficult to regain stability. At lean condition the combustor undergoes blowout. This phenomenon limits the operational range of the industrial combustor.

These observations motivated us to focus on understanding the intermittent oscillations prior to instability and blowout situation. Thus we can suggest to incorporate certain measures to avoid the unwanted oscillations and blowout situation, which in-

creases the operational margin of the turbulent swirl combustor.

2.8 Outstanding questions

Using the tools from the dynamical system theory the thermoacoustic instability and route to chaos is established in a laboratory scale combustor. However industrial combustor is characterized by swirling turbulent flows and turbulent combustion. Therefore it is of great importance to use these tools in practical combustor. In reality, practical combustor is noisy. However the characteristics of noise and its effect on the combustion process is not clear. Analyses of the effect of noise on both linear and nonlinear stability boundaries of a thermoacoustic system is very much essential. How is the flame behaviour at the onset of instability? What is the nature of bifurcation and what determines its criticality? Occurrences of secondary bifurcation is observed in laminar burners. However the industrial burners involve turbulent combustion hence it is of great importance to investigate the secondary bifurcation and the flame response during secondary bifurcation. Further it is of great importance to characterize the intermittent oscillations observed in many of the industrial combustor under a range of operating conditions.

2.9 Objectives of the present work

Using dynamical system theory, thermoacoustic instabilities and route to chaos is established in simple lab model combustor that are having laminar flows. However, industrial combustors are characterized by swirling turbulent flows and turbulent combustion. Therefore, it is necessary to analyse the characteristics of such type of practical combustor at different operating conditions using the tools from dynamical systems theory. The objective of the present work is to understand the combustor dynamics prior to thermoacoustic instabilities and blowout condition. The specific objectives are

(i) Understanding the nonlinear behaviour of the swirl stabilized combustor at different operating conditions - Limit cycle and irregular burst oscillations.

(ii) Establish a system to detect the onset of thermoacoustic instability and thereby

improving the stability margin for a partially premixed swirl stabilized combustor.

(iii) Understanding the signature prior to a blowout in a turbulent combustor.

2.10 Overview of the thesis

This thesis work is based on the application of nonlinear time series analysis to an experimentally acquired pressure data from a premixed swirl stabilized combustor. Nonlinear behaviour of the combustor at different operating conditions was analysed using this technique. Significant contributions related to this work by different researchers were established in Chapter 2. Experimental setup and instrumentation for measuring data are discussed in Chapter 3. Experimental investigation of the nonlinear behaviour of the swirl stabilized combustor at the various operating condition is discussed in Chapter 4. Nonlinear time series techniques applied for the analysis of the acquired data are described in Chapter 5. The technique for detecting the onset of instabilities and its control are explained in chapter 6. The onset of a blowout is explained in chapter 7. Chemiluminescence images corresponding to the different operating condition is explained in chapter 8. The conclusion from the study is listed in Chapter 9.

CHAPTER 3

EXPERIMENTAL SETUP AND MEASUREMENTS

In this chapter, we describe the experimental setup and the instrumentation used to acquire the data required for the analysis of the combustion dynamics of a swirl stabilized combustor. Swirler provides an inner and outer recirculation zones, where the unburned fuel-air mixture thoroughly mixed with hot combustion products. The flame is stabilized in this region.

3.1 Experimental setup

A schematic representation of a swirl stabilized burner with an axial swirl generator mounted on a central bluff body is used for the study as shown in Fig.3.1. The central body is positioned in such a way that the edge of the centre body and the dump plane are in the same vertical plane. The experimental set up consists of an inlet (including plenum chamber), burner with a swirler mounted on a tube, housed near to the dump plane inside a burner of 40 mm diameter and a combustion chamber with extension ducts. The combustion chamber including the extension ducts has a length of 700 mm and a cross-section of 90mm x 90 mm. The length of the combustion chamber can be increased by adding extension chambers of same cross-section with required length. However the length up to the upstream of the dump plane is held constant. Provisions for two transparent windows with quartz glasses of size 150 mm x 99 mm are made in the combustion chamber for optical diagnostics. A spark plug, which is mounted at the dump plane with 11kV step-up transformer is used for ignition. The Liquefied petroleum gas (LPG), which has components of 60 % butane (C_4H_{10}) and 40 % propane (C_3H_8) by volume was used as the fuel. By maintaining constant fuel flow rate ($\dot{m}_f$), the air flow rate ($\dot{m}_a$) increases gradually for getting a progressive increase in Reynolds number with an uncertainty of 4.7 % (or decrease in equivalence ratio, ϕ). The Reynolds number of the flow was computed using the expression $Re = 4\dot{m}D_1/(\pi\mu D^2)$, where $\dot{m}$ is the mass of fuel-air mixture, D_1 is the diameter of the swirler, D is the diameter

of the burner and μ is the dynamic viscosity of the fuel-air mixture at the operating condition. The method explained in Wilke (1950) is used for correcting the Reynolds number due to the change in viscosity for the varying fuel-air ratios. The fuel (LPG) is injected through four holes of 2 mm diameter, provided radially on the circumference of a 10 mm diameter pipe. Compressed air from the compressor, after passing through the demoisturizer is introduced at the inlet of the plenum chamber through a 25 mm diameter hose. The fuel injected 100 mm upstream of the swirler mixes with the air, forming a reactive mixture which enters the combustor through the swirler. The swirler, which has 8 blades positioned at an angle of 40^0 relative to the incoming air stream, enhances the mixing between the cold reactants and hot combustion products, enabling flame anchoring at high speeds, resulting in flame compactness. The mixture reacts at the swirl stabilized combustion zone in the combustor downstream of the swirler and the hot combustion products exit the combustor through the exhaust section. A traverse mechanism is provided for positioning the swirler at different locations within the burner with a least measure of 1mm as shown in Fig.3.2.

3.2 Instrumentation for measurements

The mass flow rates of fuel and air are measured by mass flow controllers (Alicat Scientific, MCR Series) with an uncertainty of $\pm$ (0.8 % of reading + 0.2 % of full scale). The experiments were performed by continuously varying the air flow rate from 9.9 g/s to 27.7 g/s, maintaining a constant fuel flow rate of 1.1 g/s. Thus equivalence ratio was varied from 0.92 to 0.33 with an uncertainty of 2.4 %).

Unsteady pressure fluctuations are measured using piezoelectric (PCB106B50) transducers (72.5 mV/kPa, 0.48 Pa resolution and ± 0.64 % uncertainty), mounted on the pressure ports, which are 40 mm apart from each other, provided on the walls of the combustion chamber. The signals from the pressure transducers are acquired simultaneously through a 16-bit analog to digital conversion card (NI-6143) with a resolution of $\pm 0.15mV$ and an input voltage range of $\pm 5V$ at a sampling frequency of 10 kHz, over a sampling interval of 10 seconds.

High speed digital images of the CH* chemiluminescence were acquired simultaneously at a recording speed of 1000 fps using a Phantom V12.1 high speed camera with

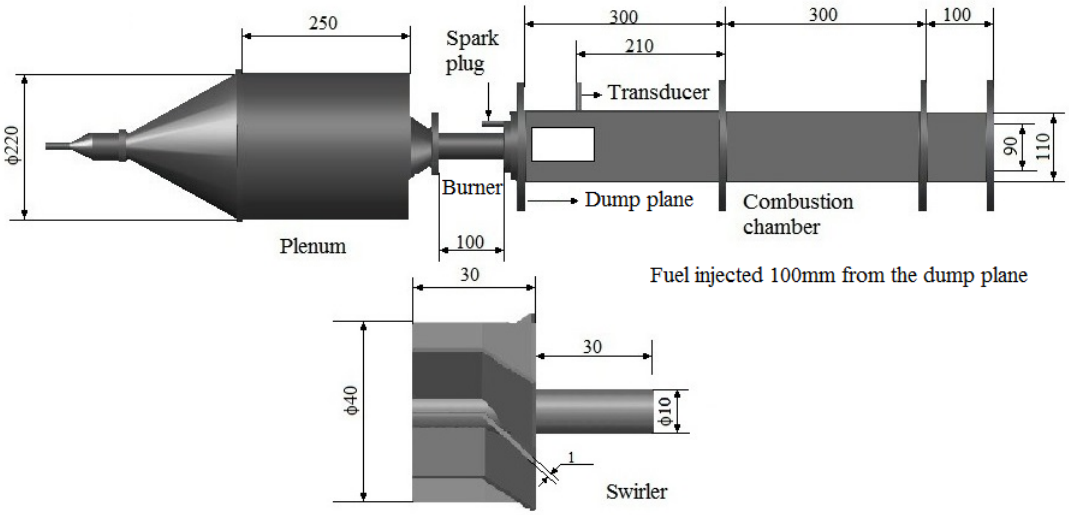

Figure 3.1: Schematic of the swirl stabilized burner experimental setup showing the position of the fuel injection point, the swirler and the pressure transducers used for pressure measurements. The length of the combustion chamber used for analysis is 700 mm which includes three extension chambers, two of length 300 mm and one of length 100 mm. The fabrication of the combustor was based on the design adapted from Komarek and Polifke (2010).

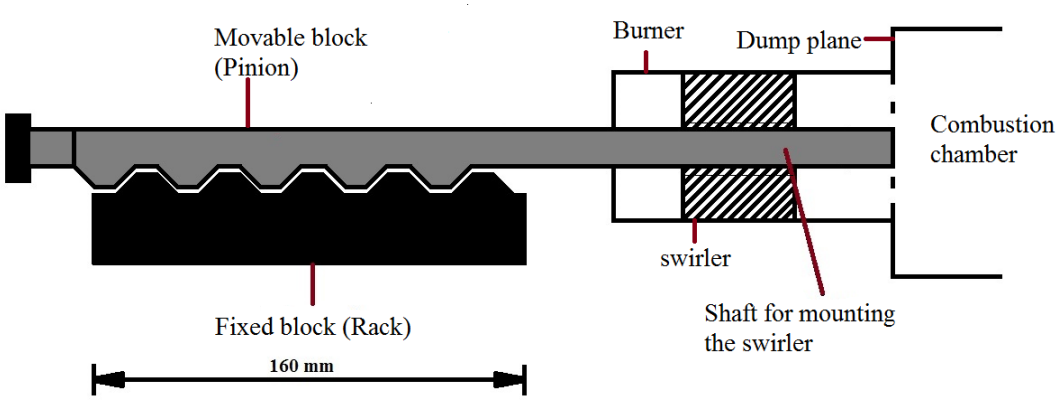

Figure 3.2: Schematic of the Rack and pinion arrangement used for mounting the swirler.

CH* filter (transmission peaks around a wave length of 431 nm and bandwidth of 10 nm) at a resolution of 1280×800 pixels.

The exponential decay rates of the acoustics of the combustion chamber were measured multiple times in cold condition prior to the experiments to ensure that the ambient condition did not change between the experiments. Decay rates were measured at the start of the experiments by exciting the system for a small time interval and then switching off the acoustic driver. The system decays according to the decay rate, which was found to be $32s^{-1}$ at a frequency of 133 Hz, corresponding to the fundamental frequency of the cold system. Repeatability of the experiments was ensured by ensuring that the determined acoustic damping (damping rate/decay rate) of the system are within $\pm 10\%$ of $32s^{-1}$. Time series data of pressure fluctuations were acquired at different operating conditions from the combustor using pressure transducers at different positions. The results presented in this thesis correspond to the pressure signals acquired using pressure transducer at a distance of 90 mm from the dump plane; data from other transducers reveal the same findings.

CHAPTER 4

SELF-EXCITED OSCILLATIONS IN A SWIRL STABILIZED PARTIALLY PREMIXED LABORATORY COMBUSTOR: LIMIT CYCLE AND INTERMITTENCY

Experiments were performed by continuously varying the air flow rate from 9.9 g/s (stable combustion, ϕ = 0.92) to 27.7 g/s (blow off, ϕ = 0.33), maintaining a fuel flow rate of 1.1 g/s. We provide a 10s settling time for the experimental setup to reach the equilibrium condition. The following characteristics are observed.

4.1 Dominant frequency and pressure amplitude variations

The time series data of pressure oscillations were acquired using a pressure transducer, mounted near the dump plane, for every operating conditions and plot the spectrum of oscillations using Fast Fourier Transform (FFT) with a bin size of 0.33Hz. Figure 4.1a shows the variation of dominant frequency (frequency corresponding to the peak pressure amplitude in the FFT) of oscillations and peak pressure (peak of the FFT) at different operating conditions with respect to flow Reynolds number, keeping the mass flow rate of fuel ($\dot{m}_f$) constant. The flow Reynolds number is defined as Re = $\rho v d/\mu$, where ρ is the mixture (fuel and air) density, v is the bulk flow velocity with respect to the burner diameter, d is the burner diameter and μ is the viscosity of the mixture at atmospheric condition. The Reynolds number has an uncertainty of 4.7 %. However Fig. 4.1b represents the fluctuations of amplitudes of pressure oscillations (peak of the FFT) near the dump plane with Reynolds number (Re) for the same mass flow rate of fuel. In Fig. 4.1a, a gradual increase of the dominant frequency of oscillations are observed within the range of Reynolds numbers of air flow from 1.8×10^4 to 2.6×10^4.

Further, between Reynolds numbers 2.1×10^4 and 2.6×10^4, the dominant frequency of oscillations (Fig. 4.1a) and pressure amplitudes (Fig. 4.1b) increases almost linearly with mean velocity of flow (or Reynolds number) and undergoes limit cycle oscillations.

This increase in frequency with Reynolds numbers exists till a Reynolds number of 2.6×10^4. Chakravarthy et al. (2007a and b) and Lieuwen (2002) reported that this kind of increase in frequency with Reynolds number is due to the existence of hydrodynamic instabilities. The amplitude of limit cycle oscillations attain a maximum value of approximately 1900 Pa for further increase of Reynolds number up to 3×10^4 (Fig. 4.1b). However in the Reynolds number range between 2.6×10^4 and 3×10^4 the acoustic oscillations are dominant. That is the acoustic time scale is greater than the hydrodynamic time scale. Thus in this region the dominant frequency is constant. In the subsequent region, the frequency of oscillations increases further followed by sudden shift to a lower frequency. Further, at higher Reynolds numbers, the frequency of oscillations increases with increasing Reynolds number. These types of transitions are presented by Chakravarthy *et al.* (2007a) in a bluff body combustor, wherein the acoustic oscillations "lock-on" to the vortex shedding frequency for a certain range of Reynolds number. At around a Reynolds number of 3.5×10^4 the acoustic mode shift to the vortex shedding frequency.

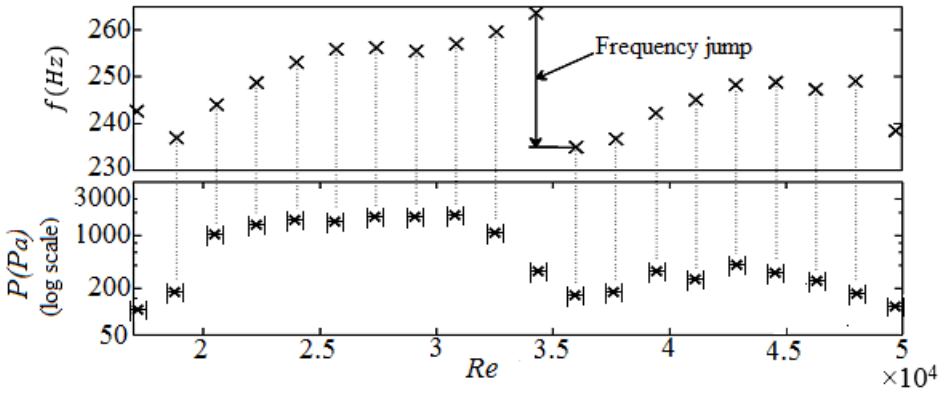

Figure 4.1: Shows the variation of frequency of oscillations and pressure amplitude (Peak of FFT in log scale) with flow Reynolds numbers for continuously varying air flow rates from 9.9 g/s to 27.7 g/s (up to blowout) with constant fuel flow rate of 1.1 g/s. The fundamental frequency of the combustor = 250Hz.

The sudden drop followed by an increasing trend in the dominant frequency of oscillations for higher Reynolds numbers were observed in Fig. 4.1a. However, during

this region a rise and fall in amplitude of pressure oscillations was observed, indicating yet another possible transition regime (Fig. 4.1b).

4.2 Transition from low amplitude oscillations to limit cycle oscillations

The combustor undergoes low amplitude noisy oscillations for a Reynolds number of 1.8×10^4 (mass flow rate of air 9.9 g/s) and for a constant fuel flow rate (1.1 g/s). These low amplitude noisy oscillations transitioned to high amplitude discrete tonal oscillations as and when the flow Reynolds number increases further. The corresponding FFT are shown in Fig. 4.2.

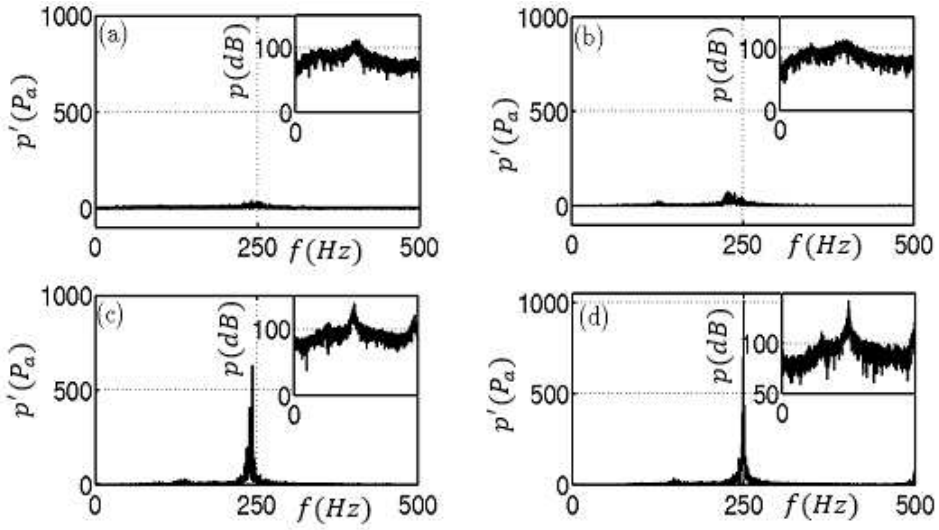

Figure 4.2: Represents FFTs corresponding to the transition from low amplitude noisy oscillations to limit cycle oscillations. Fig. 4.2a corresponds to a flow Reynolds number of 1.8×10^4 and mass flow rate of air 9.9 g/s. Fig. 4.2b corresponds to a flow Reynolds number of 1.9×10^4 and air mass flow rate of 10.9 g/s. Fig. 4.2c corresponds to a flow Reynolds of 2.1×10^4 and air mass flow rate of 11.9 g/s. Figure 4.2d corresponds to a flow Reynolds number of 2.3×10^4 and air mass flow rate of 12.8 g/s. Fuel flow rate is maintained constant at 1.1 g/s.

Figure 4.2a represents the FFT for a Reynolds number of 1.8×10^4 (air flow rate 9.9 g/s) with an equivalence ratio ϕ = 0.92. The amplitude of pressure oscillations

are much smaller (below 500 Pa) compared to the amplitude of limit cycle oscillations (approximately 1900 Pa). These relatively low amplitude noisy oscillations signify combustion noise (Nair *et al.* 2013a). A broadband spectrum due to turbulence with one superimposed peak corresponding to the duct resonance is observed in the FFT (Fig. 4.2a, shown in dB scale at inset).

During the transition from low amplitude combustion noise to high amplitude oscillations, the noisy oscillations are amplified by the combustion process as shown in Figures 4-2(b-d). Notice the narrowing of the peak in Figures 4.2b and 4.2c eventually leading to a sharp peak as shown in Fig. 4.2d. For stable operating condition, these broadband peaks are at lower amplitude and remains in these narrow range of amplitude values. As the Reynolds number reaches 2.6×10^4 (corresponding to an air flow rate of 14.8 g/s, $\phi = 0.62$), the low amplitude broadband combustion noise at low inlet air flow rates becomes transformed to discrete high amplitude tonal oscillations.

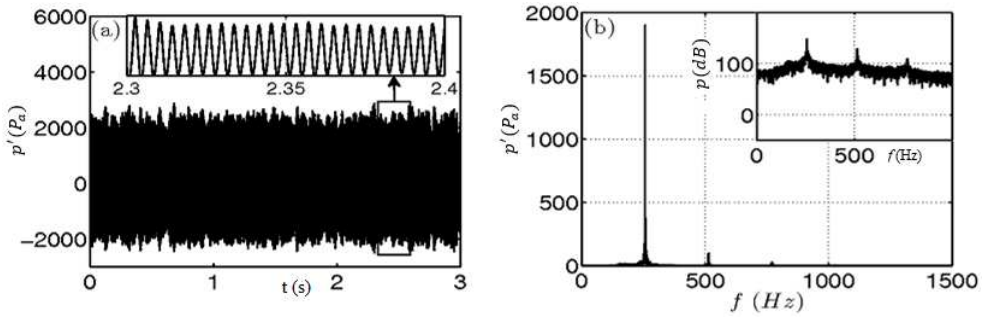

Figure 4.3: Represents the time trace of pressure signal and the corresponding FFT for limit cycle oscillations. The Reynolds number of flow is 2.6×10^4. Mass flow rate of air is 14.8 g/s and fuel is 1.1g/s. Equivalence ratio, $\phi = 0.62$.

These high amplitude tonal oscillations with a dominant frequency are usually referred to as limit cycle oscillations (Lieuwen 2002). The time trace of pressure signal corresponding to limit cycle oscillations are as shown in Fig 4.3a. Figure 4.3b represents the FFT corresponding to such a limit cycle oscillations. Between a Reynolds number of 2.1×10^4 and 3×10^4 the combustor undergoes limit cycle oscillation. In this region, flow-acoustic lock-on may occur similar to the scenario reported by Chakravarthy *et al.* (2007b) in a non-premixed half-dump combustor for a wide range of operating conditions. They concluded that the excitation of high amplitude discrete tone oscilla-

tions from low amplitude noisy oscillations is due to flow-acoustic lock-on. Two low amplitude harmonics are also seen in Fig. 4.3b. These low amplitude harmonics of the instability mode of the combustor were excited possibly because of system nonlinearity. This result is consistent with Lieuwen (2002), who pointed out that the low amplitude harmonics of the acoustic mode of the combustor are excited by system nonlinearity.

4.3 Transition from limit cycle oscillations to irregular burst oscillations

After attaining the limit cycle oscillations, a frequency shift from 265Hz to 235Hz (Reynolds number between 3.3×10^4 and 3.9×10^4) followed by a further increase in frequency is observed for further increase in Reynolds number as shown in Fig. 4.1a. At a Reynolds number of about 3.9×10^4 (21.7 g/s air flow rate, $\phi = 0.42$), the pressure signal consists of loud and quiet zones as shown in Fig. 4.4. The periodic motion is interrupted by occasional irregular bursts and the behavior of the system switches back and forth between the loud (periodic) and quiet (aperiodic) zone. Such a behaviour in a gas turbine combustor was reported by Hong *et al.* (2005, 2008 a, 2008b) and Arndt *et al.* (2010). The fluctuations are apparently periodic for a particular time intervals and are called laminar phases (Pomeau and Manneville 1980), indicating periodic behaviour. The corresponding time traces (short interval) of pressure signal is shown at the inset. The quiet phase, which is shown at the inset is similar to the time series during the occurrence of combustion noise. These quiet phases are randomly and abruptly disturbed by a burst oscillations that have a finite duration.

We can identify the burst oscillations by the amplitude of the acoustic field while running the combustor. Finally a decrease in frequency just before blowout accompanied by a decrease in pressure amplitude is observed. These transitions of combustor dynamics for different operating conditions can also be analysed by plotting the bifurcation diagram.

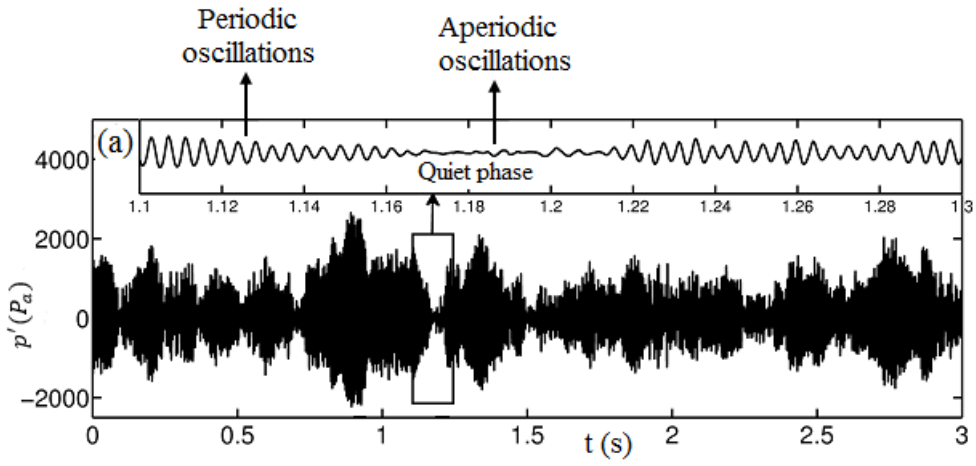

Figure 4.4: Time trace pressure signal corresponding to noisy and quiet phase with time trace of pressure signals at the inset for the flow Reynolds number of 3.9×10^4. Mass flow rate of air is 21.7 g/s and fuel flow rate maintained at 1.1 g/s. Equivalence ratio $\phi = 0.42$.

4.4 Bifurcation diagram

In nonlinear dynamics, the term bifurcation refers to a sudden qualitative change in the behaviour of dynamical system when some control parameter is varied by a small amount [Kabiraj *et al.*, 2011, Kabiraj and Sujith 2012a). Figure 4.5 represents the bifurcation diagram plotted with the peak pressure amplitude as the measure and the flow Reynolds numbers when the Reynolds number of the flow is varied. The amplitude of the pressure oscillations is relatively small and almost constant initially for a very small range of Reynolds numbers which represent stable combustion. For further increase in Reynolds numbers, the amplitude of the pressure oscillations increases from low amplitude noisy oscillations to limit cycle oscillations. These increasing trends in the amplitude of pressure oscillations followed by high amplitude oscillations (noisy limit cycle oscillations) are as shown in the bifurcation diagram (Fig. 4.5).

Complex combustion dynamics such as the occurrence of irregular pressure oscillations was observed at Reynolds numbers higher than 3.3×10^4.

From the bifurcation diagram, it is observed that, when the Reynolds number of flow increases, the combustor goes through three different regions: (1) low amplitude oscil-

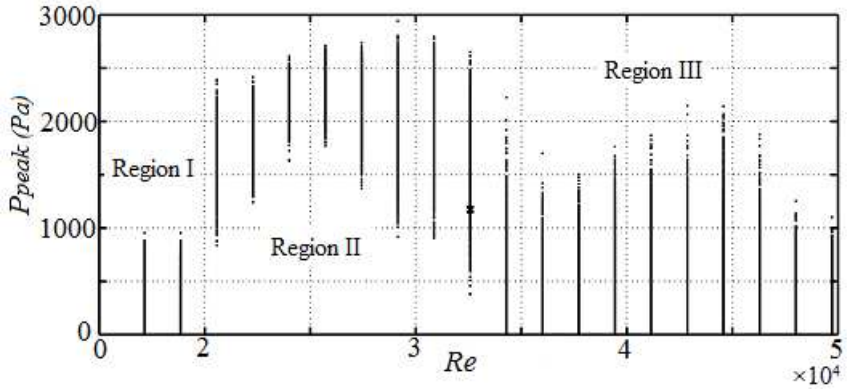

Figure 4.5: Represents the bifurcation diagram of pressure peaks acquired from a transducer near the dump plane with flow Reynolds numbers corresponding to low amplitude noisy oscillations to the blowout point. The flow Reynolds number varies from 1.8×10^4 to 4.9×10^4. The mass flow rate of air is varied from 9.9 g/s to 27.7 g/s. Mass flow rate of fuel is maintained constant at 1.1 g/s.

lations, (2) limit cycle oscillations and (3) pressure oscillations with irregular increase and decrease of the amplitude of oscillations. The low amplitude and the limit cycle oscillations have been reported by various authors in different combustors (Lieuwen 2002, Nair *et al.* 2013a, and Hong *et al.* 2005). However, the bifurcation from limit cycle oscillations to irregular pressure oscillations is a complex phenomenon that needs further examination.

The power spectral analysis of the acquired pressure data provides only a limited understanding towards interpreting the complex combustor dynamics at various operating conditions. To extract more information about the inherent nonlinearity associated with the combustion dynamics, we perform nonlinear time series analysis (Abarbanel 1996), which is discussed in the Chapter 5.

4.5 Interim conclusion

This chapter describes the experimental investigation of the occurrence of self-excited oscillations in a swirl stabilized partially premixed combustor operating at different air flow rates by maintaining constant fuel flow rates. Qualitatively different combustion

dynamics were revealed from the acquired time trace of pressure data. Transition from low amplitude noisy oscillations (combustion noise) to high amplitude limit cycle oscillations is observed by increasing the air flow Reynolds number or decreasing the global equivalence ratios. Lowering the equivalence ratio further, irregular bursts were formed.

CHAPTER 5

NONLINEAR DYNAMICS USED FOR THE ANALYSIS

5.1 Dynamical systems Theory

A swirl stabilized combustor undergoes complex combustion dynamics on decreasing the equivalence ratio up to blowout. The analysis of pressure fluctuations acquired during these operating conditions help us to understand this complex combustion dynamics. Low amplitude oscillations, called combustion noise (Nair and Sujith 2013) at high equivalence ratio (≈ 1) transmitted to irregular burst oscillations through limit cycle oscillations when the equivalence ratio reached to a very low value (≈ 0.33).

A systematic and efficient investigation to both the linear (Trefethen and Embree 2005) and nonlinear behaviour of the system (Burnley 1996) can be performed using tools from dynamical systems' theory. Dynamical system's approach aims to model the time evolving dynamics of physical systems.

Jahnke and Culick (1993) discussed the conditions under which stable limit cycles of a linearly unstable system may exist, and conditions under which bifurcation of the limit cycle may occur. Although Culick and co-authors have applied some of the concepts from dynamical system theory such as continuation methods (Burnley 1996, Ananthkrishnan *et al.* 2005), till recently thermoacoustic instability has not been posed in the framework of dynamical systems theory. However in recent years Sujith and co-workers, a group from IIT Madras, has posed the combustion instability problem in the framework of dynamical systems theory (Subramanian 2011, Kabiraj *et al.*, 2012a, Subramanian *et al.*, 2010, Balasubramanian and Sujith 2008, Kabiraj 2012b, Kabiraj *et al.*, 2012c, Kabiraj *et al.*, 2010, Kabiraj and Sujith 2011).

Complex thermoacoustic oscillations have been reported in the literature by a few authors. Using numerical continuation analysis of solid rocket motors Jahnke and

Culick (1993) have reported the possibility of quasi-periodic thermoacoustic oscillations. Sterling (1993) and later Lei and Turan (2009) have reported chaotic oscillations in a premixed combustor through numerical bifurcation analysis. Chaotic dynamics of heat release rate oscillations in a lean premixed gas turbine was reported by Fichera *et al.* (2001).

Nonlinear thermoacoustic oscillations in a simple ducted laminar premixed flame were investigated experimentally by Kabiraj *et al.* (2010) and Kabiraj and Sujith (2011) using bifurcation analysis. They reported that the system undergoes bifurcation leading to characteristically different nonlinear oscillations. Application of nonlinear time series analysis on pressure and CH* chemiluminescence (time trace flame intensity) characterises these oscillations as periodic, aperiodic or chaotic oscillations. However dynamical system theory helps to explain the nature of the obtained bifurcation. A thermoacoustic system can undergo bifurcations to states other than limit cycle oscillations and can attain the states such as quasi-periodic, period doubling, frequency locked and chaotic states which are observed in both experiments and computations.

5.2 Terms used in Nonlinear Dynamics

A brief review of the terms used in nonlinear dynamics theory (Lauterborn, 1996) is presented in this section.

5.2.1 State Space

The state of a dynamical system is geometrically as a point in a space, called state space or phase space, extend across all the dependent variables of the system. The variables are represented by $x_1, x_2...., x_n$. The initial state, at time t_0 is marked as x_0. The dynamic evolution; i.e., the change of the system with time, represented by a curve in the state space of the system called trajectory or orbit as shown Fig.5.1. The time is a parameter used for connecting the points in the state space trajectory as shown in Fig.5.1 by the two times t_1 and t_2. The system is characterized by the values of the variable corresponding to these times.

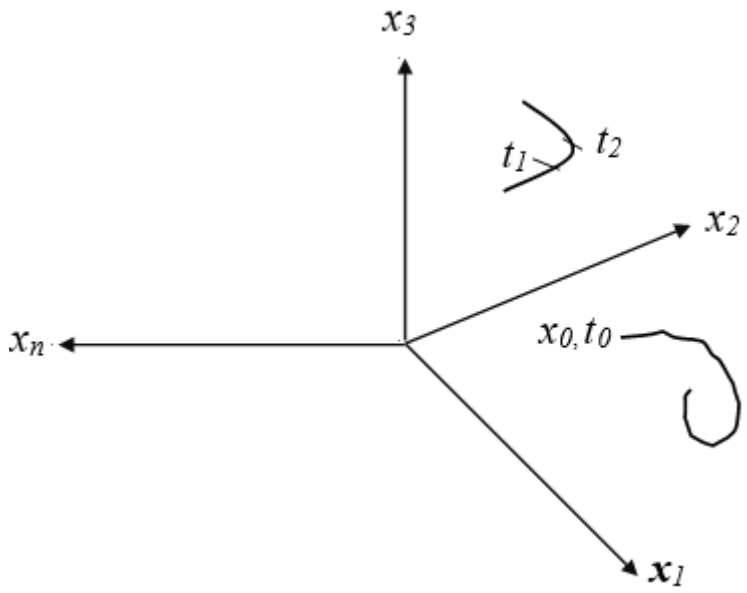

Figure 5.1: Schematic representation of state space and trajectory (Lauterborn 1996).

5.2.2 Attractor

As and when the time move on, the whole volume at initial condition remains constant for initial condition for conservative systems. However volume diminish for dissipative systems. The diminishing rate depends on the physical system as does the final volume (limit set) and its form. If the system consist of only one limit set, then it is called an attractor. However if the physical system has several attractors and each attractor attain its own set of initial condition in the course of time, then the set being called its basin (Lauterborn 1996).

Types of attractor

Fixed point: A single constant state in state space. It is a state of equilibrium or state of rest without any change and is zero dimensional.

Limit cycle: A closed trajectory in state space that is occupied again and again by the system. It is one dimensional.

Torus: An attractor which fills a two-dimensional manifold. A trajectory on the torus

undergoes a quasi-periodic motion, where two or more frequencies of irrational ratio, being present simultaneously.

Chaotic attractor: It is a strange attractor. A minimum of three dimensional state spaces are needed for continuous dynamics and fractal dimension for special cases. These attractor are characterized through fractal dimensions and their Lyapunov spectrum.

Poincare' sections: The structure of the attractor can be better viewed by Poincare' section. Structure of one dimensional attractor can also obtained through this section. In this method, a plane called Poincare' section plane is chosen in the state space for visualizing the attractor. The trajectories in the state space is intersected transversely by the Poincare' section plane. Then the attractor is displayed by plotting only the points of intersection of the attractor in the Poincare' section plane (Lauterborn 1996).

5.3 Methods of nonlinear dynamics used for the analysis

A brief review of the tools of nonlinear dynamics applied to thermoacoustic systems (Abarbanel 1996).

5.3.1 Reconstruction of phase-space

The complex combustion dynamics at different operating conditions can be readily examined by reconstructing the phase space using the acquired time series pressure data. The phase-space reconstruction of a time series data allows us to readily examine the combustor dynamics at different operating conditions. For reconstructing the phase space, we have to covert the observations with respect to time into delay vectors (state vectors), each of which has an one-to-one correspondence with one of the dynamic variables involved in the system using the time delay embedding method. For instance from the acquired pressure data $p\prime(t)$, we construct the vectors $p\prime(t), p\prime(t+\tau), p\prime(t+2\tau), ...p\prime(t+d-1)\tau$ such that the combination of these vectors provides maximum information of the combustor dynamics.

According to Taken's theorem, for an adequate reconstruction of d-dimensional system in an m-dimensional phase space using time delay is possible when $m \geq 2d + 1$ (Abarbanel, 1996, Nair *et al.*, 2013a, Nair *et al.*, 2014a, Cao, 1997, Hilborn, 2004). The average time delay embedding method (Abarbanel, 1996, Nair *et al.*, 2013a) is used for determining the appropriate time delay (τ) required for the reconstruction of phase space. The embedding dimension (d) required for the reconstruction of phase space is determined by the practical method proposed by Cao (1997).

5.3.2 Average mutual information

Average mutual information is a function of the duration between the data points of a time series. This provides useful information for determining the optimal time delay τ for embedding as well as measuring the rate of spontaneous decay of information from the time series. The average mutual information between two measurements $s(n)$ and $s(n + \tau)$ at time n and $n + \tau$ are

$$I(\tau) = \sum_{s(n)}^{s(n+\tau)} P(s(n), s(n+\tau)) log_2 \left[\frac{P(s(n), s(n+\tau))}{P(s(n)), P(s(n+\tau))} \right] \tag{5.1}$$

Where $P(s(n))$ and $P(s(n + \tau))$ are individual probability densities for the measurements and $P(s(n), s(n + \tau))$ is the joint probability density for the measurements. The optimum time delay τ_{opt} is estimated as that of τ for which the $I(\tau)$ between two delay vectors attains its first minimum (Abarbanel 1996, Nair *et al.* 2013a). The location of the first minimum is such that the examined events are independent enough to define new coordinate and is chosen as the time lag τ for the construction of the phase space.

5.3.3 Embedding dimension

The technique proposed by Cao (1997) and Kabiraj *et al.* (2012c) is used to estimate the optimum embedding dimension, the dimension at which the attractor dynamics unfold. This technique is an optimized version of the False Nearest Neighbouring (FNN) method (Abarbanel 1996), wherein one tracks the number of false neighbours to each

point in the phase space during the progressive increase of embedding dimension. A false neighbour to a point in phase space is one that moves away from it once the embedding dimension is increased. The false neighbours can be diagnosed by evaluating the vector,

$$a(i,d) = \frac{(y_i(d+1) - y_{n(id)}(d+1))}{(y_i(d) - y_{n(id)}(d))} \tag{5.2}$$

Where $i = 1, 2, ...(n - d\tau)$ and $n(i,d)$ is the index of the nearest neighbouring point in phase space to the point y_i. The dependency of the index i can be eliminated by taking the mean value of $a(i,d)$ at different values of i, as

$$E(d) = \frac{1}{(n - a\tau)} \sum_{n}^{n-a} a(i,d) \tag{5.3}$$

Here, E(d) is dependent only on the dimension d and the time lag τ. The variation from d to the next nearest dimension d+1 is determined by defining

$$E1(d) = \frac{E(d+1)}{E(d)} \tag{5.4}$$

E1(d) stop changing when the value of d is greater than d_0. Then $d_0 + 1$ are the minimum embedding dimensions for a time series coming from an attractor.

5.3.4 Return maps

Return maps are commonly used to investigate the structure of time series data from nonlinear systems. They are constructed by plotting time series data against itself lagged in time (Hilborn, 2004, Strogatz, 2000). The occurrence of extreme events such as local maxima or local minima can also be analysed by using this technique. By visualizing the trajectories in phase, the important and easily interpretable information about the acquired time series data can be displayed by these return maps. Using these maps, we study the evolution of extreme events in the combustor such as maxima and minima of pressure oscillations (points where the first derivative become zero). In the first return map, all maxima/minima of x_n are plotted against the next maxima/minima x_{n+1}. If these successive maxima/minima (for limit cycle) are equal, we have points lying on the diagonal of the plot, else it moves away from the diagonal. From these maps

we can observe the evolution of phase space trajectory on a lower-dimensional space (Kabiraj *et al.*, 2012b). In the absence of noise, for systems which undergo limit cycle oscillations, the return map is a dot on the diagonal line and for intermittent oscillations the map is spread around the diagonal (Kabiraj *et al.*, 2012b).

The hidden dynamical patterns and nonlinearity in the acquired data can also be analyzed graphically using recurrence plots, which is explained in Chapter 7.

The application of the tools of the dynamical system theory for an experimental data is explained in the Appendix A.4.

CHAPTER 6

DETECTING PRECURSORS TO INSTABILITIES AND ITS CONTROL IN A SWIRL STABILIZED TURBULENT COMBUSTOR

The devices such as combustors that are used in gas turbines, jet engines and industrial processing devices such as furnaces and burners undergoes combustion instabilities at certain operating conditions. These instabilities lead to large amplitude pressure oscillations, resulting in decreased performance and reduced life time of such devices. Controlling or avoiding and detecting the onset of these oscillatory instabilities is very much important and are a challenging task. The need for detecting and controlling the instabilities is to increase the stability margin of the combustor and to prevent (i) the occurrence of high amplitude oscillations during certain operating conditions (ii) structural damage (iii) unsteady heat release oscillations.

In almost all practical devices, during certain operating conditions, the low amplitude noisy oscillations (chaotic oscillations) undergoes transition to high amplitude periodic oscillations, called instability oscillations.

A thorough knowledge of the occurrence of the combustion instabilities is prerequisite for developing a system and a method for early detection of the onset of oscillatory instabilities in any practical devices. The transition from chaotic or low amplitude noisy oscillations to unwanted instabilities occurs in practical devices through intermittent burst oscillations. These developing oscillatory instabilities can be prevented by controlling various parameters of the device. The physical mechanism underlying the transition between combustion noise to combustion instabilities are essential for identifying the early warning signals to impending instabilities.

6.1 Evolution of the system dynamics during the onset of instabilities.

The evolution of system dynamics during the onset of instabilities are shown in Fig. 6.1. Figure 6.1a shows that up to a particular regime of Reynolds numbers the combustor undergoes low amplitude aperiodic oscillations, called stable combustion (combustion noise) (Nair *et al.*, 2013a). For further increase of Reynolds number, the combustor undergoes high amplitude tonal oscillations called instability oscillations as shown in Fig.6.1c. This transition from combustion noise to instability oscillations happens through a regime of irregular burst oscillations, referred to as intermittency in dynamical system theory as shown in Fig.6.1b. This intermittent state in a combustor is a distinct stable dynamical state compared to chaotic (stable) or unstable (periodic) states. The intermittent oscillations are characterized by intermittent bursts of high amplitude periodic oscillations that appear in a near-random fashion along with the low-amplitude aperiodic fluctuations as shown in Fig.6.1b. As the operating conditions approach towards instability, the bursts progressively last longer in time and eventually the dynamics transition completely in to periodic oscillations. Thus the intermittent oscillations can be considered as an indication of the onset of instability oscillations. The same kind behaviour was observed by Nair *et al.* (2014a) in a bluff body combustor.

To study the onset of instabilities, we need a continuous measure, that quantifies intermittency in an acquired time series pressure signal.

6.2 Intermittency in a swirl stabilized combustor

Figure 6.2 shows the intermittent burst signal obtained from a swirlstabilized combustor after the loss of chaotic behaviour and before the occurrence of self-sustained high amplitude periodic oscillations. This signal consists of bursts of high amplitude oscillations along with the region of low amplitude fluctuations. Nair *et al.* (2013b) showed that these intermittent oscillations are consequences of the presence of homoclinic orbits in the phase space of the underlying attractor. A homoclinic orbit is the one in which the unstable manifold of the hyperbolic fixed point of the system merges with its own stable manifold. That is, such orbits allow the system to move from a fixed point

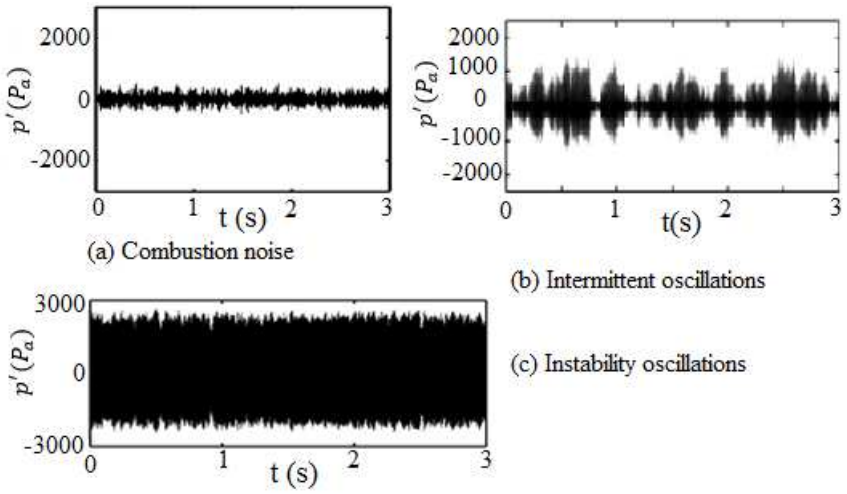

Figure 6.1: Shows the evolution of combustion dynamics during the variation of the Ryenolds number (or equivalence ratio) up to instability oscillations. (a) combustion noise (Re = 1.8×10^4 , mass flow rate of air 9.9 g/s, $\phi = 0.92$), (b) intermittent burst oscillations (Re = 2.1×10^4, mass flow rate of air11.9 g/s, $\phi = 0.71$), (c) instability oscillations (Re = 2.6×10^4, mass flow rate of air 14.8 g/s,$\phi = 0.62$), maintaining constant fuel flow rate of 1.1 g/s.

solution to an oscillatory state and back to the fixed point, which one observes in the dynamics theory as intermittent burst (Pomau and Manneville, 1980). These homoclinic orbits connect the stable and unstable branches of a hyperbolic saddle equilibrium solution. This lead to excursions of the dynamics near the vicinity of the periodic orbit which are seen as bursts of periodic oscillations in the acquired signal. Such oscillations die down to low amplitude hydrodynamic oscillations in the absence of self-sustained heat release fluctuations.

The dynamics in a swirl stabilized combustor are due to the complex interplay between two sub systems operating over different length and time scales - the acoustic and the hydrodynamic scales. Acoustics operates over a short time scale associated with the passage time of sound through the combustor, where as hydrodynamics operates over the comparatively slower flow time scales. The modulation of the acoustic subsystem by hydrodynamics, which shifts it back and forth causes to arise the intermittent burst oscillations. The unsteady pressure signal acquired at condition immediately prior to combustion instability are composed of burst of high amplitude periodic oscillations along with the regions of chaotic fluctuations. Such intermittent burst oscillations dur-

ing the onset of instability oscillations in swirlstabilized combustor are shown in Fig. 6.2. The zoomed region of the signal showed in Fig. 6.2 is composed of high amplitude periodic regions along with the low amplitude aperiodic oscillations. Such type of intermittent burst oscillations are always observed in turbulent combustors prior to the onset of instability oscillations.

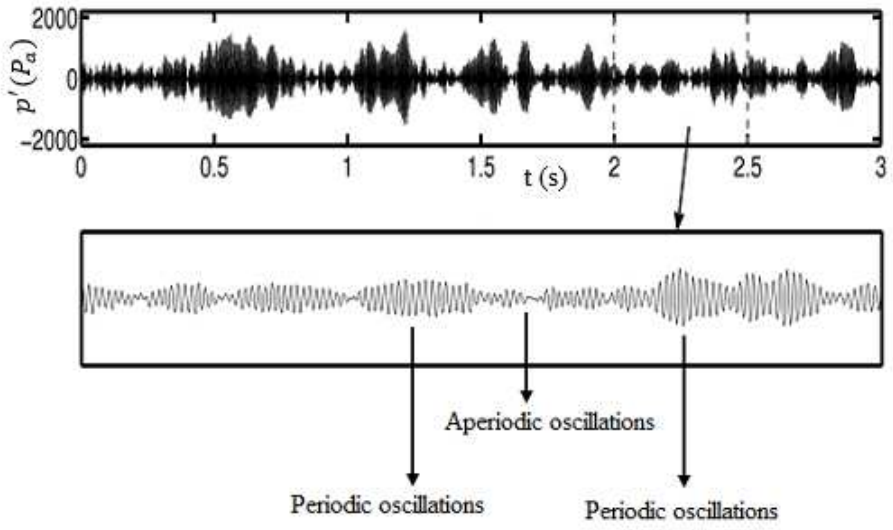

Figure 6.2: Shows the time trace of pressure signal corresponding to the intermittent burst oscillations prior to instability oscillations in a swirlstabilized combustor (Re = 2.1×10^4, mass flow rate of air11.9 g/s, global equivalence ratio, ϕ = 0.71).

In this chapter, we analysed the presence of intermittent burst dynamics in confined, compressible, turbulent flow environment prior to the transition to high amplitude periodic oscillations from low amplitude chaotic fluctuations (combustion noise). Based on this analysis we develop a system and method for early detection of onset of oscillatory instabilities in practical devices where in transition to instability from chaotic or noisy behaviours happens through intermittent bursts. The occurrence of these instability oscillations in the combustor are prevented by controlling various parameters of the combustor (Nair *et al.*, 2014b).

The onset of combustion instabilities are well understood by measuring the occurrence of intermittent burst oscillations and thus we can avoid the unwanted instability oscillations by adopting preventive measures to the system.

6.3 Measures used for early detection of instabilities

Understanding the dynamics of the transition and hence the route to instability, one has better chances of finding robust precursors that can forewarn the onset of an impending instabilities, thereby providing operators of fielded combustors with warning signals sufficiently in advance to take effective control measures (Nair *et al.*, 2014b). The following method are used for early detecting the precursor to instabilities in a turbulent swirl stabilized combustor.

Statistical measures: Based on quantifying the recurring state in dynamics using the recurrence plots.

Mathematical measures: Based on the test for chaos.

6.3.1 Statistical measures

Continuous measures that rely on intermittency in a measured signal are sought for, that can then serve as robust precursors to the onset of large amplitude periodic oscillations. This involves studying the characteristics of the aperiodic states along with the periodic bursts and the recurrence properties of the bursts.

The onset of combustion instabilities of a swirl stabilized combustor can be evaluated based on quantifying the recurrence state in the dynamics using the recurrence plot, which is explained in the next section.

6.3.2 Recurrence plots

Recurrence is a fundamental characteristic of dynamical systems. The recurrence pattern in the dynamics of an acquired signal can be quantified by using recurrence plots. The recurrence plots track the time at which the trajectory of the system visits roughly the same region in phase space. From the reconstructed phase space, a matrix of recurrences can be formulated by computing the pairwise distances between points in the phase space. Then the recurrence matrix $R_{(i,j)}$ as:

$$R_{(i,j)} = H(\epsilon - ||(\vec{x}_i) - (\vec{x}_j)||) \tag{6.1}$$

Where, i, j = 1.....N, number of considered states of x(i) and x(j) $\in R^m$, ϵ is a threshold or upper limit of the distance between a pair of points in the phase space to consider them as close or repeat, $\Pi.\Pi$ is Euclidean norm and H is the Heaviside step function(Nair *et al.*, 2014a, Nair *et al.*, 2013a, Li and Yao, 2008). An optimum value of the threshold distance is important for recurrence plots. For our recurrence plots, a value equal to 15% of the attractor diameter, which is defined as the maximum distance between pair of points in the phase portrait is used.

The recurrence matrix is a 2D symmetric matrix composed of 0s and1s and the plot is a 2D representation of the matrix as the trajectories evolve in time. 0 (zero) corresponding to black point, those time intervals when the pairwise distance are less than ϵ. 1(one) corresponding to white point, those instances when the pairwise distances exceed the threshold. The black dots mark a recurrence of a dynamical state and white dots for the non-occurrence of the state. Both axes in the recurrence plot are time axes (Nair *et al.* 2014a). The impending instability can be established by counting the number of black points in the recurrence plots. The construction of recurrence plots is explained in the next sub-section.

6.3.3 Construction of Recurrence plots

For constructing the recurrence plot, we have to fix a threshold value ϵ_0, which depends on the size of the attractor for that operating condition. If we fix $\epsilon = \epsilon_0$, we will get a quantifiable precursor across different Reynolds numbers. The value of ϵ_0 is fixed slightly higher than the size of the attractor obtained at the lowest operational Reynolds number. The recurrent rate of the dynamics obtained by measuring the density of the recurrence point.$R_{ij} = 0$, for black points and 1 for white points. This density of points in the recurrence plot seen to decrease on approach of combustion instability (Nair *et al.*, 2014a). Figure 6.3 shows the number of black points decreases as the system approaches instability. That is the system exceeds the threshold value. This decrease in density of black points corresponds to the decrease in time spent by the system in aperiodic states. This can be measured by a quantity τ_o, which quantified how long the system remains in a particular dynamical state (chaotic). The value of τ_o tends to zero when the system reached combustion instability.

Figure 6.3 shows the unsteady pressure signal and the corresponding recurrence plots during the evolution of instability oscillations from the low amplitude combustion noise. The recurrence plot for chaotic or combustion noise is grainy. This is due to the fact that the dynamics at this working condition is chaotic with little repeatability in the patterns. On the other hand the recurrence plot during the instability oscillations displays the pattern of diagonal lines, indicating high repeatability (recurrence) in the dynamics. The broken diagonal lines indicates the presence of noise in the system. However the recurrence plot for the intermediate regime has perforated black patches along with white patches. This is because the system moves back and forth between low amplitude or chaotic oscillations (black patches) and high amplitude instability oscillations (white patches). These are the patterns corresponding to intermittent burst oscillations (Klimaszewska and Zebrowski, 2009) and thus this plot helps to clearly identify the route to instability in a swirl stabilized turbulent combustor.

The statistical measures can be applied to quantify the recurrences in the signal during intermittent oscillations (Nair *et al.*, 2014a and b, 2013a). This measures can further be used as precursors to instability because they vary in a smooth fashion as the operating condition traverses intermittent regime in to instability. By tracking the probability distribution of black points or white points in the recurrence plots, measures can be constructed to distinguish the dynamics prior to combustion instability. The quantification of recurrence state in the dynamics corresponding to different operational condition is established in the next section.

6.3.4 Quantifying the recurring state in the dynamics

The recurrence state in the dynamics can be quantified by counting the number of black points in the recurrence plot. This can be used as an indication, which for warn an impending instability (Nair *et al.*, 2014a, 2014b, 2013a). The density of black points in a recurrence plot measures the recurrence rate in the dynamics of the system and can be obtained as

$$RR = \frac{1}{(N_0 - d_0\tau_{opt})^2} \sum_{i,j=1}^{N_0 - d_0\tau_{opt}} R_{ij} \tag{6.2}$$

Where RR- Recurrence rate, N_0- length of the pressure time series, d_0 - Optimum embedding dimension, τ_{opt} -optimum time delay, $d_0\tau_{opt}$ -length of delay vectors.R_{ij} =

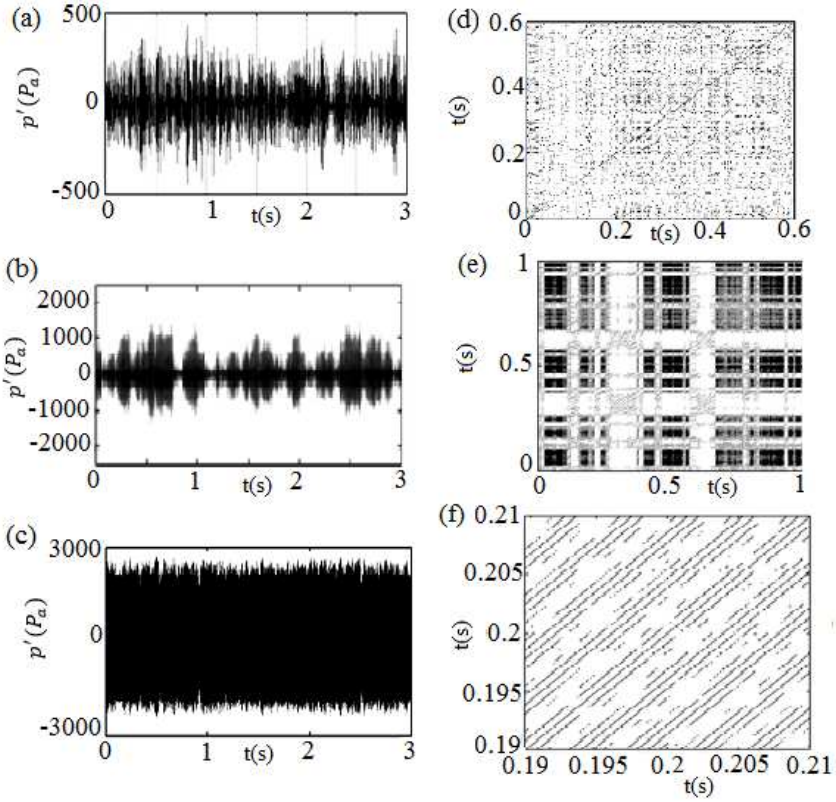

Figure 6.3: Shows unsteady pressure signals (left column) and the corresponding recurrence plots (right column) acquired during combustion noise (first row), intermediate intermittent regime (middle row) and combustion instability (last row). The threshold for the recurrence plot was taken to be $\epsilon = 0.15\lambda$, where λ is the size of the attractor, defined as the maximum distance between pairs of points in the phase space. The black patches in the intermittent oscillations correspond to regions of low amplitude pressure fluctuations.

0 for a black point and 1 for a white point (Nair *et al.*, 2014a and b). The variation of recurrence rate with respect to Reynolds number is shown in Figure 6.4.

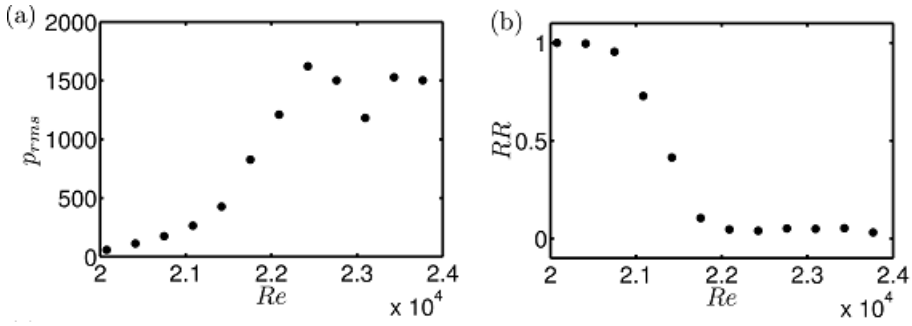

Figure 6.4: Shows the plot for the statistical measures of intermittency obtained through recurrence quantification with the r.m.s values of the pressure signals acquired from the swirl stabilized turbulent combustor for a fuel flow rate of 0.55g/s. (a) r.m.s values of unsteady pressure signal (p_{rms}), (b) Recurrence rate of dynamics (RR) which measure the density of points in the recurrence plot.

The recurrence rate decreases as the system approaches instability. As and when the system attains instability, the recurrence rate attains zero value (Fig. 6.4b). The number of black points also comes down as the system reached instability because the pairwise distance at this condition exceeds threshold value.

Since the black points in the recurrence plot represents the recurrence state of a dynamics, the decrease in density of black points corresponds to the decrease in the time spent by the system in aperiodic sates. This can be measured by a quantity called average passage time and is explained in the next sub-section.

Average passage time

The time spent by the system in a particular dynamic state, represented as average time τ_0, can be defined as

$$\tau_0 = \frac{\sum_{v=v_{min}}^{N_0 - d_0\tau_{opt}} vP(v)}{\sum_{v=v_{min}}^{N_0 - d_0\tau_{opt}} P(v)} \tag{6.3}$$

Where τ_0, quantifies how long the system remains in a particular dynamical state (chaotic fluctuations), $P(v)$, being the frequency distribution of the vertical/horizontal black lines of length v in the recurrence plot, and v_{min} is a suitable lower limit for ν to prevent noise corruption (Nair *et al.*, 2014a and b, 2013a). The variation of average time with respect different Reynolds number is shown in Fig. 6.5.

It is observed that the value of τ_0 decrease in a smooth fashion although at different rates from chaotic low-amplitude combustion noise to high-amplitude periodic combustion instability. Hence we expect this quantity to tend towards 0 as the system transitions completely into periodic oscillations. The amount of order/disorder in the system can also be measured by a parameter called Shannon entropy s of the signal, which can be obtained through the recurrence plot.

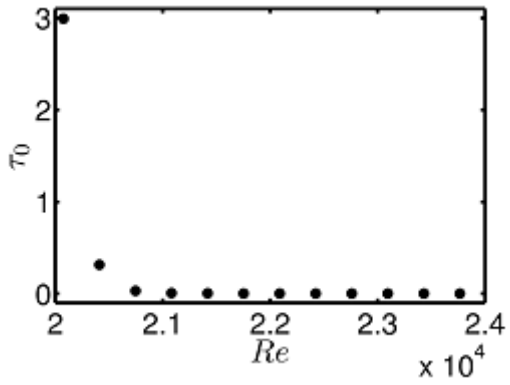

Figure 6.5: Shows the average passage time spent by the dynamics in aperiodic fluctuations (τ_0) with respect to Reynolds number. The value of τ_0 will correspond to the duration of data acquisition (3s in the present case) at conditions of combustion noise.

Shannon entropy

The unpredictability of information content can be measured by using Shannon entropy. It quantifies the expected value of the information contained in a message (Marwan *et al.*, 2007, Gao and Cai, 2000, Nair *et al.*, 2014a and b, 2013a). Higher Shannon entropy is observed for more disorganized systems since it contains more information. The amount of information contained in a given message is defined as the negative of a certain sum of probability, and is given by the expression (Nair *et al.,* 2014a),

$$s = -\sum_{l=l_{min}}^{N_0-d_0\tau_{opt}} p(l)ln(p(l)) \tag{6.4}$$

where, p(l) is the probability that a diagonal line has length l , and p(l) is given by

$$p(l) = \frac{P(l)}{\sum_{l=l_{min}}^{N_0-d_0\tau_{opt}} P(l)} \tag{6.5}$$

Where $P(l)$ is the frequency distribution of the black diagonal lines of length l and l_{min} is the suitable lower limit for l to prevent noise corruption. Figure 6.6 shows the variation of Shannon entropy with respect to Reynolds number. The Shannon entropy measures the order/disorder in the system. The Shannon entropy tends to zero when the system leading towards instability as shown in Fig. 6.6.

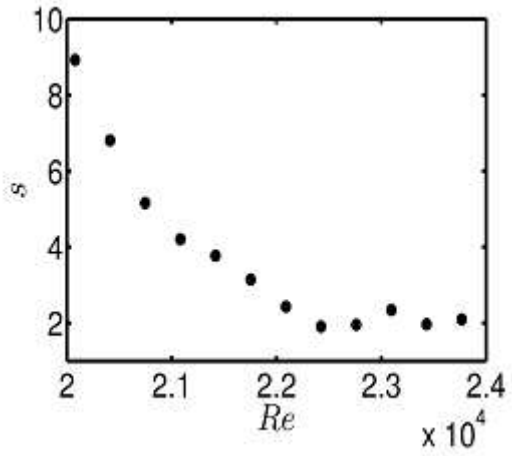

Figure 6.6: Plot of Shannon entropy Vs Reynolds number. Entropy s of the diagonal length distribution decrease in a smooth fashion from chaotic low-amplitude combustion noise to high-amplitude periodic combustion instability.

That is, a decrease in entropy indicates that the system is approaching a state of regular or an emergence of order out of disorder (chaos). At this regular state, the recurrence plot consists of only black parallel diagonal lines and the system oscillates in an ordered manner. Here we found the probability of black diagonal line be l after fixing a minimum value for l as l_{min}. Higher value of s means more information we can potentially gain once we know the outcome of the experiment. Shannon entropy give a way to quantify the potential reduction in our uncertainty once we learnt the outcome of the probabilistic process. The value of s = 1 means we gain one bit of information or our uncertainty reduced by 1 bit.

The relative merits of these defined precursors as early warning signals for the occurrence of instability were gauged by comparing with the r.m.s value of pressure fluctuations (see Fig.6.4a). We see that the new precursors perform as well as (for example RR) and often times better (see the variation of τ_0 or s) than P_{rms}. Thus we see that these

measures show a variation in behaviour well before the operating condition approaches instability. More generally, we can possibly use such precursors as early warning signals to an impending instability in a variety of turbulent flow systems encountering periodic oscillations.

Mathematical measures based on the test for chaos can also be used for determining the onset set of instabilities.

6.3.5 Mathematical measures: Based on a test for chaos

Burst method

In burst method the early detection of onset of instability is done by tracking the intermittent bursting behaviour preceding the transition to instability from chaos (Nair *et al.* 2014b, 2013b). The burst, which is a sudden spike in the amplitude of the measured signal which decay after a short duration. The occurrence of such burst in the measured signal leads to an intermittent switching behaviour of the signal between low and high amplitudes. This is often the case in high Reynolds number flows where the chaotic oscillations undergo the transition to instability oscillations through intermittent burst.

In this method a threshold value for the amplitude of the burst is fixed. In our study we fixed a threshold value of the burst amplitude as 500 Pa (see Fig.6.4a). Then we compare the measured signal with the threshold of the signal and count the number of bursts in the signal above this threshold value. The occurrence of burst in the signal increases the amplitude of pressure signal beyond the threshold value. The repeated occurrence of these burst oscillations above the defined threshold value can be used as a precursor to the occurrence of the combustion instability (see Appendix A.2)

Peak method

The onset of impending instability can be determined by counting the number of peaks N in the signal above a user defined threshold (ξ) for a time duration t (Nair *et al.*, 2014b). The threshold will be fixed corresponding to the acceptable levels of amplitude of the device. Time duration $t = 400\tau_{min}$ and the number of peaks above the user defined threshold be N and the total number of peaks in the signal within this time duration

be N_{tot}. Then the probability of the combustor to attain instability is $N/N_{tot} = p$, which is the measure of proximity of the device to attain instability. The value of p increases smoothly towards 1 for the increase of Reynolds number (Re) towards instability as shown in Fig. 6.7. A suitable threshold value for p can be set for the probability of the combustor to attain instability. Thus when a measured value of p exceeds the defined threshold, a control unit suitably ensures that the combustor to operate within the stable limit by controlling various parameters, thereby increases the stable limit. The schematic representation is explained in Appendix A.3.

The results on applying the peak method on the swirlstabilized backward facing step combustor for signals acquired at various Reynolds number is as shown in Fig. 6.7. The value of p lie reasonably near to 0 for chaotic combustion which is stable. A smooth departure of p from 0 indicates the precursor for impending combustion instability which happens as the Reynolds number is increased. The results presented are for the entire 3s data. By setting threshold at a value of say 0.25 for p, operators can be informed of an impending instability in advance so that appropriate control measures can be taken.

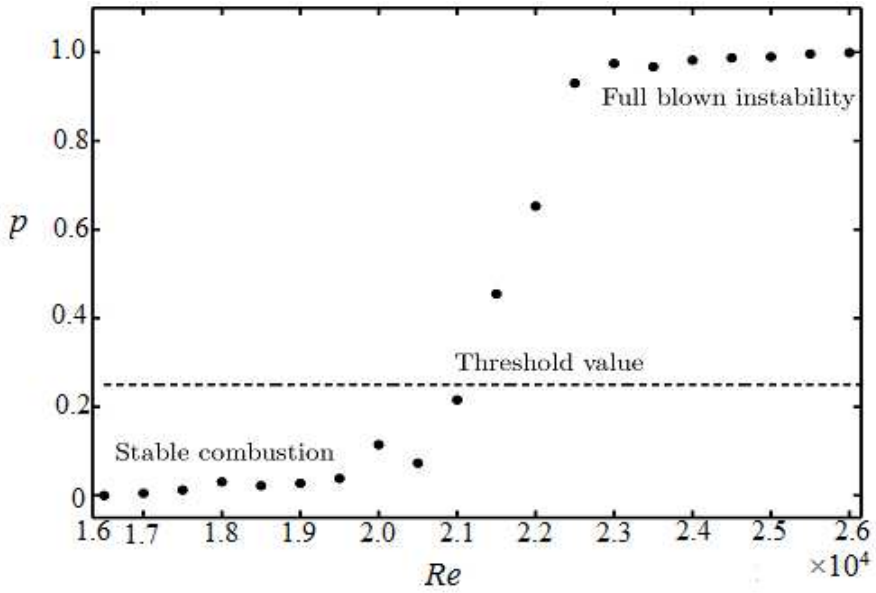

Figure 6.7: Shows a measure based on the number of peaks crossing a set threshold value applied on the dynamic pressure data obtained from a combustor in a particular configuration as the parameters moved towards instability.

Bifurcation diagram (Nair *et al.* 2014a) can be drawn by tracking the peaks in a

measured signal and plotting them as a function of control parameter (Reynolds number, Re). A supercritical Hopf bifurcation of the acoustic system is observed in a swirl-stabilized combustor, when the system moving from combustion noise to combustion instability. However due to turbulence, the peak amplitudes shift across a range of values even during combustion instability. This effect can be overcome by counting the number of peaks (N) in the signal $\phi(j)$ for a time duration of 3s above a threshold value (ξ), which would correspond to the .acceptable level of amplitude for the system. A threshold value of 500 Pa, which is corresponding to the level of pressure fluctuations in the system during stable regimes of operation is taken as the acceptable level in our study. If N_{tot} is the total number of peaks that happen within the time duration of 3s then the probability of the system to attain the instability as $f = N/N_{tot}$, where f is the measure of the proximity of the system to attain instability.

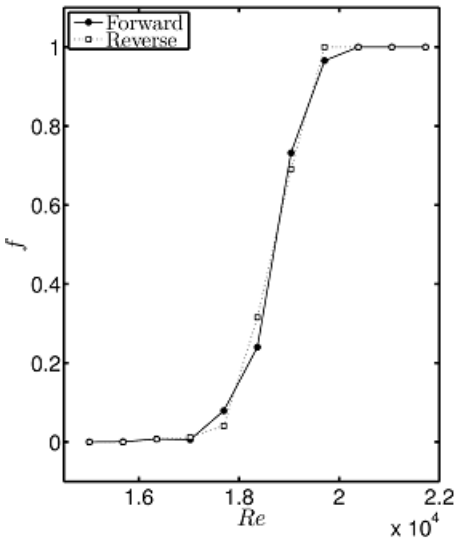

Figure 6.8: Bifurcation diagram obtained through burst count for the transition from chaotic combustion noise to high amplitude combustion instability for a swirl stabilized backward facing step combustor (fuel flow rate = 0.55g/s). The nature of bifurcation to combustion instability can be identified as supercritical. The threshold was set at 500 Pa. Similar results were obtained at other fuel flow rates.

In the Bifurcation diagram (Nair *et al.* 2014a and b), the value of f vary smoothly as the control parameter Re traverses a regime of stable operation towards combustion instability. This variation is due to the presence of an intermediate intermittent burst regime in which the pressure signal occasionally cross the threshold and leads to increase in f. These intermittent excursions keep increasing as flow condition approaches

combustion instability and finally f tends towards a value of 1 as shown in Fig. 6.8.

In the next sub-section we describe mathematical methods, which gave an indication that how close the operating conditions are to impending combustion instability.

Maximum Lyapunov exponent, λ

The usual test for detecting a deterministic dynamical system whether it is chaotic or non-chaotic is the calculation of maximum lyapunov exponent λ (Gottwald and Melbourne 2004, Zachilas and Psarianos 2012). A positive largest lyapunov exponent ($\lambda > 0$) indicates chaotic behaviour. The nearby trajectories separate exponentially for $\lambda > 0$ and close each other for $\lambda < 0$; shows system is chaotic and non-chaotic respectively. The maximum lyapunov exponent λ can be computed using the expression (Zachilas and Psarianos 2012).

$$\lambda(t) = \lim_{t \to \infty} ln \left| \frac{\xi(t)}{\xi(t_0)} \right| \tag{6.6}$$

Where $\xi(t_0)$ and $\xi(t)$ are the measuremets corresponding to the time t = 0 and t respectively of the distance between two points of the nearby orbits . $\lambda(t)$ is the average exponential deviation of two adjacent orbits as shown Fig. 6.9 and is known as Maximum lyapunov exponent.

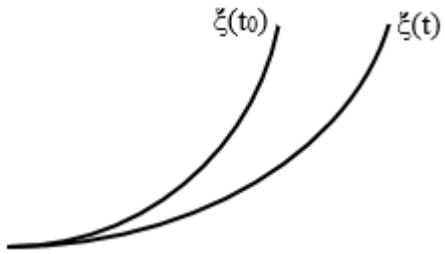

Figure 6.9: Schematic diagram representing two consecutive orbits in the phase space diagram for determining the Lyapunov exponent λ. The value of $\lambda > 0$ for chaotic system and ≤ 0 for periodic system.

This approach has lot of disadvantages. This method can not be applied directly

to exponetial data. However it can be applied to experimental data by using Takens embedding theory. This method is very much suitable for dynamical systems whose equations are known. However for situations where the equations are unknown and also if we wish to analyse the experimental data by evaluating λ, then we have to construct phase portrait, in which computing time is large. A numerically computed small positive Lyapunov exponent does not give any definite conclusion, rather this method is not suitable for noisy systems. Due to this complexities we are not able use this method for our analysis. At this situation we used a method proposed by Gottwald and Melbourne (2004) called 0-1 test, which is a binary test for characterizing the regular and chaotic dynamics in dynamical systems.

0-1 test

The 0-1 test (Gottwald and Melbourne 2004, 2005, 2009a, 2009b, Zachilas and Psarianos 2012) tell apart the state between order and chaos in a deterministic dynamical sytem. This test distinguish the transition from a chaotic regime to an ordered state from a time series of masurements. The following are the major advantage of this test:

(i) Since this test can be directly apply to time series data, there is no need of constructing the phase portrait. Thus reduces time elapsed for analyzing the data.

(ii) This test applicable equally good to discrete and continuous time series data, experimetal data and maps, ordinary and partial differential equations; i.e, this method is applicale to any dynamical sytems irrespective of the form and nature of the system.

(iii) This test gave a definite conclusion for small positive computed value from zero.

Figure 6.10 shows the schematic representation of the application of 0-1 test on the acquired time series pressure data.

We identified the presence of chaos in a given time series data of pressure signal by using the 0-1 test. The pressure signal p(t) is measured by ensuring that the acquired value at each instant provides essentially little information about the future values at stable operation. That is we have to sample the data at a time interval corresponding to the minimum of the average mutual information (AMI). Practically we use the sampling time as $\tau_{opt} = T/4$, T is the natural acoustic period of oscillation in the combustion

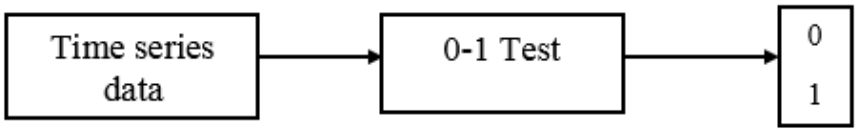

Figure 6.10: Schematic diagram representing the 0-1 test applied on the acquired pressure data from the partially premixed swirl stabilized combustor during different operating conditions.

chamber. We formulate the translational variables q_c and r_c from the measured signal p(t) for t = 1,2...N and $(t_{i+1} - t_i) = \tau_{min}$, where c is chosen randomly between 0 and π (Nair *et al.* 2013a, 2014b) as,

$$q_c = \sum_{j=1}^{n} p(t)cos(tc) \tag{6.7}$$

$$r_c = \sum_{j=1}^{n} p(t)sin(tc) \tag{6.8}$$

The diffusive or non- diffusive behaviour of q_c and r_c can be investigated by analysing the mean square displacement $M_c(n)$.

$$M_c(n) = \lim_{N\to\infty} \frac{1}{N} \sum_{(t=1)}^{N} [q_c(t+n) - q_c(t)]^2 + [r_c(t+n) - r_c(t)]^2 \tag{6.9}$$

Where N is the size of the measured signal and n is the value up to which $M_c(n)$ is calculated. The mean square displacement of these translation variables can be computed for different values of $c(\pi/5, 4\pi/5)$. If the dynamics is regular, then $M_c(n)$ is a bounded function in time and for chaotic, it scales linearly with time. In the definition of $M_c(n)$ the value of n should be very much less than N ($n \ll N$). However a limit is assured for $M_c(n)$ by calculating for $n \leq n_{cut}$, where $n_{cut} \ll N$. We found that better result is obtained for $n_{cut} = N/10$, where n_{cut} represents the value of index up to which the mean square displacement ($M_c(n)$) is calculated. The test for chaos is based on the growth rate of $M_c(n)$ as function of n. To ensure better convergence with the

same asymptotic growth rate, we used a modified mean square displacement as

$$D_c(n) = M_c(n) - V_{osc}(n) \tag{6.10}$$

Where, $V_{osc}(c, n)$ is the oscillating term, which could be removed from the mean square displacement as

$$V_{osc}(c, n) = \langle p(t) \rangle^2 \frac{1 - cosnc}{1 - cosc} \tag{6.11}$$

in which

$$\langle p(t) \rangle = \lim_{N \to \infty} \frac{1}{N} \sum_{t=1}^{N} p(t) \tag{6.12}$$

The asymptotic growth rate k_c of the modified mean square displacement is obtained from the correlation of the vectors ζ and Δ, where $\zeta = (1, 2, ..., n_{cut})$ and $\Delta = D_c(1), D_c(2), ...D_c(n_{cut})$. That is $k_c = corr(\zeta, \Delta)$. The value of k_c allow one to distinguish two types of behaviour possible in systems such as chaotic and non-chaotic dynamics of the combustor. The asymptotic growth rate k_c is a function of c for both regular and chaotic dynamics. For regular (periodic) dynamics $k_c = 0$ for all values of c. However k_c is large for isolated value of c. To ensure robustness of the measure to outliers and resonances, the median value of k_c say K is calculated for different c values. The plot of K Vs parameter, in our case is Reynolds number (R_e) was shown in Fig. 6.11. $K \to 0$ for periodic or regular dynamics and $K \to 1$ for noisy or chaotic signals.

The results on applying the 0-1 test for chaos on the swirl stabilized backward facing step combustor for signals acquired at various Reynolds number is shown in Fig. 6.11. The values lie reasonably near to 1 for chaotic combustion which is stable. A smooth departure from 1 indicates the onset of impending combustion instability which happens as the Reynolds number is increased. The results presented are for the entire 3s data which brings in some graininess due to amplitude modulations. By setting threshold at a value of say 0.9 for K, operators can be informed of an impending instability in advance so that appropriate control measures can be taken.

In a swirl stabilized turbulent combustor, the transition to instability would be as-

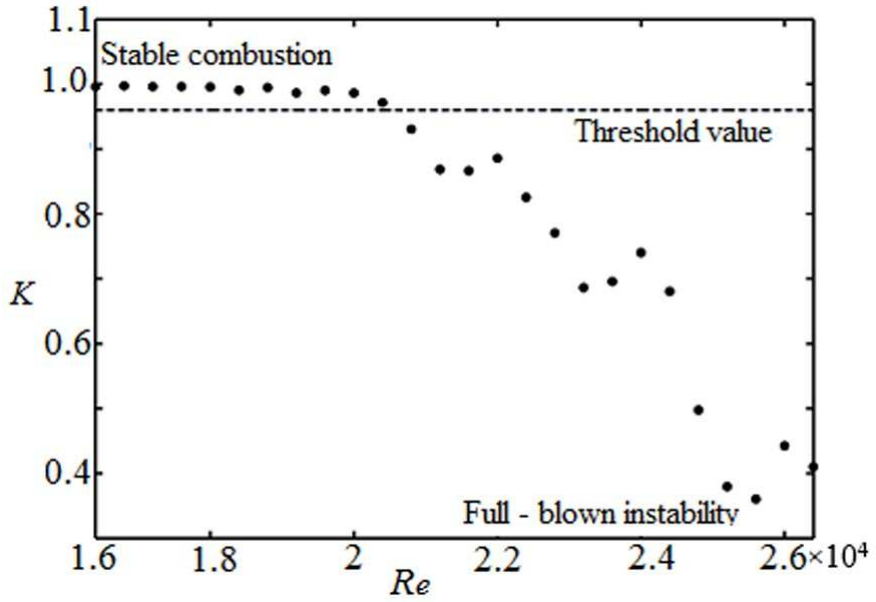

Figure 6.11: Shows a measure based on the 0-1 test applied on the dynamic pressure data obtained from a combustor in a particular configuration as the parameters are moved towards instability.

sociated with a decrease in the value of K from 1 to a lower value, depends on the turbulence level as shown in Figure 6.11. Higher the intensity of turbulence at instability, higher the departure of K from zero at instability. Here we fix a threshold value for K, based on the stable operating condition. Upon crossing this value we can say that the system going towards instability mode. At this stage, we configure the control unit suitably to control various parameters of the combustor and maintain the combustor under stable operating condition.

The 0-1 test for chaos was applied on the pressure measurements acquired at various operating conditions (or Reynolds numbers), starting from low amplitude combustion noise to high amplitude combustion instability (Nair *et al.* 2013b, 2014b). The measure of K almost close to 1 during the stable combustion, which indicates combustion noise is chaotic. As and when the flow Reynolds number increases towards instability condition, the value of K gradually starts decreasing and eventually reaching close to zero at the onset of instabilities. As the loss of chaos occurs in smooth manner, we can use the measure of K as a precursor to impending instability. By choosing a threshold value for K, that corresponds to the stable combustion (initial stages of loss of chaos), operators

get to know well in advance of an impending instability so that control action may be taken through modification of control parameters to prevent the onset condition.

We successfully devised the controller (Appendix A.1) that determines the proximity of the combustor to instability that utilizes the 0-1 test for chaos. We used the entire 3s data for this analysis. The test perform robustly even with a poor sampling rate of 1kHz, with 500 samples of data. That is the data acquisition for 500ms for an instability frequency of around 250Hz. Here since the measures falls smoothly as the operating conditions approach onset, suitable control action may be taken by modifying operational parameters to prevent high amplitude oscillations. Thus the stability margin of practical systems can safely estimated without encountering instabilities.

6.4 Interim Conclusion

The present study identifies the onset of instabilities through statistical and mathematical methods. We identified that the departure from chaos as an early warning signal for the onset of instabilities. From the recurrence plots, corresponding to the onset of instabilities,we estimated the recurrence rate, average time and the shannon entropy for identifying the onset of instabilities. We determined a threshold value for the safe operation of the combustor using the Mathematical methods. By providing suitable control measures during the onset of instabilities, the operational boundary of the practical combustors can be increased.

CHAPTER 7

ONSET OF BLOWOUT CHARACTERISTICS OF A PARTIALLY PREMIXED SWIRL STABILIZED TURBULENT COMBUSTOR

Experiments were conducted using a laboratory scale partially premixed swirl stabilized combustor for different global equivalence ratios (0.92 to 0.33). The time series data of pressure fluctuations acquired during this period were analysed using nonlinear time series analysis explained in Chapter 5. When the combustor was operated at an equivalence ratio 0.92, combustion noise, indicated by broadband low amplitude pressure oscillations, were observed. As the equivalence ratio is decreased to 0.62, the oscillations change their characteristics from combustion noise to limit cycle oscillations, indicated by high amplitude discrete tones. Further decreasing the equivalence ratio to 0.42 and lower, the periodic motion is interrupted by occasional irregular bursts and the system switches back and forth between the noise (periodic) and quiet (aperiodic) zone. On reducing the equivalence ratio further, the system reaches blowout condition.

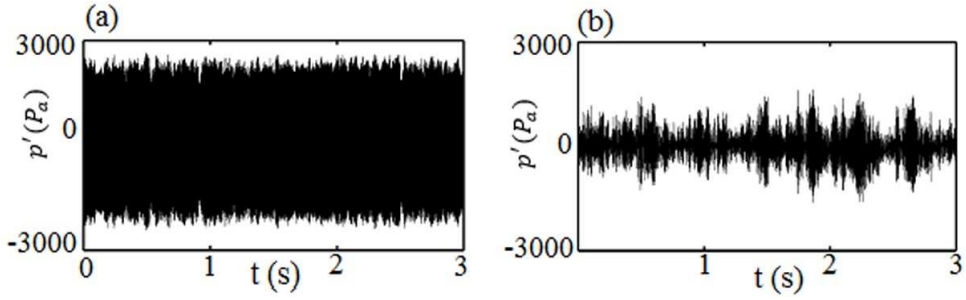

Figure 7.1: (a) pressure signal corresponding to limit cycle oscillations. The Reynolds number of flow is 2.6×10^4. The mass flow rate of air is 14.8 g/s and fuel is 1.1g/s. Equivalence ratio, ϕ = 0.62. (b) Pressure signal near blowout condition. The Reynolds number of flow is 3.9×10^4. Mass flow rate of air is 21.7 g/s and fuel is 1.1g/s. Equivalence ratio, ϕ = 0.42.

The low amplitude combustion noise and limit cycle oscillations have been studied by various researchers in different combustors (Lieuwen 2002, Chakravarthy *et al.*,

2007a and b). Nair *et al.* (2014a) observed an intermittent behaviour during the transition to periodic oscillations from chaotic oscillations in a bluff body combustor. Gotoda *et al.* (2014) recently reported that the intermittent behaviour is also a route to low dimensional chaos from regular thermoacoustic oscillations in a partially premixed gas turbine model combustor during blowout. However further study is needed to understand more about the transition charactristics of self sustained high amplitude oscillations towards lean blowout. This transition characteristic is represented in Fig. 7.1. Figure 7.1a shows the time trace of the pressure signal corresponding to the limit cycle oscillations. The corresponding FFT (Fig.7.3a) shows a single peak along with super harmonics indicates that the combustor undergoes high amplitude oscillations. Irregular bursts oscillations followed by blowout is observed for further increase in Reynolds number as shown in Fig 7.1 b.

The time series data in the regime passed through by the thermoacoustic system during irregular burst oscillations is composed of high amplitude periodic burst and low amplitude aperiodic oscillations as shown in Fig. 7.2.

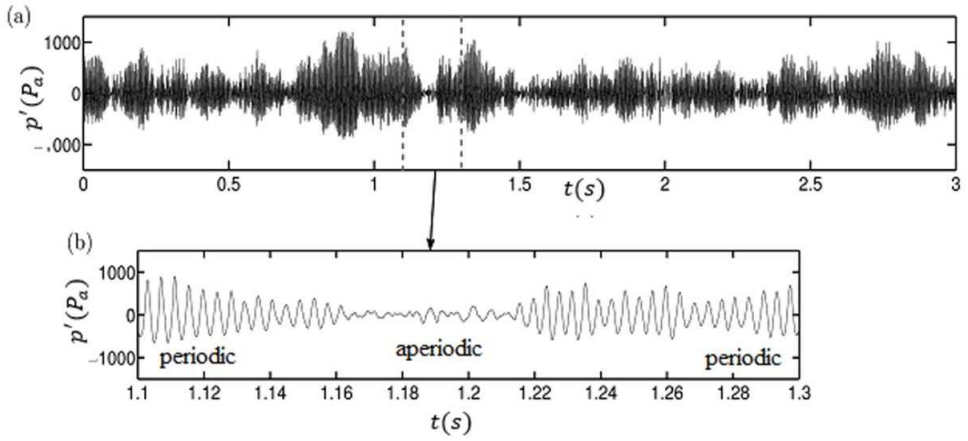

Figure 7.2: Time traces of pressure signal corresponding to noisy and quiet phase for the flow Reynolds number of 3.9×10^4. Mass flow rate of air is 21.7 g/s and fuel flow rate maintained at 1.1 g/s. Equivalence ratio $\phi = 0.42$.

The pressure spectra (Fig. 7.3) shows an increasing trend in the spectral content at low frequencies corresponding to the transition from limit cycle oscillations to this intermittent burst oscillation. This can be attributed to the appearance of these bursts in a near random fashion, typically at time scales larger than the acoustic time scales.

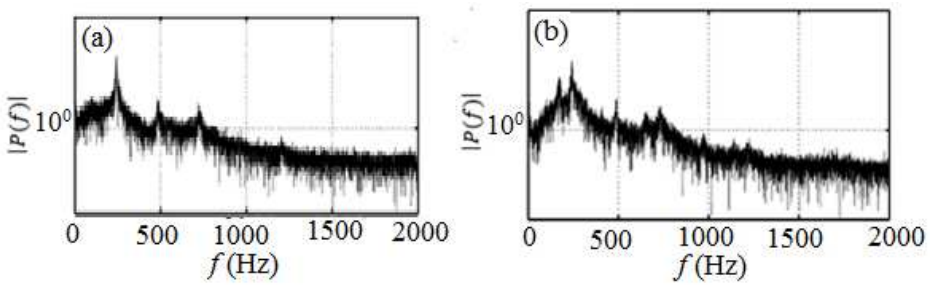

Figure 7.3: Pressure spectra corresponding to (a) limit cycle with the flow Reynolds number of 2.6×10^4. Mass flow rate of air is 14.8 g/sec. Equivalence ratio $\phi = 0.62$. (b) Intermittent oscillations with a flow Reynolds number of 3.9×10^4. Mass flow rate of air is 21.7 g/s. Equivalence ratio $\phi = 0.42$. Mass flow rate of fuel is maintained constant at 1.1 g/s. The fundamental frequency of the combustion chamber is 250Hz.

Due to the complexity of the combustor dynamics at different operating conditions, the corresponding spectral analysis of the acquired pressure data provides only a limited understanding of the combustor dynamics. More information about the nonlinearities inherent in the combustor dynamics can be extracted using nonlinear time series analysis (Abarbanel 1996, Strogatz 2000).

Combustion dynamics, which are dominated by complex dynamic processes involving a significant level of determinism when operating under fuel lean conditions (Nair *et al.*, 2013a). Presently, thermoacoustic systems are associated with limit cycle oscillations. Recently, both experimental and computational studies performed by Kabiraj *et al.* (2011, 2012c) and Kabiraj and Sujith (2012b) on laminar burners indicate that a thermoacoustic system can undergo secondary bifurcation to states such as frequency locked, quasi-periodic, period doubling, intermittent and chaotic states. Similar type of bifurcations and route to chaos was also observed by Kashinath *et al.* (2014) and Kashinath (2013) in a ducted premixed flame.

Industrial combustors are often characterized by swirling turbulent flows and turbulent combustion and hence they are inherently noisy. They display intermittent oscillations under a range of operating conditions. Nair et al. (2014a, 2013b) investigated this type oscillation prior to the occurrence of instability. However, no studies have been performed to characterize intermittency prior to blowout in turbulent combustors.

Therefore, it is of great importance to characterize the occurrence of intermittency in industrial combustors, which is the signature prior to flame blowout, using the tools from dynamical systems theory.

This chapter describes the experimental investigation of the occurrence of intermittent burst oscillations prior to flame blowout using the dynamical system theory explained in Chapter 5.

7.1 Combustor behaviour at different operating conditions

Using the technique for nonlinear time series analysis (Chapter 5), the combustor dynamics at different operating conditions were analysed by plotting the phase portrait and the return map.

7.1.1 Reconstruction of phase portrait and return map for stable combustion (Region I, Fig.4.5)

By constructing the phase portrait and return map we are able to understand the complex combustion dynamics at different operating conditions. Figure 7.5a shows the phase portrait and 7.5b represents the return map corresponding to the stable combustion with a flow Reynolds number of 1.8×10^4. The corresponding mass flow rate of air is 9.9 g/s and fuel (LPG) is 1.1 g/s respectively with a global equivalence ratio of 0.92. At this operating condition, the peak of the amplitude of pressure oscillations are well below 500 Pa and can be interpreted as combustion noise. The FFT (Fast Fourier Transform) at this condition shows broad band oscillations with a broad peak as can be seen from Fig. 7.4. The amplitude spectra in dB scale is shown in the inset.

The trajectory during noisy combustion is close to the fixed point in phase portrait as shown in Fig. 7.5a indicating that the thermoacoustic system during that period corresponds to combustion noise. Relatively small amplitude of the combustion noise spreads the data points around the fixed points (Lieuwen 2002). The combustor behaviour during various operating conditions can also be studied by plotting the return

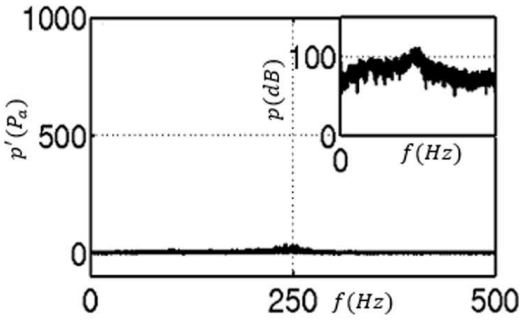

Figure 7.4: FFT with pressure oscillations corresponds to a flow Reynolds number of 1.8×10^4 and mass flow rate of air 9.9 g/s. Equivalence ratio = 0.92, Fuel flow rate is maintained constant at 1.1 g/s. The amplitude spectra also showed in dB scale at the inset.

map using the time series data acquired experimentally. Figure 7.5b shows the first return map corresponding to stable combustion with an equivalence ratio of 0.92.

During stable combustion, the concentration of all data points near the origin in the diagonal line, shows that the variability in pressure fluctuations is less. All the maxima of pressure fluctuations are nearly the same during the successive events; however, because of combustion noise the points spread around zero. This indicates that the thermoacoustic system undergoes low amplitude noisy oscillations during "stable operation".

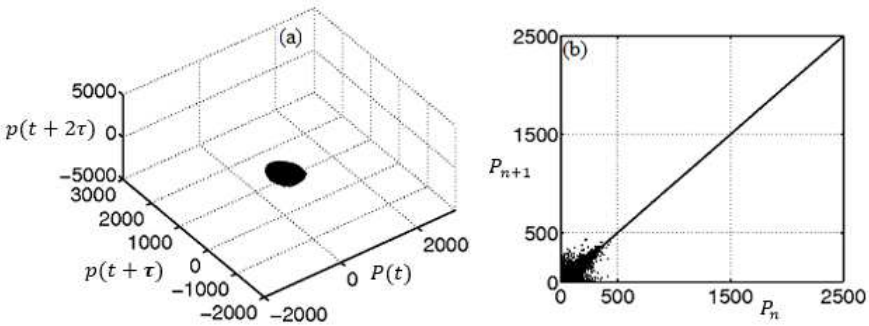

Figure 7.5: Represents the phase plot and the return map corresponding to the noisy combustion. Reynolds number of flow is 1.8×10^4. Mass flow rate of air is 9.9 g/s and the fuel flow rate is 1.1 g/s. Equivalence ratio, $\phi = 0.92$.

Upon increasing the Reynolds number further, the thermoacoustic system undergoes limit cycle oscillations.

7.1.2 Reconstruction of phase portrait and first return map for limit cycle oscillations (Region II, Fig. 4.5)

Figure 7.6a shows the phase portrait for combustion dynamics with stable limit cycle oscillations. The fixed point became unstable and the trajectory forms a closed curve around this unstable fixed point. A banded limit cycle shown Fig. 7.6a indicating a cycle to cycle variation in pressure amplitude, which in turn indicates the "noisy nature" of the oscillations present in the system. This is consistent with the result reported by Lieuwen (2001). The formation of harmonics during limit cycle oscillations as shown in corresponding FFT (Fig.7.3a) causes the distorted shape for the phase portrait. Lieuwen (2002) also pointed out that the presence of small amplitude harmonics along with the occurrence of the combustion instability is an indication of the system nonlinearities.

The first return map during limit cycle oscillations are shown in Fig.7.6b. A large excursion of data points away from zero along the diagonal line is observed during the lowering of global equivalence ratio or increasing the Reynolds number. The amplitude of pressure oscillations attained a maximum at about an equivalence ratio of 0.62 and the combustor undergoes limit cycle oscillations. These limit cycle oscillations are represented by scattering of points between 2000 and 2500 Pa in the first return map as shown in Fig. 7.6b. The scattering of points between 2000 and 2500 Pa (high pressure state) is because of cycle to cycle fluctuations of high amplitude pressure oscillations. That is, the transition from low amplitude noisy oscillations to high amplitude limit cycle oscillations are observed when the data points which are initially spread near zero in the first return map (Fig. 7.5b) move along the diagonal line to the high amplitude region (Fig. 7.6b).

7.1.3 Evolution of irregular burst oscillations from limit cycle oscillations

At higher Reynolds numbers, the transition of limit cycle oscillations to irregular pressure oscillations is observed in the bifurcation diagram shown Fig. 4.5 (Chapter 4). However, this bifurcation occurs through a frequency jump at a Reynolds number of 3.5x 10^4 as shown in Fig. 4.1 (Chapter 4).

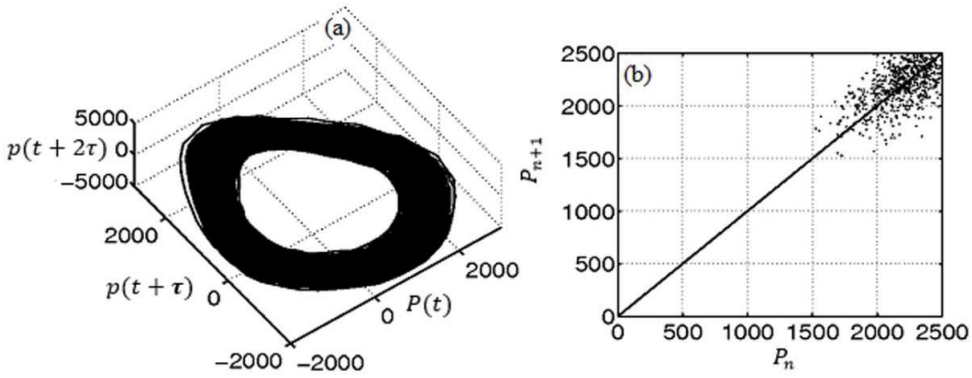

Figure 7.6: (a) The phase portrait and (b) the return map for the stable limit cycle oscillations. Flow Reynolds number is 2.6×10^4. Mass flow rate of air is 14.8 g/s and mass flow rate of fuel is maintained at 1.1g/s. Equivalence ratio, $\phi = 0.62$.

Figure 7.7 shows the evolution of irregular burst oscillations from limit cycle oscillations through Fast Fourier Transform (FFT). The corresponding flow Reynolds numbers varying between 3.3 x 10^4 and 3.9 x 10^4 (mass flow rate of air varying from 18.8 g/s to 21.7 g/s). The FFT of pressure oscillations prior to the frequency jump (region II in Fig. 4.5) is shown in Fig. 7.7a. A narrow peak of high amplitude along with the instability mode ($\sim 250Hz$) is observed in this operating condition (Re = 3.3 x 10^4). This indicates that the system attains a frequency nearing to the fundamental frequency during limit cycle oscillations.

For further increase of Reynolds number, the FFT shows two peaks (Fig. 7.7b) at relatively low amplitudes, in which one of the peaks corresponds to limit cycle oscillations. When we increase the Reynolds number further, the frequency of oscillations shifts in the region of low frequency range as shown in Fig.7.7b. The FFT shows two peaks (Fig. 7.7b) in the low frequency range. One of the peaks corresponds to the frequency of the limit cycle in region II of Fig. 4.6. During this operating condition, the oscillations are predominant with a frequency of 155 Hz at an amplitude of 163 Pa, instead of 258 Hz and 1224 Pa (Fig. 7.7a). These resulting changes of the predominance of oscillations happen through a frequency jump. Then the system goes through a regime of intermittency. The intermittent occurrence of periodic oscillations increases the spectral content at low frequencies as shown in Fig. 7.3b. That is, we can say that the burst oscillations occur apparently randomly, at a time scale larger than the acoustic

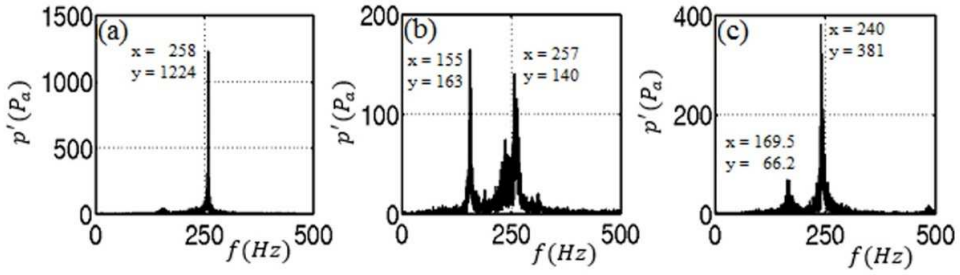

Figure 7.7: Represents the FFT's corresponds to the transition from limit cycle oscillations to irregular burst oscillations through a frequency jump. Figure 7.7a, corresponds to a flow Reynolds number of 3.3 x 10^4 and mass flow rate of air is 18.8 g/s. Equivalence ratio, $\phi = 0.52$. Figure 7.7b, corresponds to a flow Reynolds number of 3.5 x 10^4 and mass flow rate of air is 19.8 g/s. Equivalence ratio, $\phi = 0.46$. Figure 7.7c, corresponds to a flow Reynolds number of 3.9 x 10^4 and mass flow rate of air is 21.7 g/s. The fuel flow rate is maintained at 1.1 g/s. Equivalence ratio, $\phi = 0.42$.

time scale. When we increase the Reynolds number of flows beyond this value, the frequency and amplitude of oscillations increases further as shown in Fig. 7.7c. Now the combustor exhibits irregular burst oscillations. That is, the pressure oscillations switch from high amplitude to low amplitude in an irregular manner.

7.1.4 Irregular burst oscillations (Region III, Fig. 4.5)

At a Reynolds number of about 3.9 x 10^4 (21.7 g/s air flow rate, $\phi = 0.42$), the pressure signal consists of loud and quiet zones as shown in Fig. 7.8a and the corresponding FFT is shown in Fig. 7.7c. That is the system undergoes occasional irregular burst oscillations, which interrupts the periodic motion of the system. Thus the behaviour of the system switches back and forth between the loud (periodic) and quiet (aperiodic) zone. Such a behaviour in a gas turbine combustor was reported by Hong *et al.* (2005, 2008a, 2008b) and Arndt *et al.* (2010). These apparent periodic (loud) fluctuations for a particular time interval are called "laminar phases" (Note that this is not the same as laminar flows) (Pomeau and Manneville 1980, Schuster, 2005). Figure 7.8b shows the short interval FFT of the laminar phase with a predominant frequency indicating periodic behaviour. The corresponding time traces (short interval) of pressure signal are shown in the inset. The FFT of the quiet phase is shown in Fig. 7.8c and is similar

to the time series during the occurrence of combustion noise. These quiet phases are randomly and abruptly disturbed by burst oscillations that have a finite duration. We can identify the burst oscillations by the amplitude of the acoustic field while operating the combustor. Further reduction in the equivalence ratio up to 0.33, the combustor undergoes blowout. Thus, these irregular burst oscillations are interpreted as the signature prior to the combustor blowout.

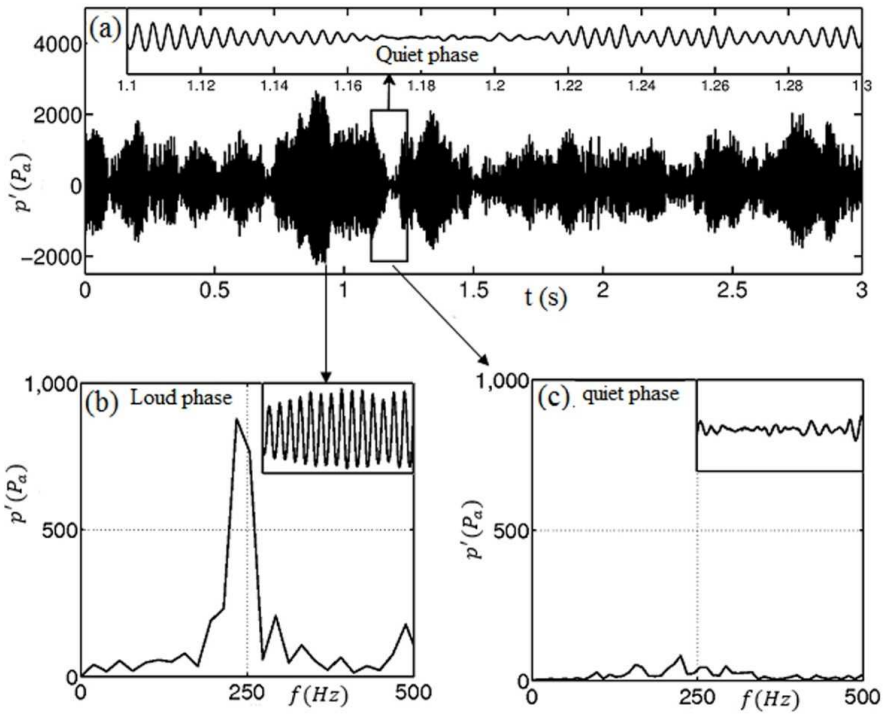

Figure 7.8: Time traces pressure signal and the FFT are corresponding to noisy and quiet phase with time trace of pressure signals at the inset for the flow Reynolds number of 3.9 x 10^4. Mass flow rate of air is 21.7 g/s and fuel flow rate maintained at 1.1 g/s. Equivalence ratio $\phi = 0.42$.

Nair *et al.* (2013a) observed similar kind of behaviour prior to the onset of instability oscillations. However these irregular burst oscillations, that are originated at two different scenarios can be differentiated based on the rate of occurrence of loud (periodic/laminar) and quiet (aperiodic) phases in the signal. The rate of occurrence of high amplitude burst oscillations (laminar phases) become more frequent and last longer in time when the combustor approaches limit cycle oscillations and finally system attains limit cycle oscillations. On the other hand the rate of occurrence of low amplitude oscillations (quiet phases) become more frequent and last longer in time when the combustor

approaches blowout and eventually system attains blowout condition.

These complex irregular bursting behaviours, which is the signature near the combustor blowout, can be studied by plotting the phase plot and return maps of the acquired pressure data corresponding to this regime. Thus we can avoid blowout during the unwanted situations by implementing the necessary measures in the system, like that reported by Muruganandam *et al.* (2012) and Muruganandam and Seitzmann (2005).

Reconstructed phase portrait and return map for the irregular burst oscillations

Figure 7.9 is the phase portrait corresponding to the irregular burst oscillations in the combustor.

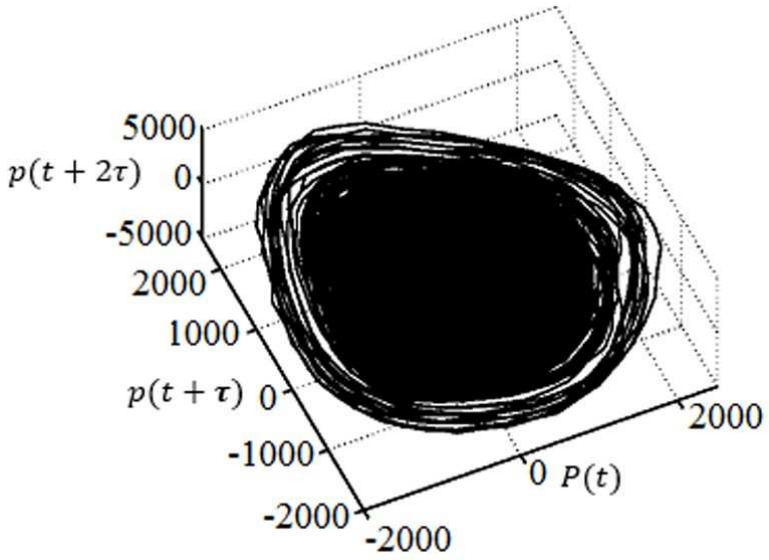

Figure 7.9: Phase portrait corresponding to the irregular bursts. The air flow Reynolds number is 3.9 x 10^4. The mass flow rate of air is 21.7 g/s and fuel flow rate is maintained at 1.1 g/s. Equivalence ratio, $\phi = 0.42$.

The outer trajectory of the phase portrait shows a high amplitude oscillation zone similar to the case of limit cycle oscillations. However the inner trajectory of the phase portrait shows a low amplitude oscillation zone similar to the combustion noise. These high and low amplitude regions have been referred to as noisy and quiet regions respectively by Arndt *et al.* (2010). That is the combustor possibly undergoes reignition and

extinction (Stohr 2011). In nonlinear dynamics this type of irregular burst oscillations is referred as intermittency.

Figure 7.10 shows the return maps corresponding to the intermittent burst oscillations, observed at an equivalence ratio of 0.42. During this period the points are spread all along the diagonal line. Lowering the global equivalence ratio further, these points move towards the high pressure zone and then back to low pressure zone as indicated in Fig. 7.10a and 7.10b respectively.

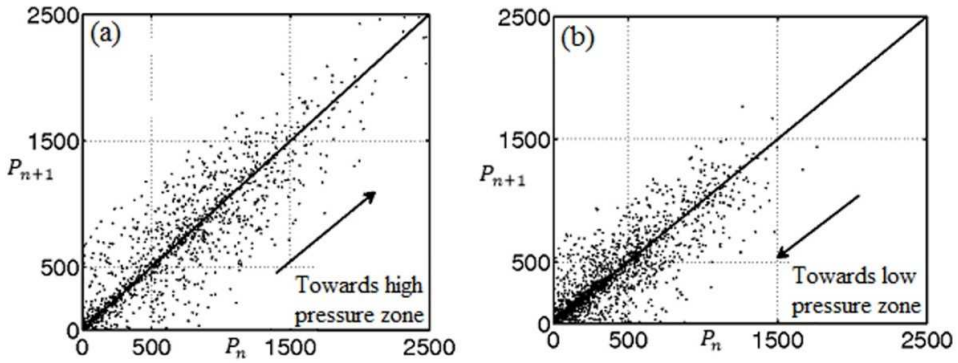

Figure 7.10: Return maps corresponding to the irregular burst: (a) Noisy phase. The air flow Reynolds number is 3.9 x 10^4. Mass flow rate of air is 21.7 g/s and fuel flow rate is maintained at 1.1 g/s. Equivalence ratio, $\phi = 0.42$. (b) Quiet phase. The air flow Reynolds number is 4.0 x 10^4. Mass flow rate of air is 22.7 g/s and fuel flow rate is maintained at 1.1 g/s. Equivalence ratio, $\phi = 0.40$.

The points clustered near to zero on the diagonal line correspond to low amplitude aperiodic oscillations (Fig.7.5b). In Fig. 7.10a the points move away from the zero point with a drift from diagonal line indicates the burst (laminar) phase, which represents periodic high amplitude oscillations. In Fig. 7.10b, the points moved towards the zero point along with the drift from diagonal line indicates the quiet (aperiodic) phase. The intermittent behaviour is the switching between these two phases as shown in Fig. 7.10a and 7.10b respectively.

This kind of irregular switching between periodic and aperiodic behaviour was observed by Kabiraj *et al.*(2012c, 2012b) and Kabiraj and Sujith (2012b) in a ducted premixed conical flame, when they varied the flame location beyond a particular point. They characterized these irregular switching between periodic and aperiodic behaviour

as intermittency (Abarbanel 1996, Klimaszewska and Zebrowski 2009, Hilborn 2004). They reported that the system behaviour exhibits transitions from low amplitude to high amplitude oscillations and characterized it as intermittency.

The same kind of behaviour was studied theoretically in the pioneering work of Pomeau and Manneville (1980) on dissipative dynamical systems during the transition of a stable periodic behaviour to an unstable chaotic behaviour. They found that the fluctuations are apparently periodic during long time intervals called laminar phases (quiet phase) and this regular periodic behaviour is disrupted randomly and abruptly by a burst. A new laminar phase starts at the end of this finite duration burst. The instability of periodic motion occurs when the burst starts at the end of the laminar phase. For us, the burst phase is the same as laminar phase. That is the bursts/laminar phase is at high amplitude.

The complex combustor dynamics can also be visualized by analysing the patterns in the recurrence plots, which is a graphical representation of the hidden dynamical patterns and nonlinearities in the data and was explained in Chapter 6. Different behaviours of the dynamical system create different recurrence patterns (Klimaszewska and Zebrowski 2009).

7.2 Recurrence plots

These plots are introduced in this chapter to characterize the stable and unstable combustion dynamics of a swirl stabilized combustor at different operating conditions.

7.2.1 Recurrence plots for different operating conditions

Recurrence plots can be used to visualize the combustion dynamics of a swirl stabilized combustor at different operating conditions. By visualizing the trajectories in phase space, the recurrence plots display important and easily interpretable information about time series data. Different recurrence patterns in the plot indicate different behaviour of the dynamical system. Noise fills the plots with homogeneously distributed black points. Long lines parallel to the main diagonal of the recurrence plot are due to periodic orbits without noise. The occurrence of intermittency results in various char-

acteristic shapes or patterns in the recurrence plots. When intermittency occurs in a dynamical system, horizontal and vertical lines are obtained in the plot. These lines are corresponding to laminar phases (Klimaszewska and Zebrowski 2009).

Recurrence plot for limit cycle oscillations

Applying these techniques from dynamical system theory, the following characteristics of the partially premixed swirl stabilized combustor at different operating conditions were analysed. Figure 7.11 shows the recurrence plot for stable limit cycle oscillations with a ball size $\epsilon < 0.15$. The lines parallel to, but offset from the main diagonal indicates that the state of the system visit themselves multiple times the same region of an attractor at different times.

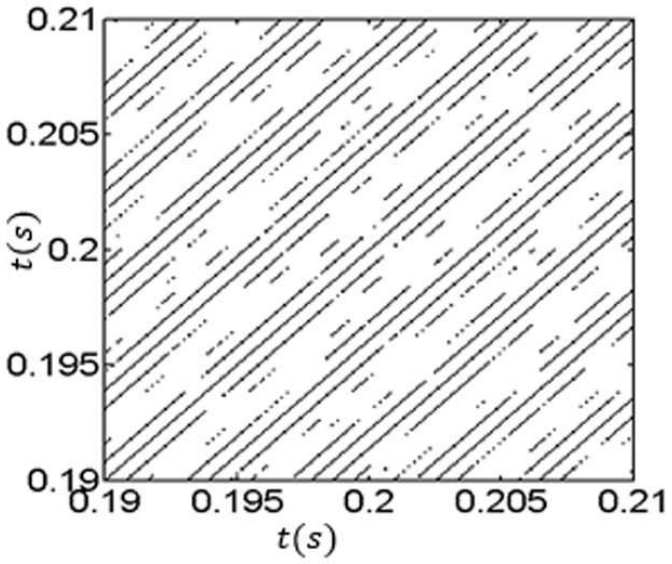

Figure 7.11: Shows the recurrence plot for the stable limit cycle oscillations. Flow Reynolds number is 2.6 x 10^4. Mass flow rate of air is 14.8 g/s and mass flow rate of fuel is maintained at 1.1g/s. Equivalence ratio, $\phi = 0.62$. Ball size, $\epsilon < 0.15$.

Equally spaced diagonal lines parallel to the main diagonal was observed by Kabiraj *et al.* (2012c) for the systems having periodic behaviour in the absence of noise. These sets of lines parallel to the main diagonal lines is the signature of limit cycle oscillations (Klimaszewska and Zebrowski 2009). However due to the presence noise and turbulence in the swirl stabilized combustors, gaps appear in the lines parallel to

the main diagonal line as shown in Fig. 7.11. Since the vertical distance between the diagonal line is constant, this plot represents the periodic limit cycle orbit.

Followed by limit cycle oscillations, a complex bifurcation of the combustor dynamics was observed at higher Reynolds numbers.

Recurrence plot for irregular bursts

Recurrence plots can also be used for analysing the occurrence of the irregular burst (intermittency) oscillations in a turbulent combustor. Figure 7.12a shows the recurrence plot for intermittency.

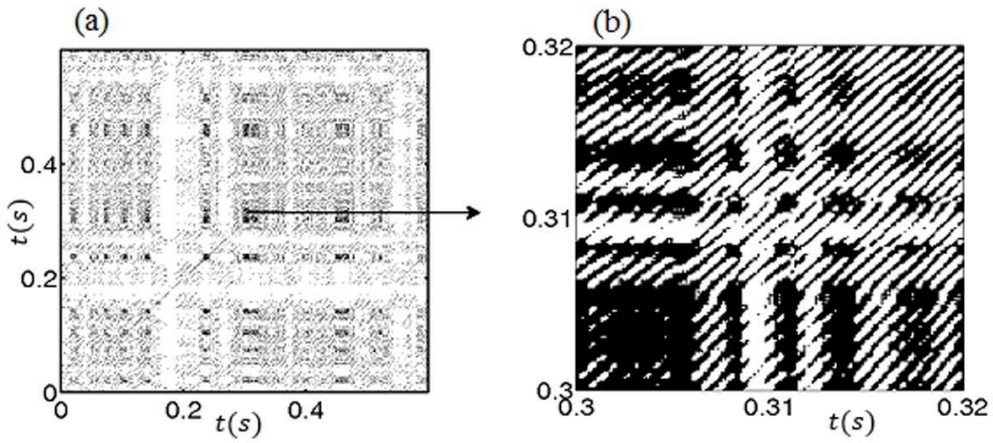

Figure 7.12: Shows the recurrence plot for the irregular burst oscillations. Flow Reynolds number is 3.9 x 10^4. Mass flow rate of air is 21.7 g/s and mass flow rate of fuel is maintained at 1.1g/s. Equivalence ratio, $\phi = 0.42$.

During the occurrence of intermittency in combustors, uniformly white perforated type structures and black patches (Klimaszewska and Zebrowski 2009) are observed in the recurrence plot as seen in the elongated structure shown in Fig. 7.12b. The white perforated structure corresponds to the system trapped in high amplitude regime (burst/laminar phase) and the black patches corresponds to the system trapped in low amplitude regime(quite phase). Figure 7.12b shows the zoomed view of the recurrence plot during intermittency.

Subsequent to intermittent behaviour, the combustor undergoes blowout. Therefore recurrence plots could be used to analyse the approach to blowout.

7.3 Interim Conclusions

This chapter describes an experimental investigation of the nonlinear characteristics of a turbulent combustor operating at different air flow rates up to blowout by maintaining constant fuel flow rate. Combustion dynamics prior to blowout regime was characterized by performing nonlinear time series analysis of the acquired pressure data up to blowout ($\phi = 0.33$). The transition characteristics from low amplitude noisy oscillations to high amplitude limit cycle oscillations was observed by increasing the air flow Reynolds number or decreasing the global equivalence ratios. Further lowering the equivalence ratio, irregular bursts were formed prior to blowout. These combustion dynamics at different operating condition of the combustor were analysed by phase space reconstruction and return map using nonlinear time series analysis. The combustor attain high amplitude oscillations when the attractor attains a periodic orbit (limit cycle). However the intermittent behaviour was observed when the oscillations switching back and forth between a quiet state and a high amplitude state. These states are also characterized through the application of recurrence plots. The intermittency in our system is characterized by analysing the intermittent state using recurrence plots. Subsequent to this intermittent behaviour, the flame blowout occurs. Thus the lead up to blowout may be analysed by observing the intermittent behaviour.

CHAPTER 8

HIGH SPEED IMAGING OF THE TURBULENT REACTING FLOW-FIELD

High-speed digital images of the CH* chemiluminescence were acquired simultaneously with pressure data at a recording speed of 1000 fps using a Phantom V12.1 high speed camera with CH* filter (transmission peaks around a wavelength of 431nm and bandwidth of 10nm) at a resolution of 1280 x 800 pixels. The flame images corresponding to the stable combustion, limit cycle oscillations and irregular burst oscillations were acquired simultaneously with a pressure data.

8.1 High- speed flame imaging during stable combustion

For higher values of equivalence ratios ($\phi \geq 0.5$), the flame is sustained on both inner and outer recirculation zones. Most of the time flame appears near to the combustion chamber wall. Figure 8.1 (b-e) represents the instantaneous images corresponding to the stable combustion (pressure amplitude $\leq$ 500Pa), with an equivalence ratio of 0.92. Similar images were presented by different authors (Hong *et al.*, 2005, 2008a, Arndt *et al.*, 2010).

8.2 High-speed flame imaging during Limit cycle oscillations

The transition from stable combustion to combustion with stable limit cycle oscillations occurs at an equivalence ratio of 0.62 with a pressure amplitude of about 1900 Pa.

Figure 8.2 (b-e) shows the sequence of images corresponding to limit cycle oscillations. Simultaneously extended and compacted images are observed during these

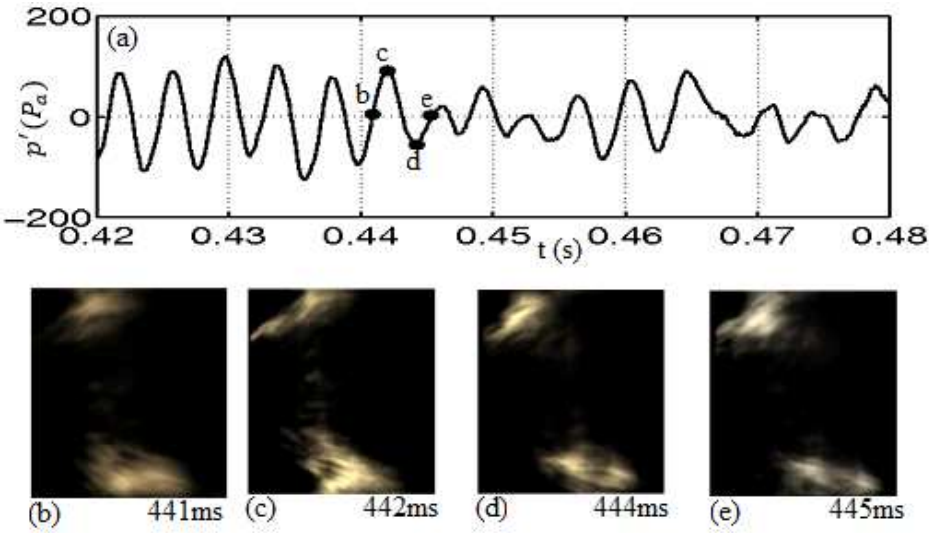

Figure 8.1: (a) represents the time trace of pressure signal, (b-e) represents the instantaneous flame images corresponding to the low amplitude combustion oscillations using a high- speed camera. Re = 1.8 x 10^4, $\dot{m}_a = 9.9g/sec, \dot{m}_f = 1.1g/s$ and $\phi = 0.92$..

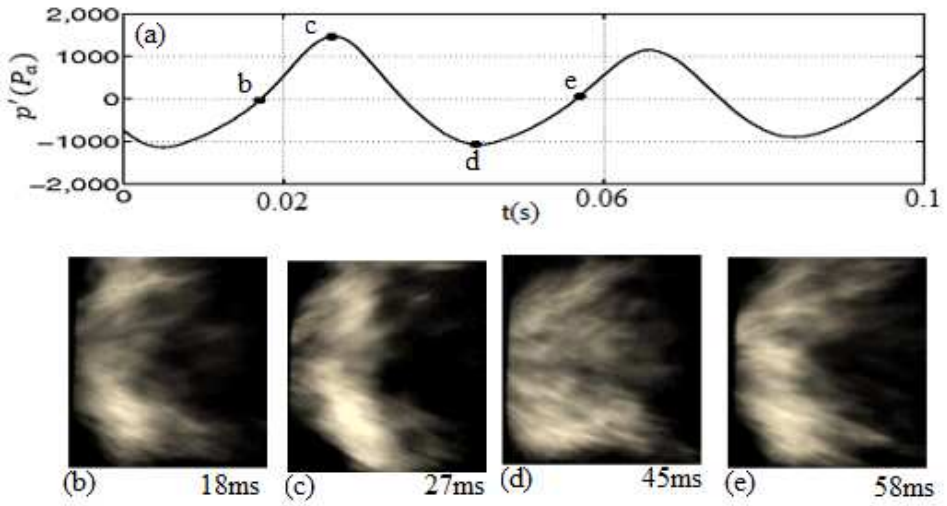

Figure 8.2: (a) represents the time trace of pressure signal, (b-e) represents the instantaneous flame images corresponding to limit cycle oscillations using a high-speed camera. Re = 2.6 x 10^4, $\dot{m}_a = 14.8g/s, \dot{m}_f = 1.1g/s$ and $\phi = 0.62$.

oscillations. This is speculated due to the domination of vortices that are formed by the interaction between chamber acoustic and hydrodynamic instabilities (Schadow *et al.*.1989). They observed that the combustion which is initially at the core is proceeded towards downstream due to the presence of vortices. We observed low and high amplitude pressure oscillations when the flame is compacted near (Fig.8.2 b and e) and extended (Fig 8.2 c and d) away from the dump plane. This may be due to the influence of phase between pressure and heat release rate fluctuations. The main reaction zone is located near the dump plane. At this zone the periodic ignition of the flame, the growth of flame, flame burnout and ignition source entrainment into fresh fuel and air mixture occur repetitively. Similar kind of flame structure was observed by Hong *et al.* (2008b).They represented as mode 1 flame behaviour.

8.3 High-speed flame imaging during irregular burst oscillations

Figure 8.3 shows the sequence of flame images for an equivalence ratio of 0.42. For low values of equivalence ratios, a conical flame is sustained by an inner recirculation zone. The flame in the outer recirculation zone appears and disappears during this operating condition. Such type of behaviour was observed by Hong *et al.* (2008b). They represented as mode 2 flame behaviour, which shows alternate noisy and silent periods sequentially. We observed the occurrences of high amplitude pressure oscillations when the flame with conical shape is attached (Fig. 8.3 (b-f)) near to the dump plane. However low amplitude pressure oscillations are established during the detachment (Fig. 8.3h) from the dump plane and subsequent stabilization at an axial position. An M-like shape is observed during the quiet state as shown in Fig. 8.3g. Similar results were shown by Arndt *et al.* (2010) in a gas turbine model combustor. They observed that the flame undergo lift- off during the transition from the noisy state to quiet state. However, the flame reattached during the transition from quiet state to noisy state. This type of transition is called intermittency in dynamical system theory. We observed a dark (low amplitude) region during intermittency in the flame as shown in Fig. 8.3i. These regions are speculated to be due to local extinction within the flame zone.

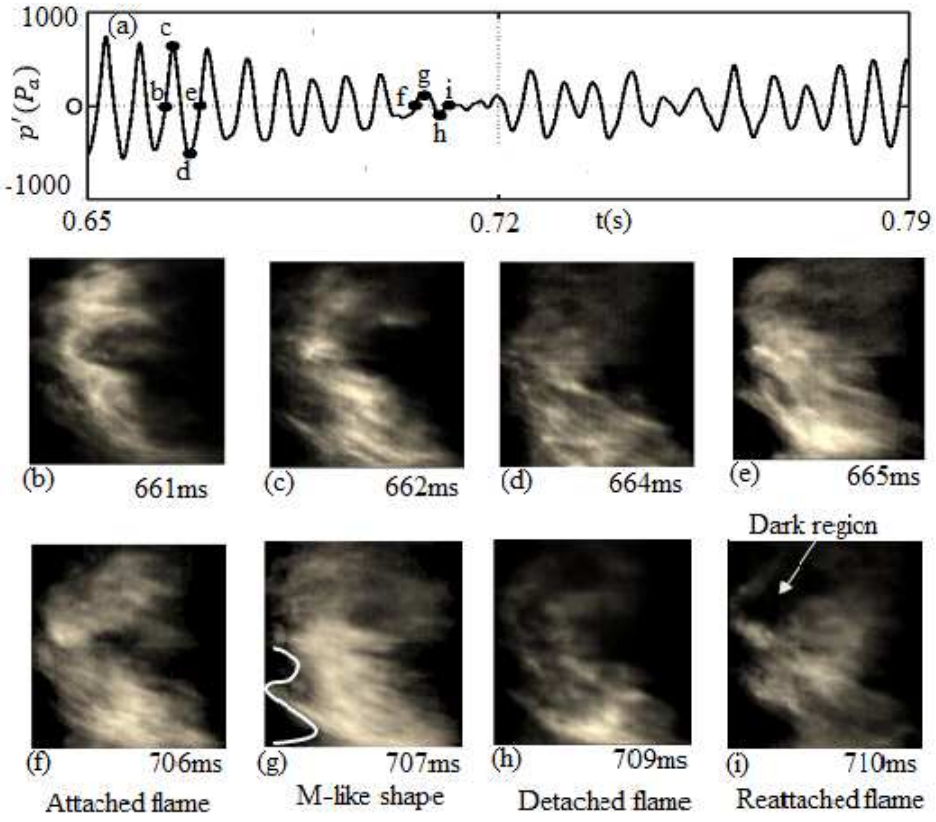

Figure 8.3: (a) represents the time trace of pressure signal, (b) represents the instantaneous flame images corresponding to the combustion with irregular bursts (intermittency) by a high-speed camera. Re = 3.9 x 10^4, $\dot{m}_a = 21.7g/s, \dot{m}_f = 1.1g/s, \phi = 0.42$. Figures b-e represents the sequence images corresponding to the periodic high amplitude oscillations (burst phase). Figures 8.3 f-i represents the sequence of images corresponding to the aperiodic low amplitude oscillations (quiet phase).

8.4 Interim summary

The complex flame dynamics was visualized by using chemiluminescence high-speed flame images. Flames images that correspond to low amplitude oscillations near to the dump plane indicate stable combustion. However the extended and compacted images of the flame indicates limit cycle oscillations. The flame alternatively detaches and then reattaches at the dump plane during the intermittent state. The reattachment may be because of reverse flow of hot gases within the central recirculation zone. Dark zones are also observed during the detachment and is speculated to be due to local extinction.

CHAPTER 9

CONCLUSION AND FUTURE WORK

The present research work describes an experimental investigation of the nonlinear characteristics of a partially premixed swirl stabilized combustor operating at different air flow rates by maintaining a constant fuel flow rate. Bifurcation diagram indicates that the combustor undergoes a transition from low amplitude chaotic oscillations (combustion noise) to high amplitude limit cycle oscillations on increasing the air flow Reynolds number which in turn decreases the global equivalence ratios. Lowering the equivalence ratio further, the combustor switches between periodic burst oscillations and low amplitude aperiodic oscillations in an apparently random fashion.

Significant information regarding the dynamical pattern and inherent nonlinearity associated with combustion dynamics at different operating conditions are shown qualitatively through phase portraits, return maps, and recurrence plots.

During stable combustion (chaotic oscillations), we observed that the attractor is near to the fixed point whereas during limit cycle oscillations the attractor attains a periodic orbit. The intermittent behaviour was observed when the oscillations were moving back and forth between a quiet state (near fixed point) and a high amplitude state (near to the periodic regime). These states are also characterized through the application of recurrence plots. The precursor to an impending instability is investigated by estimating the recurrence rate, average trapping time and by Shannon entropy of the combustor dynamics in a particular state. This helps to warn an operator of fielded systems sufficiently early so that necessary control measures can be adopted to avoid unwanted oscillations. Thus, we can increase the stability margin of the combustor. We determined a threshold value for the safe operation of the combustor using 0-1 test, which helped to increase the operational boundary of the practical combustors.

The dynamics of the system prior to blowout condition were characterized by analyzing the patterns observed in the recurrence plots. Thus we established that the intermittency is a signature prior to blowout.

The intermittency in our system is characterized by analyzing the intermittent state using recurrence plots. Such type of oscillations is observed in turbulent combustors prior to combustion instability and blowout. Thus, intermittency can be considered as a characteristic feature of any turbulent flow field which presages the imminent events such as combustion instability and blowout. Thus, it would be interesting to verify the generality of such intermittent states in any flow field, irrespective of whether laminar or turbulent. It would also be interesting to declare the proposed method for identifying the precursors of imminent events and for fixing a threshold value for a stable limit in any kind of flow fields.

The complex flame dynamics was visualized by using high-speed flame images. The flame image that corresponds to low amplitude oscillations near to the dump plane indicates stable combustion. However with the extended and compacted flame with respect to the dump plane indicate limit cycle oscillations. The flame alternatively detaches and reattaches at the dump plane during the intermittent state. The reattachment is because of reverse flow of hot gases within the central recirculation zone. Dark zones are also observed during the detachment and is speculated to be due to local extinction.

APPENDIX A

DETECTION AND CONTROL UNITS FOR COMBUSTION INSTABILITIES

A.1 Detection unit based on 0-1 test for detecting the onset of instabilities.

Figure A.1 shows the block diagram comprising the components used in the system for detecting instability for a device such as a combustor using 0-1 test.

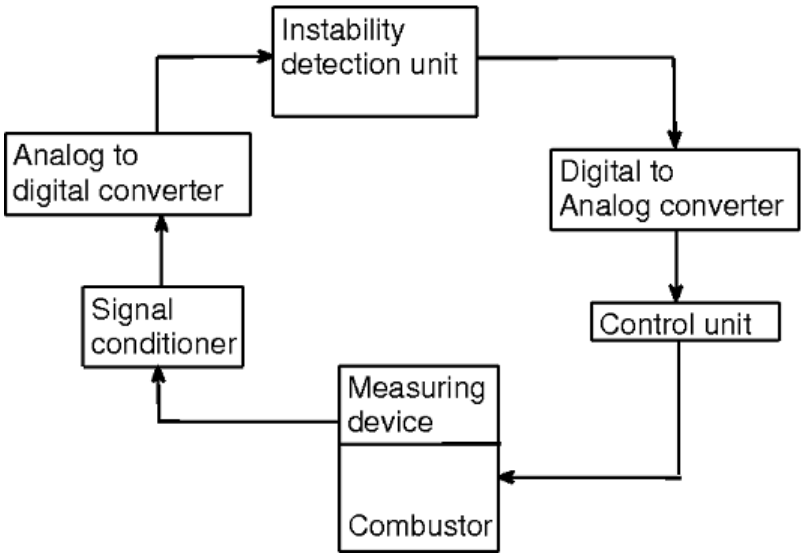

Figure A.1: shows the block diagram of a system for early detection of onset of instabilities in practical systems using 0-1 test.

The system consists of a measuring device; signal conditioner, analog to digital convertor, instability detecting unit, Digital to analog convertor and a control unit. .

Measuring device: The measuring device is configured to generate signals corresponding to the dynamics occurring inside the combustor. This is provided on the device which is to be prevented from instability oscillations for indicating the instabilities.

Signal conditioner: The analog signal coming from the measuring unit is manipulated using a signal conditioner to satisfy the requirement for an analog to digital

convertor.

Analog to digital convertor: The analog to digital convertor converts the analog signal to digital signal such that the signal can be processed in the instability detecting unit.

Instability detection unit: The instability detecting unit is configured to measure the stability of the combustor from the signal generated by the dynamics inside the combustor. Based on the time series signal generated by the measuring device, this instability detecting unit diagnose whether the dynamics of the combustor is chaotic/noisy or non- chaotic/ periodic.

Analysis of the signal by the detector unit: The signal $\phi(j)$ is measured such that the measured value at each instant provides essentially no information about future values. To accomplish this, the instability detection unit sample the measured signal at time interval corresponding to the first minimum of the average mutual information of the signal $\phi(j)$.

Digital to analog convertor: The digital to analog convertor converts the digital signal coming from the instability detecting unit to an analog signal suitable for the control unit.

Control unit- The control unit is configured to control various operating parameters in the combustor as per the information coming from the instability detecting unit. Thus avoid the occurrence of combustion instability.

In this test from the available spectrum of a dynamical system we determine the binary quality such as 0-1. The nature of the dynamical system is irrelevant for employing this method. This method is applicable to data generated from maps, ODE, PDE and is also applicable to noisy experimental data.

A.2 Detection unit based on burst method for detecting the onset of instabilities

Early detection of onset of instabilities can be obtained by counting number of intermittent bursts in the measured signal preceding the transition to instability from chaos.

The system consists of a measuring device, a sensor, an instability detecting unit (not shown in figure), and a control unit.

Measuring device: The measuring device is configured to generate signals corresponding to the dynamics occurring inside the combustor. This is provided on the device which is to be prevented from instability oscillations for indicating the instabilities.

Sensor: The unit also includes a sensor configured to acquire signal from the device to which the system is incorporated. The acquired signal then reaches the instability detection unit where the instability is determined.

Instability detection unit: The instability detection unit diagnose the stability of the combustor from the signals that are generated by the measuring device. This is a programmed unit that requires the sampling rate (Fs) for which the signal is obtained. The signal is acquired such that the sampling rate is approximately 10 times the maximum frequency (Fmax) one wishes to prevent, as any device generally starts the operation at a stable condition. In our experiment the sampling rate at which the signal is obtained is related to the location of the minimum of average mutual information (τ_{min}). Thus the obtained sampling rate for which the signal could be revised as Fs = 10/ ÏĎmin. After fixing the sampling rate the system could be used for detecting the precursor to instability oscillations. The detection unit generate appropriate signals corresponding to the instability oscillations and transfer the signals to the control unit.

Control unit: This unit controls the various operating parameters of the combustor based on the information obtained from the instability detection unit. A suitable threshold is set for the number obtained by the instability detection unit such that when the threshold is crossed, the control unit suitably ensures that the combustor remains in stable operating condition, by controlling various parameters in the combustor thereby increasing the stability margin of the combustor.

The onset of instabilities in the combustor is determined by examining the bursts generated within the device prior to instability. Bursts refer to a sudden spike in the amplitude of the measured signal which decays after a short duration. The occurrence of such bursts in the measured signal leads to an intermittent switching behaviour of the signal between low and high amplitudes. In high Reynolds number flow devices where the transition from chaotic behaviour to oscillatory instability happens through

intermittent bursts. Similar kind of behaviour is common in systems with high levels of noise in which the transition to instability happens through a region characterized by intermittent bursts.

A.3 Peak method for detecting the onset of instabilities

The onset of impending instabilities is determined by counting the number of peaks (N) in the signal above a user defined threshold ξ for a time duration t. The threshold ξ would correspond to the acceptable levels of amplitude of the combustor. This unit includes a signal conditioner, threshold logic, a comparator, a gating signal, a counter and a control unit. The control unit further includes at least one digital to analog converter, an air flow controller and fuel flow controller as shown in Fig. A.2. The signal generated inside the combustor is determined by means of appropriate sensors (not shown in Fig.). Further the measured signal is amplified by the signal conditioner. The gating signal generated by an internal gating circuit controls the time duration t of signal acquisition. The threshold logic includes fixed threshold ξ, such that when the threshold logic is applied on the gated signal, the peak in the signal above the threshold ξ is determined. The measured signal is compared with the threshold ξ of the signal by a comparator. A counter is included in the circuit for counting the number of peaks in the signal above the threshold ξ.

The occurrence of burst in the signal increases the amplitude of pressure signal beyond the threshold value and the threshold logic circuit generates a signal indicating the occurrence of peak above the threshold. Further, the counter counts the number of peaks within the gating period (N) and transmits the information based on this number (N) to the control unit. The control unit includes the air flow controller, which regulate the functioning of air flow control valve and fuel flow controller to regulate the functioning of fuel flow control valve, both of which can be adjusted such that the combustor is prevented from instabilities. A digital to analog converter is provided to convert the digital signal coming from the control unit to analog signal for use in air flow controller and fuel flow controller.

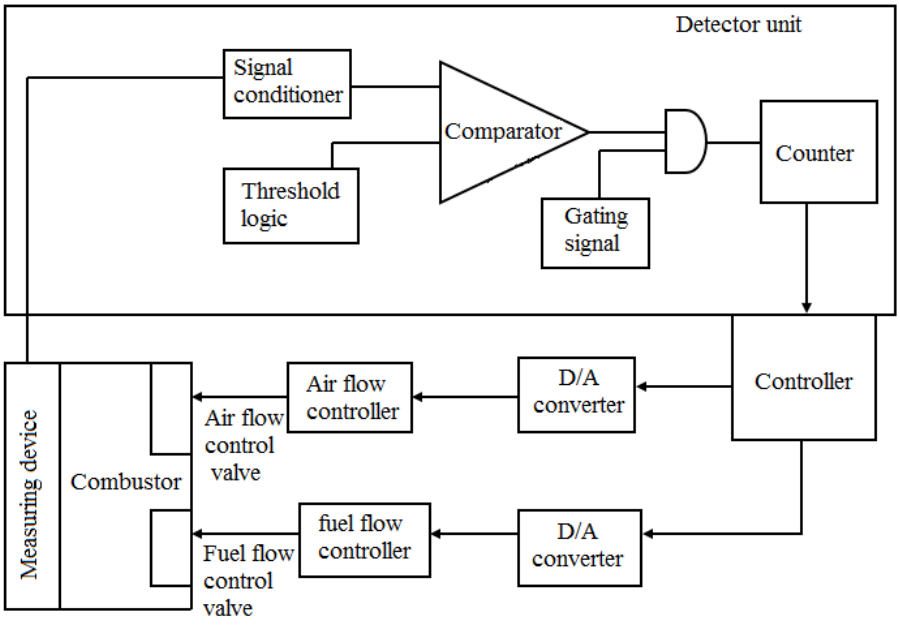

Figure A.2: shows the block diagram of a system for early detection of onset of instabilities in practical systems by counting the burst behaviour generated within the combustor.

A.4 How to apply the tools of dynamical system theory for an experimental data

At first we have to acquire time series data of a parameter (say pressure, $p(t)$). This time series data consists of inherent dynamics of a system from which we acquire data. To unfold the dynamics we have to reconstruct the acquired time series data in a higher dimensional space using Takens' time delay embedding method, which is called phase portrait. The delay period τ for formulating the state space vectors $p(t+\tau)$, $p(t+2\tau)$ can be determined from average mutual information method (see Chapter 5). The embedding dimension suitable for reconstruction of phase portrait is determined by using Cao's embedding method (see Chapter 5). We can also plot return maps (see Chapter 5) for getting more information about the inherent dynamics of the system. For understanding the hidden dynamical pattern we have used recurrence plots during different operating conditions.

REFERENCE

1. **Altay, H. M., R. L. Speth, D. E. Hudgins,** and **A. F. Ghoniem** (2009). The impact of equivalence ratio oscillations on combustion dynamics in a backward-facing step combustor. *Combustion and flame dynamics,* **156**, 2106 - 2116.

2. **Bender, C., F. Zhang, P. Habisreuther, H. Buchner,** and **H. Bockhorn.**, chapter 2, *Measurement and simulation of combustion noise emitted from swirl burners. Combustion noise*, Springer, Nov 2008.

3. **Candel, S.** and **D. Durox**, (2004). Flame interactions as a source of noise and combustion instabilities. 10th AIAA/CEAS Aeroacoustics Conference, *AIAA* 2004 - 2928.

4. **Candel, S** (2002). Combustion dynamics and control: Progress and challenges, *Proceedings of the Combustion Institute*, **29**, 1-28.

5. **Chiu, H. H.** and **M. M. Summerfield**, *Theory of combustion noise*. Acta austronautica, vol.1, 967 âĂŞ 984, Pergamon Press, 1974.

6. **Culick, F. E. C.** (1994). Some recent results for nonlinear acoustics in combustion chamber. *AIAA Journal*, **32**(1), 146-169.

7. **Culick, F. E. C.** (2006). Unsteady motions in combustion chambers for propulsion systems, Vol. AG-AVT-039, RTO AGARDograph.

8. **Dowling, A. P.** (2003). The challenges of lean premixed combustion. *Proceedings of the international gas turbine congress*, November 2-7, IGTC2003 Tokyo KS-5.

9. **Ducruix S., T. Schuller, D. Durox,** and **S. Candel** (2005). Combustion instability mechanisms in premixed combustors. *progress in Astronautics and Aeronautics*, AIAA, Virginia, **210**.

10. **Durox, D., T. Schuller,** and **S. Candel** (2002). Self-induced instability of a premixed jet flame impinging on a plate. *Proceedings of the combustion institute*, **29**, 69 - 75.

11. **Fichera, A., C. Losenno** and **A. Pagano** (2001). Experimental analysis of thermoacoustic combustion instability. *Applied Energy*, **70**, 179-191.

12. **Fritsche, D., M. Furi** and **K. Boulouchos** (2007). An experimental investigation of thermoacoustic instabilities in a premixed swirl-stabilized flame. *Combustion and Flame*, **151**, 29-36.

13. **Gotoda. H., H. Nikimoto, T. Miyano,** and **S. Tachibans** (2011). Dynamic properties of combustion instability in a lean premixed gas turbine combustor. American institute of physics, *chaos*, **21**, 013124, 1-11.

14. **Gouldin F. C., R. N. Halthore,** and **B.T. Vu** (1984). Periodic oscillations observed in swirling flows with and without combustion, *20th symposium (international) on combustion/ The combustion institute*, 269 - 276.

15. **Grinstein F. F.** and **C. Fureby** (2005). LES studies of the flow in a swirl combustor. *Proceedings of the combustion institute*, Pittsburgh PA, **30**, 1791- 1798.

16. **Hilborn, R. C.,** *Chaos and Nonlinear Dynamics: An Introduction for scientist and Engineers*. Second Edition. Oxford University Press, 2000.

17. **Hong, J. G., K. C. Oh, U. D. Lee** and **H. D. Shin** (2008). Generation of Low-Frequency Alternative Flame Behaviours in a Lean Premixed Combustor. *Energy & Fuels*, **22**, 3016-3021.

18. **Hong, J. G., U. D. Lee, K. C. Oh, H. D. Shin, K. Tanaka, S. Tanimura,** and **K. Fuji** (2005). An effect of fuel flow modulation on the combustion instability in a model gas turbine combustor. *5th Asia - pacific conference on combustion*, the university of Adelaide, Adelaide, Australia, 17-20.

19. **Huang. Y.** and **Y. Vigor** (2005). Effect of swirl on combustion dynamics in a lean- premixed swirl stabilized combustor. *Proceedings of the combustion institute*, **30**, 1775-1782.

20. **Kabiraj L., A. Saurabh, P. Wahi** and **R. I. Sujith** (2012). Route to chaos for combustion instability in ducted laminar premixed flames. *Chaos*, **22**, 023129.

21. **Kabiraj, L.** and **R. I.Sujith** (2012b). Nonlinear self-excited thermoacoustic oscillations: intermittency and flame blowout, *Journal of Fluid Mechanics*, **713**, 376- 397.

22. **Kim, K. T., J.G. Lee, B.D. Quay** and **D. Santavicca** (2011). Experimental investigation of the nonlinear response of swirl-stabilized flames to equivalence ratio oscillations. *Journal of Engineering for Gas Turbines and Power*, **133**, (021502), 1 - 8.

23. **Klimaszewska, K.** and **J.J. Zebrowski** (2009). Detection of the type of intermittency using characteristics patterns in recurrence plots, *Physical Review E*, **80**, 1-14, (026214).

24. **Lauterborn, W.** (1996). Nonlinear dynamics in Acoustics. *Acustica*, acta acustica, **82**, Suppl.1.

25. **Lieuwen.T., H. Torres, C. Johnson, B. R. Daniel** and **B. T. Zinn** (2001). A Mechanism for Combustion Instabilities in Premixed Gas Turbine Combustors. *Journal of Engineering for Gas Turbines and Power*, **123**(1), 182-190.

26. **Manneville. P,** and **Y. Pomeau** (1979). Intermittency and the Lorenz model. *Physics letters*, 24th December, 75A (1.2).

27. **Najm H. N.** and **A. F. Ghonim** (1994). Coupling between vorticity and pressure oscillations in combustion instability. *Journal of Propulsion and Power*, **10**, 769-776.

28. **Palies. P., D. Durox, T. Schuller** and **S. Candel** (2010). The combined dynamics of swirler and turbulent premixed swirling flames. *Combustion and flame*, **157**, 1698 - 1717.

29. **Paschereit, C.O., E. Gutmark,** and **W. Weisenstein** (1999). Coherent structures in swirling flows and their role in acoustic combustion control. *Physics of fluids*, **11**(9), 2667-2678.

30. **Polifke, W.,** VKI Lecture Series. March, 2004.

31. **Rayleigh, J. S. W.** (1878). The explanation of certain acoustical phenomena. *Nature*, **18**, 319-321.

32. **Reddy A.P., R. I. Sujith,** and **S.R. Chakravarthy** (2006). Swirler flow field characteristics in a sudden expansion combustor geometry, *Journal of propulsion and power*, **22**(4), July âĂŞ August 2006.

33. **Samaniego, J. M., B. Yip, T. Poinsot,** and **S. Candel** (1993). Low- FrequencyCombustion Instability Mechanisms in a Side-Dump Combustor. *Combustion and Flame*, **94**, 363 - 380.

34. **Shadow, K. C.** (2001). Combustion Dynamics: Passive Combustion Control. Paper presented at the RTO AVT Course on Active Control of Engine Dynamics held in Brussels, Belgium, 14-18 May and published in RTO-EN-020.

35. **Strahle, W. C.** (1971). On combustion generated noise. *Journal of Fluid Mechanics*, **49**(02), 399-414.

36. **Syred. N.** and **M. Beer** (1974). Combustion in swirling flows: A Review. *Combustion and Flame*, **23**,143-201.

37. **Yu, K. H., A. Trouve,** and **J. W. Daily** (1991). Low frequency pressure oscillations in a model ramjet combustor. *Journal of Fluid Mechanics*, **232**, 47-72.

38. **Takens. F.,** Detecting strange attractors in turbulence. In **R. David** and **L. S. Young** (eds), *Dynamical systems and Turbulence: Lecture Notes in Mathematics*, volume 898, Springer Berlin/ Heidelberg, Warwick, 1980, 366-381. .

39. **McManus, K. R., T. Poinsot,** and **S. M. Candel** (1993). A review of active control of combustion instabilities, *Progress in Energy and Combustion Science*, 19, 1-29.

40. **Rogers, D. E.** and **F. E Marble** (1956). A mechanism for high-frequency oscillation in ramjet combustors and afterburners, *Jet Propulsion*, Copyright by American Rocket Society, 456-462.

41. **Strahle, W. C.** (1978). Combustion noise, *Progress in Energy and Combustion Science*, **4**, 157-176.

42. **Nair, V., G. Thampi,** and **R. I. Sujith** (2013a). Intermittent bursts presage the onset of instability in turbulent combustors, *n3l - Int'l Summer School and Workshop on Non-Normal and Nonlinear Effects in Aero and thermoacoustics*, June 18-21, Munich.

43. **Schwarz, A.** and **J. Janicka** (eds), *Combustion noise*, Springer-Verlag, XVII, 291p, 2009.

44. **Chakravarthy, S. R., R. Sivakumar,** and **O.J Shreenivasan** (2007a). Vortex-acoustic lock-on in bluff-body and backward-facing step combustor, *Sadhana*, **32**, 145-154.

45. **Chakravarthy, S. R., O.J Shreenivasan, B. Boehm, A. Dreizler,** and **J. Janicka** (2007b) Experimental characterization of onset of acoustic instability in a non-premixed half-dump combustor, *Journal of the Acoustical Society of America*, **122**, 120-127.

46. **Huang, Y.** and **V. Yang** (2009). Dynamics and Stability of lean premixed swirl stabilized combustion. *Progress in energy and combustion science*, **35**, 293-364.

47. **Komarek, T.** and **W. Polifke** (2010). Impact of swirl fluctuations on the flame response of a perfectly premixed swirl burner, *Journal of Engineering for Gas Turbines and Power*, **132** (061503), 1-7.

48. **Sutton, G. P.** and **O. Biblarz**. *Rocket propulsion elements*. 7th ed. John Wiley and sons; 2000.

49. **Mongia, H. C., T. J. Held, G. C. Hsiao,** and **R. P. Pandalai**. *Incorporation of combustion instability issues into design process, GE aero-derivative and aero engines experience*. Chapter 3, In: **T. Lieuwen** and **V. Yang**, (eds), *Combustion Instabilities in Gas Turbine Engines: Operational Experience, Fundamental Mechanisms, and modelling*, 210, Progress in Astronautics and Aeronautics, (2005), 43- 63.

50. **Broda J. C., S. Seo, R. J. Santoro, G. Shirhattikar** and **V. Yang** (1998). An experimental study of combustion dynamics of a premixed swirl injector, *Proceedings of the combustion institute*, **27**, 1849-1856.

51. **Seo, S.** (2003). Combustion instability mechanism of a lean premixed gas turbine combustor, *KSME International Journal*, **17**(6), 906-913.

52. **Huang, Y.** and **V. Yang** (2004). Bifurcations of a flame structure in a lean premixed swirl stabilized combustor: transition from stable to unstable flame, *Combustion and Flame*, **136**, 383-389.

53. **Lieuwen, T. C.** (2002). Experimental investigation of limit cycle oscillations in an unstable gas turbine combustor, *Journal of Propulsion and Power*, **18**(1), 61-67.

54. **Sterling, J. D.** (1993). Nonlinear analysis and modelling of combustion instabilities in a laboratory combustor, *Combustion Science and Technology*, **89**,167-179.

55. **Kabiraj, L., R. I. Sujith,** and P. Wahi (2012). Investigating the dynamics of combustion driven oscillations leading to lean blowout, *Fluid Dynamics Research*, **44**, 1-12.

56. **Kabiraj, L.** and **R. I. Sujith** (2012). Bifurcation analysis and Observation of intermittency in combustion-driven thermoacoustic oscillations, *AIAA*, 1-11.

57. **Jahnke, C. C.** and **F.E.C. Cuclik** (1994). An application of dynamical systems theory to nonlinear combustion instabilities, *Journal of Propulsion and Power*, **10** (4), 508-517.

58. **Kabiraj, L., R. I. Sujith,** and **P. Wahi** (2011). Experimental studies of bifurcations leading to chaos in a laboratory scale thermoacoustic system, *Proceedings of ASME Turbo Expo* June 6-10, Vancouver, Canada. GT 2011-46149.

59. **Kabiraj, L., A. Saurabh, R. I. Sujith,** and **P. Wahi** (2012). Bifurcations of self-excited ducted laminar premixed flames, *Journal of Engineering for Gas Turbines and Power*, **134** (3), 031502.

60. **Hong, J. G., K. C. Oh, U. D. Lee,** and **H. D. Shin** (2008b). Effect of the unmixedness of unburned gases on the pressure fluctuations in a dump combustor, *Energy and Fuels*, **22**, 2221-2228.

61. **Arndt, C. M., A.M. Steinberg, I.G. Boxx, W. Meier, M. Aigner,** and **C.D. Carter** (2010). Flow-field and flame dynamics of a gas turbine model combustor during transition between thermoacoustically stable and unstable states, *Proceedings of ASME Turbo Expo 2010; Power for Land Sea and air* GT2010, June 14-18, Glasgow, UK, 1-11.

62. **Strogatz, S. H.,** Nonlinear Dynamics and Chaos: With Applications To Physics, Biology, Chemistry, And Engineering (Studies in Nonlinearity). Copy right by Westview press, 2001.

63. **Kabiraj, L** and **R. I. Sujith** (2012). Dynamics of thermoacoustic oscillations and lean flame blowout, *Proceedings of the ASME 2012 Turbine Technical Conferences & Exposition Turbo Expo*, June 11-15, Bella Center, Copenhagen, Denmark, GT 2012 - 68696.

64. **Nair, V., G. Thampi,** and **R. I. Sujith** (2014). Intermittency route to thermoacoustic instability in turbulent combustors, *Journal of Fluid Mechanics*, **756**, 470-487.

65. **Kabiraj, L., Saurabh, A., Karimi, N., Sailor, A., Mastorakos, E., Dowling, A. P.** and **Paschereit, C. O** (2015). Chaos in an imperfectly premixed model combustor. Chaos: An Interdisciplinary *Journal of Nonlinear Science*, **25**(2), 023101.

66. **Nair, V., G. Thampi, S. Karuppusamy, S. Gopalan,** and **R. I. Sujith** (2012). *System and method for predetermining the onset of impending oscillatory instabilities in practical devices*, provisional patent, filed 26th October, 2012.

67. **Gottwald, G. A.** and **I. Melbourne** (2004). A new test for chaos in deterministic systems, *Proceedings of the Royal Society of London*, A, 460 (2042), 603-611.

68. **Zachilas, L.** and **I. N Psarianos** (2012). Examining the chaotic behaviour in Dynamical Systems by Means of the 0-1 Test. *Journal of Applied Mathematics*, 681296.

69. **Nair, V., G. Thampi, S. Karuppusamy, S. Gopalan,** and **R. I. Sujith** (2013b). Loss of chaos in combustion noise as a precursor of impending combustion instability, *International journal of spray and combustion dynamics*, **5**(4), 2013, 273-290.

70. **Stohr, M., I. Boxx, C. Carter,** and **W. Meier** (2011). Dynamics of lean blowout of a swirl-stabilized flame in a gas turbine model combustor, *Proceedings of the combustion institute* **33**, 2953-2960.

71. **Nair, S** and **T. Lieuwen** (2007). Near blow off dynamics of a Bluff body stabilized flame, *Journal of Propulsion and Power*, **23**(2), 423-429.

72. **Muruganandam, T. M.** and **J. M. Seitzmann** (2012). Fluid mechanics of lean blow out precursors in gas turbine combustors, *International Journal of Spray and Combustion Dynamics*, **4**(1), 29-60.

73. **Muruganandam, T.M., S. Nair, D. Scarborough, Y. Neumeier, J. Jagoda, T. Lieuwen,** and **B. Zinn** (2005). Active control of lean blow-out for turbine engine combustors, *Journal of Propulsion and power*, **21**(5), 807-814.

74. **Yi, T.** and **E. J. Gutmark** (2007). Real time prediction of incipient Lean Blowout in gas turbine combustors, *AIAA Journal*, **45**(7), 1734-1739.

75. **Bompelly, R., T. Lieuwen** and **J.M. Seitzman** (2009). Lean blowout and its sensing in the presence of combustion Dynamics in a premixed swirl combustor. 47th AIAA Aerospace Sciences Meeting Including The New Horizons Forum and Aerospace Exposition 5-8 January 2009,Orlando, Florida. *AIAA* 2009-982.

76. **Mukkopadhyay, A., R. R Chaudhari, T. Paul, S. Sen,** and **A. Ray** (2013). Lean Blow-Out Prediction in Gas Turbine combustors using Symbolic Time Series Analysis, *Journal of Propulsion and Power*, **29**(4), 950-960.

77. **Gotoda, H., Y. Shinoda, M. Kobayashi, Y. Okuno,** and **S. Tachibana** (2014). Detection and control of combustion instability based on the concept of dynamical system theory, *Physical Review E*, **89**(2) (022910).

78. **Wilke, C. R.** (1950) A viscosity equation for gas mixtures. *J. Chem. Phys.* **18**, 517-519.

79. **Lieuwen, T. C** (2002). Experimental investigation of limit cycle oscillations in an unstable gas turbine combustor, *Journal of Propulsion and Power*, **18**(1), 61-67.

80. **Pomeau, Y** and **P. Manneville**, (1980). Intermittent Transition to Turbulence in Dissipative Dynamical Systems, *Commun Math Phys*, **74**, 189-197. .

81. **Abarbanel,H. D. L,** *Analysis of observed chaotic data*, Institute for Nonlinear Science, University of California-San Diego ,1996 (Book).

82. **Nair, V** and **R.I. Sujith,** (2013). Identifying homoclinic orbits in the dynamics of intermittent signals through recurrence quantification, *Chaos*, **23**(3), 09, (033136).

83. **Trefethen, L. N** and **M. Embree,** (2005). Spectra and Pseudospectra: The Behaviour of Nonnormal Matrices and Operators, Princeton University Press.

84. **Burnley, V. S** *Nonlinear combustion instabilities and stochastic sources*, PhD thesis, California Institute of Technology, Pasadena, 1996.

85. **Jahnke C. C** and **F.E.C. Culick,** (1993). An application of dynamical systems theory to nonlinear combustion instabilities. *AIAA*, **93**-0114, 31^{st} Aero science meeting and Exhibit Reno, Nevada, January 11- 14.

86. **Ananthkrishnan, N; S. Deo** and **F. E. C. Culick,** (2005). Reduced-order modeling and dynamics of nonlinear acoustic waves in a combustion chamber, *Combustion Science and Technology*, **177**, 221âĂŞ247.

87. **Subramanian, P** (2011). *Dynamical systems approach to the investigation of thermoacoustic instabilities*. PhD thesis, Indian Institute of Technology Madras, Chennai, India, 2011.

88. **Subramanian, P; S. Mariappan, R. I. Sujith** and **P. Wahi,** (2010). Bifurcation analysis of thermoacoustic instability in a horizontal rijke tube. *International Journal of Spray and Combustion Dynamics*, **2**, 325-356.

89. **K. Balasubramanian, K** and **R. I. Sujith,** (2008). Non-normality and nonlinearity in combustion acoustic interactions in diffusion flames. *Journal of Fluid Mechanics*, **592**, 29âĂŞ57.

90. **Kabiraj, L A. Saurabh, P. Wahi, R. I. Sujith,** (2010). Experimental study of thermoacoustic instability in ducted premixed flames: periodic, quasi-periodic and chaotic oscillations. *In Int'l Summer School & Workshop on Non-Normal and Nonlinear Effects in Aero-and Thermoacoustics*, Technische University at Munchen, Germany, May 17-21.

91. **Kabiraj, L** and **R. I. Sujith** (2011). Nonlinear self-excited oscillations in a thermoacoustic system.In 4th International Symposium. *Bifurcations and Instabilities in Fluid Dynamics*,Barcelona, Spain, July 18-21, 2011.

92. **Lei, S** and **A. Turan,** (2009). Nonlinear/chaotic behaviour in thermoacoustic instability. *Combustion Theory and Modelling*, **13**, 541âĂŞ557.

93. **Cao, L,** (1997). Practical method for determining the minimum embedding dimension of a scalar time series, *Physica D* **110**, 43-50.

94. **Nair, V; G. Thampi, R.I. Sujith,** (2014c). Engineering precursors to forwarn the onset of an impending combustion instability, *Proceedings of ASME Turbo Expo 2014*, June 16-20, GT2014-26020, Germany.

95. **Li, G. X** and **B. F. Yao,** (2008). Nonlinear dynamics of cycle-cycle combustion variations in a lean-burn natural gas engine, *Applied Thermal Engineering*, **28**, 611 - 620.

96. **Gottwald, G. A** and **I. Melbourne,** (2004). A new test for chaos in deterministic systems, *Proceedings of the Royal Society of London*, A 460, No.2042, 603-611.

97. **Zachilas, L** and **I. N Psarianos,** (2012). Examining the chaotic behaviour in Dynamical Systems by Means of the 0-1 Test, *Journal of Applied Mathematics*, 681296.

98. **Gottwald, G. A** and **I. Melbourne,** (2005). Testing for chaos in deterministic systems with noise, *Physica D*, Nonlinear Phenomena, **212**, No.1-2, 100-110.

99. **Gottwald G. A** and **I. Melbourne,** (2009a). On the implementation of the 0-1 test for chaos, *SIAM Journal on Applied Dynamical Systems*, **8**(1), 129-145.

100. **Gottwald, G. A** and **I. Melbourne,** (2009b) On the validity of the 0-1 test for chaos, *Nonlinearity*, **22**(6), 1367- 1382.

101. **Nair. V,** (2014d). *Role of intermittency in the onset combustion instability*, Ph.D thesis, Department of Aerospace Engineering, Indian Institute of Technology, Madras.

102. **Schuster, H. G** and **W. Just,** *Deterministic Chaos: An Introduction*, Fourth, Revised and Enlarged Edition, WILEY-VCH Verlag GmbH and Co. KGaA, Weinheim, (2005). (Book).

103. **Schadow, K. C., E. Gutmark, T. P Parr, D. M. Parr, K. J. Wilson** and **J. E. Crump** (1989). Large-Scale Coherent Structures as Drivers of Combustion Instability. *Combustion Science and Technology*, **64**, 167-186.

104. **Annaswamy, A. M., M. Fleifil, J. P. Hathout,** and **A. F. Ghonim** (1997). Impact of linear coupling on the design of active controllers for the thermoacoustic instability. *Combustion Science and Technology*, **128**, 131-180.

105. **Subramanian, P.** and **R. I. Sujith** (2011). Non-normality and internal flame dynamics in premixed flame-acoustic interaction. *Journal of Fluid Mechanics*, **679**,315-342.

106. **Schuller, T., D. Durox,** and **S. Candel** (2003). Self-induced combustion oscillations of laminar premixed flames stabilized on annular burners. *Combustion and Flame*, **135**(4), 525-537.

107. **Wu, X., M. Wang,** and **P. Moin** (2001). Combustion instability due to the nonlinear interaction between sound and flame. Centre for Turbulence Research, Annual Research Briefs.

108. **Shreekrishna., S. Hemachandra,** and **T. Lieuwen** (2010). Premixed flame response to equivalence ratio perturbations. *Combustion Theory and Modelling*, **14**(5), 681 - 714.

109. **Hargrave, G. K** and **S. Jarvis** (2006). A Study of Premixed Propagating Flame Vortex Interaction. *Journal of Visualization*, **9**(2), 179-187.

110. **Coats, C. M** (1996). Coherernt Structures in combustion. *Prog. Energy Combust.* **22**, 427-509.

111. **Syred, N., W. Fick, T. O'doherty** and **A. J. Griffiths** (1997). The Effect of the Precessing Vortex Core on Combustion in a Swirl Burner. *Combustion Science and Technology*, **125**(1-6), 139-157.

112. **Hammer, P. W., N. Platt, S. M. Hammel, J. F.Heagy** and **B. D. Lee** (1994). Experimental Observation of On-Off Intermittency. *Physical Review Letters*, **73**(8),1095-1098.

113. **Strahle, W. C,** (1972). Some results in combustion noise. *Journal of Sound and Vibration*, **23**(1), 113-125.

114. **Kotake, S.** (1975). On combustion noise related to chemical reactions. *Journal of Sound and Vibration*, **42**(3), 399-410.

115. **Nair, V** and **R. I. Sujith** (2014). Multifractality in combustion noise: predicting an impending combustion instability. *Journal of Fluid Mechanics*, **747**, 635-655.

116. **Marwan, N., M. C Romano, M. Thiel** and **J. Kurths** (2007). Recurrence plots for the analysis of complex systems. *Physics Reports*, **438**, 237-329.

117. **Gao, J** and **H. Cai** (2000). On the structures and quantification of recurrence plots. *Physics Letters A*, **270**, 75-87.

118. **Kashinath, K., I. C Waugh** and **M. P. Juniper** (2014). Nonlinear self-excited thermoacoustic oscillations of a ducted premixed flame: bifurcations and routes to chaos. *Journal of Fluid Mechanics*, **761**, 399-430

119. **Kashinath, K.** (2013). *Nonlinear phenomenon in thermoacoustic systems with premixed flames*, PhD Thesis, University of Cambridge, Cambridge, UK.

LIST OF PAPERS BASED ON THESIS

1. 1. Nair, V., **Thampi, G.**, Karuppusamy,S., Gopalan, S., and Sujith, R.I Loss of chaos in combustion noise as a precursor of impending combustion instability. *International Journal of Spray and Combustion Dynamics*, 5.4, 273-290, (2013).

2. Nair, V., **Thampi, G.**, and Sujith, R.I. Intermittency route to thermoacoustic instability in turbulent combustors. *Journal of Fluid Mechanics*.

3. **Thampi, G.**, and Sujith, R.I Intermittent burst oscillations: The signature prior to flame blow-off in a turbulent swirl stabilized combustor. *Journal of Propulsion and Power* (accepted for publication).

4. Nair, V., **Thampi, G.**, and Sujith, R.I. Engineering Precursors To Forewarn The Onset Of An Impending Combustion Instability. *ASME Turbo Expo* 2014 (GT2014-26020), June 16-20, (2014).

5. Nair, V., **Thampi, G.**, and Sujith, R.I Intermittent Burst Presage the Onset of Combustion Instability in Turbulent Combustors. *n3l- Int'l Summer School and Workshop on Non-Normal and Nonlinear Effects in Aero-and Thermoacoustics,* Munich, June 18-21, (2013).

Patents filed

6. Nair, V., **Thampi, G.**, Karuppusamy, S., Gopalan, S., and Sujith, R.I., 2012. 1. System and method for pre-determining the onset of impending oscillatory instabilities in practical devices, Provisional patent, filed Oct.26.